EXPLORING THE OCCURRENCE OF HORIZONTAL GENE TRANSFER AND ITS ROLE IN THE EVOLUTION AND ADAPTATION OF *FUSARIUM VERTICILLIOIDES*

by

SHAN GAO

(Under the Direction of Anthony Glenn and Scott Gold)

ABSTRACT

Fusarium species are diverse and economically important soilborne phytopathogenic fungi. Though *Fusarium verticillioides* potentially infects various plants, it plays a diverse role in the ecosystem as both a significant pathogen of corn, causing root, kernel, seed, and stalk rots, and as a symptomless intercellular endophyte of maize. We hypothesize that the economically important maize pathogen and symptomless endophyte, *F.verticillioides*, is a good candidate for horizontal gene transfer (HGT) detection given its versatile lifestyles. Horizontal gene transfer, the exchange and stable integration of genetic material between different evolutionary lineages, is believed to shape genomes and populations and produce a gain of adaptive advantages. To identify such phenomenon in *F.verticillioides*, a genome-wide identification of HGT events using a phylogenomic pipeline was conducted followed by manual curation, obtaining 117 strong HGT candidates of which most were putatively acquired from bacteria. Functional categorization of these candidates implicated several enriched biochemical activities compared to the frequency of such genes within the genome. Multiple interesting HGT candidates that are narrowly distributed within fungi or induced only under specific environmental conditions were identified. A prime exemplar was FVEG_10494, a strong HGT candidate with orthologs in only

a few *Fusarium* species, and it was highly and specifically up-regulated under nitric oxide (NO) challenge. Secondly, functional characterization was performed on two catalase/peroxidase genes named *FvCP01* and *FvCP02*, which were previously identified as HGT candidates broadly distributed among ascomycetes. *In vitro* hydrogen peroxide (H_2O_2) sensitivity and quantitative reverse transcription-PCR (qRT-PCR) analyses suggest differential responses of these two genes to *in vitro* versus *in planta* oxidative challenges. *FvCP01* seems to be largely involved in non-host-mediated H_2O_2 stress while *FvCP02* is mainly responsible for oxidative challenge derived from the host. Lastly, a project was initiated to develop a chemical-inducible expression system in *F.verticillioides* based on a system used in plants.

INDEX WORDS: *Fusarium verticillioides*, horizontal gene transfer, phylogenomic pipeline, nitric oxide, catalase/peroxidase, hydrogen peroxide, chemical-inducible expression

EXPLORING THE OCCURRENCE OF HORIZONTAL GENE TRANSFER AND ITS ROLE IN THE EVOLUTION AND ADAPTATION OF *FUSARIUM VERTICILLIOIDES*

by

SHAN GAO

BS, China Agricultural University, China, 2012

A Dissertation Submitted to the Graduate Faculty of The University of Georgia in Partial Fulfillment of the Requirements for the Degree

DOCTOR OF PHILOSOPHY

ATHENS, GEORGIA

2017

EXPLORING THE OCCURRENCE OF HORIZONTAL GENE TRANSFER AND ITS ROLE IN THE EVOLUTION AND ADAPTATION OF *FUSARIUM VERTICILLIOIDES*

by

SHAN GAO

Major Professor:	Anthony Glenn Scott Gold
Committee:	Ronald Walcott Marin Brewer Li-Jun Ma

Electronic Version Approved:

Suzanne Barbour

Dean of the Graduate School

The University of Georgia

May 2017

DEDICATION

I would like to firstly thank my family members, my father, Shaoliang Gao and my endearing grandma, Yuqing Zhang, who have been taking good care of me since I was born. Without their encouragement and open mind, I would never have the courage and determination to grasp the opportunity of pursuing doctoral education in the United States, let alone the chance of appreciating the ethnically and racially diverse culture and traveling around the world. Next, special thank you to the love of my life, Xiao Zhang, a confident, gentle and responsible man, whose endurance and positive attitude throughout the nearly five-year transnational love relationship are greatly appreciated. I deeply believe the love will be engraved on our weal-and-woe sharing lifetime. At last, to my dear mom and grandpa, who will be forever remembered and missed. I hope you can be proud that I grow into an independent, optimistic, and well-educated woman and you will continue witnessing how I am about to start a lively family and seek the value in my life.

ACKNOWLEDGEMENTS

Great appreciation to my supervisors, Dr. Anthony Glenn and Dr. Scott Gold, for their directions during the pursuit of my doctoral degree. You are always there to care, to help, and to encourage. Dr. Glenn is like an amiable and reliable friend who always patiently and attentively listens to my needs and doubts. Dr. Gold is like a thoughtful and witty father who cares about me the moment I arrived in the States. I am still on the road to become an independent and qualified scientist, but without your promotion and guidance, I will barely set my foot on the ground of science. I would also like to thank my committee members, Dr. Ron Walcott, Dr. Marin Brewer, and Dr. Li-Jun Ma for the valuable suggestions and efforts to my project. In addition, I want to thank my collaborators, Dr. Jennifer Wisecaver, Dr. Antonis Rokas, Yong Zhang, and Dr. Li Guo. It is such a great honor to work with you all and I benefit a lot from the three-laboratories cooperation. Moreover, I would like to thank our wonderful technicians Nicole Crenshaw and Larry Pierce for the scientific training and technical help. Last but not least, special thank you to my labmate and officemate, Manisha Rath, for the experimental help and emotional encouragement.

TABLE OF CONTENTS

LIST OF TABLES

Page

LIST OF FIGURES

Page

CHAPTER 1

INTRODUCTION AND LITERATURE REVIEW

Research Objectives

The aim of this research project was to explore the occurrence of horizontal gene transfer (HGT) and characterize the role of HGT candidates in *Fusarium verticillioides.* Approaches implemented were designed to identify genome-wide HGT events and functionally characterize selected HGT candidates in *F. verticillioides.* Together, the findings provide a view of how HGT has shaped the *F. verticillioides* genome and biology. Moreover, the functional characterization of select interesting HGT candidates supported their contributions to adaptive advantage of *F. verticillioides.*

As a facultative plant pathogen commonly associated with maize (*Zea mays*), *F. verticillioides* causes a number of diseases including root, kernel, seed, and stalk rots. It also can cause stand reductions and stunting due to seedling blight [1]. The infection of *F. verticillioides* in the field is hard to detect and is facilitated by insect or herbivore damage, making it an opportunistic hemibiotroph [2]. Beyond its pathogenic nature, *F. verticillioides* can be a symptomless intercellular endophyte present in seeds and throughout the host plant [3]. Along with variable effects on seed germination and seedling health [1], the fungus can also reduce grain quality by contamination with fumonisin mycotoxins. The fumonisins threaten human and animal health upon consumption of contaminated food [4]. Carcinogenic and cytotoxic, the

fumonisins are associated with several diseases in farm animals, such as porcine pulmonary edema syndrome and leukoencephalomalacia in horses [5, 6]. Human maladies, including esophageal cancer, neural tube defects [6], and stunting in children [7], are associated with chronic *F. verticillioides* contaminated corn intake. In addition, fumonisins can disrupt ceramide biosynthesis in maize roots and are associated with overall symptoms of seedling disease [8]. Fumonisins concentrations in corn are recommended not to exceed 2 μg/kg body weight per day for humans [9].

In contrast to vertical gene transfer from parent to offspring, HGT is defined as the exchange and stable integration of genetic material between different evolutionary lineages [10]. HGT breaks species boundaries and generates new biological diversity. HGT is rampant in prokaryotes and shapes the genomes and populations of prokaryotes [10-13]. In terms of HGT events in eukaryotes, multiple factors may act as barriers to its occurrence. For instance, eukaryotic features, including the existence of a nuclear envelope and the storage of genetic information in chromatin, can potentially block HGT [14]. In addition, many eukaryotes are multi-cellular and thus separate their germline and somatic cells, which creates a physical defence against vertical transmission and retention of past HGT events [14]. The RNA interference (RNAi) system and RNAi-based silencing mechanisms operating in mitotic and meiotic cells should also contribute to scrutinize and eliminate transferred genes [15]. Furthermore, incompatibility of gene promoters and intron-splicing systems may impede post HGT event function/retention between eukaryotic genomes or between eukaryotic and prokaryotic genomes [16]. Despite this, with the rapid increase in publicly accessible eukaryotic genomic data, a growing body of evidence suggests HGT is an underestimated factor in the

evolution of eukaryotic genomes [14, 16-18]. For example, a broad search for prokaryote derived HGT events in 60 fully sequenced fungal genomes revealed 713 transferred genes [19].

HGT events are generally categorized based on the involvement of different combinations of donors and recipients, with the most abundant putative HGT cases found between prokaryotes and eukaryotes. The first category involves the transfer of genes facilitated by primary and subsequent endosymbiosis, such as the hypothesis of massive endosymbiotic gene transfer (EGT) occurring during organellar evolution [20, 21]. Although the number of nuclear genes in eukaryotes acquired from bacterial sources varies significantly between species, with estimates ranging from zero to hundreds, most described HGT events in eukaryotes are associated with bacterial gene donors [16]. In contrast, few cases of eukaryotic-to-prokaryotic HGT have been reported, one example is a eukaryotic fructose bisphosphate aldolase (FBA) acquired by abundant marine C*yanobacteria* [22]. The biased transfer orientation, on one hand, may be related to the emphasis on examining eukaryotic nuclear genomes for evidence of HGT of bacterial origin and the large prokaryotic genomic data available [16]. On the other hand, bacterial genomic features such as the absence of introns (avoid incorrect or inefficient intron splicing in a foreign genome) and the clustering of functionally related genes in operons (may benefit for the acquisition of an entire pathway through one transfer) might favor the prokaryote-eukaryote transfer [16]. The immensity of bacterial populations compared to eukaryotic populations may also enhance the odds of prokaryote to eukaryote HGT [16]. A smaller number of eukaryote–eukaryote transfers of nuclear genes has been identified. A compelling example is the horizontal transfer of the toxin-encoding gene *ToxA* from the wheat pathogen *Stagonospora nodorum* in the 1940s to another plant pathogenic fungus, *Pyrenophora tritici-repentis* [23]. In

addition, a recent study by our group suggests two xenobiotic-degrading gene clusters, *FDB1* and *FDB2*, in *F. verticillioides* were horizontally transferred to other fungi independently [24].

Several mechanisms have been proposed to explain the occurrence and retention of HGT events in eukaryotes. Seven proposed mechanisms are described below. Proposed mechanism 1: 'You are what you eat', posits HGT via incorporation of dietary DNA into germ cells after passing through a digestive system [25]. Proposed mechanism 2: incorporation of genetic materials from intracellular symbionts or parasites or through phagotrophic food vesicles into the nuclear genome [17]. Proposed mechanism 3: bacterial transduction, transformation and conjugation in association with eukaryotes. A prime example is the widely-used *Agrobacterium*-mediated transformation for genetic manipulation of plants but also possibly fungi and other groups. Proposed mechanism 4: intimate contact might promote exchange of genetic materials between different eukaryotes. For instance, it has been shown that grafting can result in HGT that may be spatially mediated by plasmodesmata [26]. Another process favoring HGT in eukaryotes is anastomosis, which happens in fungal species and results in fusion of conidia, germ tubes and hyphae [27]. Proposed mechanism 5: transposable elements (TE) may also contribute to HGT by moving or copying genetic materials between nuclear chromosomes and mobile vectors within both prokaryotes and eukaryotes as well as between prokaryotes and eukaryotes [28, 29]. Proposed mechanism 6 and 7: new ideas have also been raised recently, including the weak-link model [30] and lightning-triggered electroporation and electrofusion [31]. The weak-link model suggests both unicellular and early developmental stages are potential entry points for foreign genes into multicellular eukaryotes. Meanwhile, Kotnik proposed the feasibility of electroporation, a method for DNA release and/or uptake and transformation, and electrofusion, a way of producing cell hybrids, as natural mechanisms of HGT triggered by lightning.

Potentially promoted by the exposure to various intimate ecological associations with both living and dead organisms [14], fungi are one of the eukaryotic groups demonstrating abundant cases of HGT events [32]. During the transfer and fixation of horizontally transferred genetic materials to the recipient's genome, multiple steps are presumed to take place [33]: the transfer of genes possessing features of the donor lineage genome, the maintenance and replication of transferred genes, the spread within the population of the recipient by vertical inheritance, and the amelioration to the genome of the recipient lineage. It is predicted that retention of acquired genes should involve function of the acquired gene in the new lineage and contribution to a selective advantage to the recipient. The following paragraphs summarize potential advantageous traits brought into fungi by putative HGT candidates.

1. *Acquisition of virulence genes promoting pathogenicity on plants and affecting host range.* Secreted effector molecules, once horizontally acquired by a fungal species from other pathogens could interfere with the same host target. The *Ave1* effector was identified in specific strains of the vascular wilt-causing pathogen *Verticillium dahliae* as well as other fungal pathogens [34]. More pertinent to this discussion, *Ave1* resembles plant proteins involved in signaling. Phylogenetic analyses strongly suggested the origin of this gene as derived from plant species, implying the use of plant-derived molecules for pathogens to manipulate the host intracellular environment. Further, the amidohydrolase encoding gene *FpAH1* in *Fusarium pseudograminearum*, which causes wheat and barley crown rot, with no previously known role in fungal pathogenesis was shown to likely originate from bacteria [35]. Deletion of this gene reduced virulence of *F. pseudograminearum* on wheat and barley.

2. *HGT enhances adaptation to the environment.* Some HGT events in fungi have been shown to be involved in niche specialization. For example, three genomic regions of foreign origin have been detected in the yeast *S. cerevisiae* EC1118, which is able to tolerate harsh wine fermentation conditions featuring high sugar and alcohol, and low oxygen, nitrogen, and vitamins [36]. The acquisition of glycosyl hydrolases (GHs) by rumen fungi from prokaryotes allows rumen fungi to effectively degrade cellulose and plant hemicelluloses in the rumen of herbivorous mammals [37].
3. *HGT of secondary metabolic clusters adding advantages to fungi.* In addition to laterally acquiring single genes, several studies showed the transfer of gene clusters, especially involved in production of secondary metabolites. For example, the entire pathway consisting of 23 genes for the production of sterigmatocystin (ST), a highly toxic secondary metabolite, was horizontally transferred from *Aspergillus nidulans* to *Podospora anserine* [38]. In another instance, the β-lactam biosynthetic cluster, a relatively simple collection of three genes, was proposed to have been transferred from bacteria to fungi [39].

So far, the gold standard method for testing HGT is phylogentic analysis showing a gene phylogeny contradicting the established species phylogeny by placing that gene in a species or shared by a group of species within a clade containing similar sequences from unrelated organisms [14]. The direction of gene transfer is usually determined by revealing the location of incongruent sequence in the gene phylogeny. For example, a fungal gene clustering with a bacteria-derived clade suggests the direction of transfer is potentially from bacteria to fungus. Though powerful, phylogenetic methods can be complex and problematic. Misinterpretation of HGT may arise from biased sample collection, limited available data and ignorance of other

evolutionary possibilities. Also, inconsistent evolutionary rates amongst species and the variable recency of an HGT event make interpretation even harder [16, 18]. Phylogeny-independent approaches (also called surrogate methods) are normally included in HGT examination to further support a proposed event. Those methods include detecting regions showing atypical genomic characteristics, observing a patchy phyletic distribution of a gene, and finding similar genes among unrelated species sharing a specific niche or geographical location [40] and so on. It is recommended that a combination of multiple independent approaches be used to confidently reveal HGT events. In some cases, alternative scenarios should be considered before interpreting HGT as the most parsimonious. For instance, gene duplication followed by differential gene loss (hidden paralogy) may falsely suggest HGT depending on the level of organismal relatedness involved [14]. Convergent evolution may also falsely implicate HGT [18].

A study in which 60 fully sequenced fungal genomes were examined shows that prokaryotic-derived HGT events are especially enriched in the Pezizomycotina, while cases are scarce in the Saccharomycotina [19]. Marcet-Houben and Gabaldon proposed that this striking difference might result from distinct lifestyles of these two groups. Consistent with this idea, it has been observed that various lifestyles and multiple niches may favor horizontal gene acquisition [41], which might be the case of *Fusarium* species. Generally speaking, most *Fusarium* species are considered as soilborne facultative pathogens, suggesting more diverse lifestyles compared to obligate pathogens. They can cause plant diseases on many horticultural, field, ornamental and forest crops in various ecosystems with varying host specificity among different species. Their soilborne nature places them in contact with myriad microbes and plant species.

Despite increasing evidence of HGT events in several *Fusarium* species [35, 42-45], a thorough analysis of how HGT has shaped the genome of *F. verticillioides* is needed, which justifies the global analysis of HGT in *F. verticillioides* under this objective. While closely related to *F. oxysporum*, which has so far been the primary focus of large-scale HGT studies, the host-associated biology of *F. verticillioides* as an endophyte of maize further justifies our objective. In addition, it has been proposed that HGT may still be underestimated in eukaryotes [17, 30], further prompting us to examine such events in *F. verticillioides*.

Previously, it was proposed that a group of fungal reactive oxygen species (ROS)-degrading enzymes, catalase/peroxidases (commonly abbreviated as KatGs) were horizontally acquired from the bacterial phylum Bacteroidetes to ancient Ascomycota [46, 47]. KatGs are bifunctional heme B-containing (Class I) peroxidases with both efficient catalase activity (Reaction 1, below) and substantial peroxidase activity (Reaction 2; **A** refers to an electron donor) with various one-electron donors [46].

$$2H_2O_2 \rightarrow 2H_2O + O_2 \qquad \textbf{Reaction 1}$$

$$H_2O_2 + 2AH_2 \rightarrow 2H_2O + 2AH \qquad \textbf{Reaction 2}$$

Among reactive oxygen species, hydrogen peroxide (H_2O_2) is the most abundant as a by-product of aerobic metabolism [47]. In plants, the level of ROS can be elevated under both abiotic and biotic stresses, such as the invasion of phytopathogens [48]. It has been revealed that H_2O_2 is involved in induction of innate immune defense and production of phytoalexins in plant cells [49]. As a diffusible small molecule that can readily cross biological membranes [50], H_2O_2 appears to be heavily involved in fungus-plant interactions [51, 52]. Hyphal growth of several biotrophic and hemibiotrophic fungal pathogens is inhibited in the host cells owing to the production of H_2O_2 by plants [53-55].

For maintaining normal metabolism, living cells need a homeostatically controlled redox potential, which is ensured by antioxidant defense systems consisting of ROS-removing molecules (e.g. glutathione) and various redox enzymes (e.g. superoxide dismutase and peroxidases) [56, 57]. KatGs appear to be efficient candidates assuming dual functions. In fungi, two groups of KatGs are present, namely KatG1 and KatG2. The KatG1 group contains more representatives than those in KatG2. In addition, all members of Group 1 are intracellular proteins, which are likely located in peroxisomes owing to the presence of a peroxisomal targeting signal. Moreover, peroxisomal localization of KatG1 from *Magnaporthe grisea, Chaetomium globosum and C. cochliodes* was confirmed by organelle separation and immunofluorescence microscopy [58]. In contrast, all representatives of the KatG2 group are extracellular heme proteins, indicated by the occurrence of an N-terminal signal sequence for secretion [46]. Most amazingly, all known fungal KatG2 genes are limited to Sordariomycetes (primarily phytopathogens and a few mycoparasites within the order Hypocreales). It is worthwhile to note that the signal sequence responsible for extracellular secretion has not been detected in Bacteroidetes, implying Sordariomycete-specific modification for secretion after HGT and gene duplication [46].Therefore, it is reasonable to expect increased virulence and efficient resistance to oxidative burst during plant attack in KatG2-harboring pathogenic fungi. Functional characterization of KatG2 in *M. oryzae* suggested the positive role of the extracellular catalase-peroxidase in fighting against H_2O_2 produced by rice during the early stages of infection [49]. In *F. verticillioides*, one gene of each KcatG group is present: the intracellular KatG1 candidate (FVEG_10866) and extracellular KatG2 candidate (FVEG_12888). Their roles in responding to *in vitro* or *in planta* oxidative stresses were addressed in Chapter 3.

An additional unrelated goal of this dissertation work involved construction of a metabolically-independent inducible fungal gene expression vector. The purpose was to generate an inducible expression system for fungal genes during *in planta* colonization. Although in many cases a strong constitutive promoter is used to drive a target gene, inducible promoters are particularly valuable for studies requiring stringent expression control to investigate temporal and spatial expression of genes. Chemical-inducible expression systems stand out from others owing to their easy application, effective regulation and avoidance of undesirable influence on endogenous physiological activities as they are quiescent in the absence of inducers [59]. To precisely regulate a gene's expression, an ideal chemical-inducible expression system should have the following properties [60, 61]: absence (the chemical inducer should not be found in targeting organism), safety (the inducer should not be toxic and have no physiological effects in targeted organisms), specificity (expression should respond only to application and/or withdrawal of a particular exogenous chemical), efficiency (the inducible promoter should exhibit very low or no basal expression level, should increase rapidly to high-level expression after inducer addition, and then return to quiescence after inducer removal), dose-dependence (the inducible system should demonstrate a high dynamic range of responses depending on inducer concentrations), applicability (the inducer should be systemically effective at a low-use-rate and convenient to apply).

Chemicals that have been used to regulate inducible gene expression in plants include tetracycline, dexamethasone, copper, estradiol, ethanol etc. [59, 62]. Regardless of how chemical-inducible expression systems are categorized, two functional components are critical for all systems. The first component (activator or repressor protein) uses a constitutive promoter to express a chemical-responsive transcription factor, while the second component (target

promoter) employs multiple copies of the transcription factor binding site linked to a minimal promoter to drive the expression of a target gene [61].

Unlike the development of various well-established chemical-inducible promoters and their extensive use in plants, only a limited number of inducible expression systems regulated by chemicals (metabolism-dependent or metabolism-independent) have been developed for fungi, among which most were studied in ascomycetous fungi, most notably, *Aspergillus* spp. So far, most *Aspergillus* inducible expression systems are highly carbon-and-nitrogen-source dependent [63]. For example, one of the most frequently used inducible promoters in *Aspergillus* expression systems, P*glaA* [63], is usually repressed by xylose but can be highly induced when maltose or starch are used as a single carbon source [64]. In addition, P*glaA* is repressed or only weakly expressed when a rich, easily metabolized carbon source such as glucose is provided, making the corresponding metabolism pathways more complicated [65]. Owing to inconvenient application [66] and unavoidable effect of conditions required to regulate metabolism-dependent promoters on the exogenous metabolism of the organisms [67], efforts have been made to develop metabolically-independent and accurately adjustable expression systems by adopting the transcriptional activation of the human estrogen receptor (hERα) [66], and the thiamine promoter system (P*thiA*) in *Aspergillus oryzae* [68] and the *Escherichia coli* tetracycline on/off system in *Aspergillus* [67, 69], etc. The first metabolism-independent inducible expression system in filamentous fungi is the ER-based system, which requires successive transformations of an activator vector harboring hER and a targeting vector containing a gene of interest downstream of the estrogen-responsive elements (EREs) into *A. niger* and *A. nidulans*. Notably, diethylstilbestrol (DES) and 17-β-estradiol can highly induce the expression of a reporter gene in

the picomolar concentration range, suggesting the impressive sensitivity of this system in *Aspergillus* species to estrogens [66].

In summary, the development of chemical-inducible expression systems, especially metabolism-independent systems, is lagging in fungi. The idea of constructing a chemical-inducible and metabolism-independent expression systems for *Fusarium* is further motivated by the successful transformation of ER-based system from plants to *Aspergillus* species [66]. In this system, inducible expression of a target gene is achieved by regulated transactivation of hER (activator vector) on three copies of ERE sequences, which are upstream of a URA3 minimal promoter followed by the target gene (reporter vector). Successive fungal transformations are required to introduce activator and reporter vectors. In contrast, by adopting the XVE system, which integrates all necessary components into a single vector, fungal transformation is only needed once. In addition, the efficiency of cloning target genes into the modified vector and fungal transformation will be enhanced by introducing the Gateway® system and employing *Agrobacterium tumefaciens*-mediated transformation, respectively. Theoretically, this system would be generally applicable to other ascomycetes, and most interestingly to phytopathogens, providing a promising way to study the interaction between phytopathogenic fungi and their plant hosts.

References

1. Munkvold, G.P., D.C. McGee, and W.M. Carlton, *Importance of Different Pathways for Maize Kernel Infection by Fusarium moniliforme.* Phytopathology, 1997. **87**(2): p. 209-17.
2. Varma, A., et al., *Endophytic Root Colonization by Fusarium Species: Histology, Plant Interactions, and Toxicity*. 2006. p. 133.
3. Bacon, C.W. and D.M. Hinton, *Symptomless endophytic colonization of maize by Fusarium moniliforme.* Canadian Journal of Botany, 1996. **74**(8): p. 1195-1202.
4. Bacon, C.W., A.E. Glenn, and I.E. Yates, *Fusarium verticillioides: managing the endophytic association with maize for reduced fumonisins accumulation.* Toxin Reviews, 2008. **27**(3-4): p. 411-446.
5. Haschek, W.M., et al., *Fumonisin toxicosis in swine: an overview of porcine pulmonary edema and current perspectives.* Environ Health Perspect, 2001. **109 Suppl 2**: p. 251-7.
6. Marasas, W.F., et al., *Fumonisins disrupt sphingolipid metabolism, folate transport, and neural tube development in embryo culture and in vivo: a potential risk factor for human neural tube defects among populations consuming fumonisin-contaminated maize.* J Nutr, 2004. **134**(4): p. 711-6.
7. Kimanya, M.E., et al., *Fumonisin exposure through maize in complementary foods is inversely associated with linear growth of infants in Tanzania.* Molecular Nutrition & Food Research, 2010. **54**(11): p. 1659-1667.
8. Williams, L.D., et al., *Fumonisin disruption of ceramide biosynthesis in maize roots and the effects on plant development and Fusarium verticillioides-induced seedling disease.* J Agric Food Chem, 2007. **55**(8): p. 2937-46.
9. Voss, K., R. Riley, and J. B. Gelineau-van Waes, *Toxicity of Fumonisins, Mycotoxins from Fusarium verticillioides*, in *Microbial Food Contamination, Second Edition*. 2007, CRC Press.
10. Doolittle, W.F., *Lateral genomics.* Trends Cell Biol, 1999. **9**(12): p. M5-8.
11. Gogarten, J.P., W.F. Doolittle, and J.G. Lawrence, *Prokaryotic evolution in light of gene transfer.* Mol Biol Evol, 2002. **19**(12): p. 2226-38.
12. Jain, R., et al., *Horizontal gene transfer accelerates genome innovation and evolution.* Mol Biol Evol, 2003. **20**(10): p. 1598-602.
13. Polz, M.F., E.J. Alm, and W.P. Hanage, *Horizontal gene transfer and the evolution of bacterial and archaeal population structure.* Trends Genet, 2013. **29**(3): p. 170-5.
14. Richards, T.A., et al., *Gene transfer into the fungi.* Fungal Biology Reviews, 2011. **25**(2): p. 98-110.
15. Aramayo, R. and E.U. Selker, *Neurospora crassa, a model system for epigenetics research.* Cold Spring Harb Perspect Biol, 2013. **5**(10): p. a017921.
16. Keeling, P.J. and J.D. Palmer, *Horizontal gene transfer in eukaryotic evolution.* Nat Rev Genet, 2008. **9**(8): p. 605-18.
17. Schonknecht, G., et al., *Gene transfer from bacteria and archaea facilitated evolution of an extremophilic eukaryote.* Science, 2013. **339**(6124): p. 1207-10.
18. Wijayawardena, B.K., D.J. Minchella, and J.A. DeWoody, *Hosts, parasites, and horizontal gene transfer.* Trends Parasitol, 2013. **29**(7): p. 329-38.
19. Marcet-Houben, M. and T. Gabaldon, *Acquisition of prokaryotic genes by fungal genomes.* Trends Genet, 2010. **26**(1): p. 5-8.

20. Kurland, C.G. and S.G. Andersson, *Origin and evolution of the mitochondrial proteome.* Microbiol Mol Biol Rev, 2000. **64**(4): p. 786-820.
21. Martin, W., et al., *Evolutionary analysis of Arabidopsis, cyanobacterial, and chloroplast genomes reveals plastid phylogeny and thousands of cyanobacterial genes in the nucleus.* Proc Natl Acad Sci U S A, 2002. **99**(19): p. 12246-51.
22. Rogers, M.B., N.J. Patron, and P.J. Keeling, *Horizontal transfer of a eukaryotic plastid-targeted protein gene to cyanobacteria.* BMC Biol, 2007. **5**: p. 26.
23. Friesen, T.L., et al., *Emergence of a new disease as a result of interspecific virulence gene transfer.* Nat Genet, 2006. **38**(8): p. 953-956.
24. Glenn, A.E., et al., *Two Horizontally Transferred Xenobiotic Resistance Gene Clusters Associated with Detoxification of Benzoxazolinones by Fusarium Species.* PLoS One, 2016. **11**(1): p. e0147486.
25. Ford Doolittle, W., *You are what you eat: a gene transfer ratchet could account for bacterial genes in eukaryotic nuclear genomes.* Trends in Genetics, 1998. **14**(8): p. 307-311.
26. Stegemann, S. and R. Bock, *Exchange of Genetic Material Between Cells in Plant Tissue Grafts.* Science, 2009. **324**(5927): p. 649.
27. Mehrabi, R., et al., *Horizontal gene and chromosome transfer in plant pathogenic fungi affecting host range.* FEMS Microbiol Rev, 2011. **35**(3): p. 542-54.
28. Gilbert, C. and R. Cordaux, *Horizontal transfer and evolution of prokaryote transposable elements in eukaryotes.* Genome Biol Evol, 2013. **5**(5): p. 822-32.
29. Walsh, A.M., et al., *Widespread horizontal transfer of retrotransposons.* Proc Natl Acad Sci U S A, 2013. **110**(3): p. 1012-6.
30. Huang, J., *Horizontal gene transfer in eukaryotes: the weak-link model.* Bioessays, 2013. **35**(10): p. 868-75.
31. Kotnik, T., *Lightning-triggered electroporation and electrofusion as possible contributors to natural horizontal gene transfer.* Physics of Life Reviews, 2013. **10**(3): p. 351-370.
32. Gladieux, P., et al., *Fungal evolutionary genomics provides insight into the mechanisms of adaptive divergence in eukaryotes.* Molecular Ecology, 2014. **23**(4): p. 753-773.
33. Eisen, J.A., *Horizontal gene transfer among microbial genomes: new insights from complete genome analysis.* Current Opinion in Genetics & Development, 2000. **10**(6): p. 606-611.
34. de Jonge, R., et al., *Tomato immune receptor Ve1 recognizes effector of multiple fungal pathogens uncovered by genome and RNA sequencing.* Proc Natl Acad Sci U S A, 2012. **109**(13): p. 5110-5.
35. Gardiner, D.M., et al., *Comparative pathogenomics reveals horizontally acquired novel virulence genes in fungi infecting cereal hosts.* PLoS Pathog, 2012. **8**(9): p. e1002952.
36. Novo, M., et al., *Eukaryote-to-eukaryote gene transfer events revealed by the genome sequence of the wine yeast Saccharomyces cerevisiae EC1118.* Proc Natl Acad Sci U S A, 2009. **106**(38): p. 16333-8.
37. Garcia-Vallve, S., A. Romeu, and J. Palau, *Horizontal gene transfer of glycosyl hydrolases of the rumen fungi.* Mol Biol Evol, 2000. **17**(3): p. 352-61.
38. Slot, J.C. and A. Rokas, *Horizontal Transfer of a Large and Highly Toxic Secondary Metabolic Gene Cluster between Fungi.* Current Biology, 2011. **21**(2): p. 134-139.
39. Brakhage, A.A., et al., *Aspects on evolution of fungal beta-lactam biosynthesis gene clusters and recruitment of trans-acting factors.* Phytochemistry, 2009. **70**(15-16): p. 1801-11.
40. Fitzpatrick, D.A., *Horizontal gene transfer in fungi.* FEMS Microbiol Lett, 2012. **329**(1): p. 1-8.
41. Gardiner, D.M., K. Kazan, and J.M. Manners, *Cross-kingdom gene transfer facilitates the evolution of virulence in fungal pathogens.* Plant Sci, 2013. **210**: p. 151-8.
42. Campbell, M.A., A. Rokas, and J.C. Slot, *Horizontal transfer and death of a fungal secondary metabolic gene cluster.* Genome Biol Evol, 2012. **4**(3): p. 289-93.
43. Ma, L.J., et al., *Comparative genomics reveals mobile pathogenicity chromosomes in Fusarium.* Nature, 2010. **464**(7287): p. 367-73.

44. Proctor, R.H., et al., *Birth, death and horizontal transfer of the fumonisin biosynthetic gene cluster during the evolutionary diversification of Fusarium.* Mol Microbiol, 2013. **90**(2): p. 290-306.
45. Tsavkelova, E., et al., *Identification and functional characterization of indole-3-acetamide-mediated IAA biosynthesis in plant-associated Fusarium species.* Fungal Genet Biol, 2012. **49**(1): p. 48-57.
46. Zamocky, M., P.G. Furtmuller, and C. Obinger, *Two distinct groups of fungal catalase/peroxidases.* Biochem Soc Trans, 2009. **37**(Pt 4): p. 772-7.
47. Zamocky, M., et al., *Molecular evolution of hydrogen peroxide degrading enzymes.* Arch Biochem Biophys, 2012. **525**(2): p. 131-44.
48. Apel, K. and H. Hirt, *Reactive oxygen species: metabolism, oxidative stress, and signal transduction.* Annu Rev Plant Biol, 2004. **55**: p. 373-99.
49. Tanabe, S., et al., *The Role of Catalase-Peroxidase Secreted by Magnaporthe oryzae During Early Infection of Rice Cells.* Molecular Plant-Microbe Interactions, 2010. **24**(2): p. 163-171.
50. Gadjev, I., J.M. Stone, and T.S. Gechev, *Chapter 3: Programmed Cell Death in Plants: New Insights into Redox Regulation and the Role of Hydrogen Peroxide*, in *International Review of Cell and Molecular Biology*. 2008, Academic Press. p. 87-144.
51. Lehmann, S., et al., *Reactive oxygen species and plant resistance to fungal pathogens.* Phytochemistry, 2015. **112**: p. 54-62.
52. Nanda, A.K., et al., *Reactive oxygen species during plant-microorganism early interactions.* J Integr Plant Biol, 2010. **52**(2): p. 195-204.
53. Mellersh, D.G., et al., *H2O2 plays different roles in determining penetration failure in three diverse plant-fungal interactions.* Plant J, 2002. **29**(3): p. 257-68.
54. Shetty, N.P., et al., *Role of hydrogen peroxide during the interaction between the hemibiotrophic fungal pathogen Septoria tritici and wheat.* New Phytologist, 2007. **174**(3): p. 637-647.
55. Vanacker, H., T.L.W. Carver, and C.H. Foyer, *Early H(2)O(2) Accumulation in Mesophyll Cells Leads to Induction of Glutathione during the Hyper-Sensitive Response in the Barley-Powdery Mildew Interaction.* Plant Physiology, 2000. **123**(4): p. 1289-1300.
56. Breitenbach, M., et al., *Oxidative stress in fungi: its function in signal transduction, interaction with plant hosts, and lignocellulose degradation.* Biomolecules, 2015. **5**(2): p. 318-42.
57. Heller, J. and P. Tudzynski, *Reactive oxygen species in phytopathogenic fungi: signaling, development, and disease.* Annu Rev Phytopathol, 2011. **49**: p. 369-90.
58. Zamocky, M., et al., *Intracellular targeting of ascomycetous catalase-peroxidases (KatG1s).* Arch Microbiol, 2013. **195**(6): p. 393-402.
59. Tang, W., X. Luo, and V. Samuels, *Regulated gene expression with promoters responding to inducers.* Plant Science, 2004. **166**(4): p. 827-834.
60. Wang, R., X. Zhou, and X. Wang, *Chemically Regulated Expression Systems and their Applications in Transgenic Plants.* Transgenic Research, 2003. **12**(5): p. 529-540.
61. Zuo, J. and N.H. Chua, *Chemical-inducible systems for regulated expression of plant genes.* Curr Opin Biotechnol, 2000. **11**(2): p. 146-51.
62. Moore, I., M. Samalova, and S. Kurup, *Transactivated and chemically inducible gene expression in plants.* Plant J, 2006. **45**(4): p. 651-83.
63. Fleissner, A. and P. Dersch, *Expression and export: recombinant protein production systems for Aspergillus.* Appl Microbiol Biotechnol, 2010. **87**(4): p. 1255-70.
64. Fowler, T., R.M. Berka, and M. Ward, *Regulation of the glaA gene of Aspergillus niger.* Curr Genet, 1990. **18**(6): p. 537-45.
65. Prathumpai, W., M. McIntyre, and J. Nielsen, *The effect of CreA in glucose and xylose catabolism in Aspergillus nidulans.* Appl Microbiol Biotechnol, 2004. **63**(6): p. 748-53.
66. Pachlinger, R., et al., *Metabolically independent and accurately adjustable Aspergillus sp. expression system.* Appl Environ Microbiol, 2005. **71**(2): p. 672-8.

67. Vogt, K., et al., *Doxycycline-regulated gene expression in the opportunistic fungal pathogen Aspergillus fumigatus.* BMC Microbiol, 2005. **5**: p. 1.
68. Shoji, J.-y., et al., *Development of Aspergillus oryzae thiA promoter as a tool for molecular biological studies.* FEMS Microbiology Letters, 2005. **244**(1): p. 41-46.
69. Meyer, V., et al., *Fungal gene expression on demand: an inducible, tunable, and metabolism-independent expression system for Aspergillus niger.* Appl Environ Microbiol, 2011. **77**(9): p. 2975-83.

CHAPTER 2

GENOME-WIDE ANALYSIS OF *FUSARIUM VERTICILLIOIDES* REVEALS THE CONTRIBUTION OF HORIZONTAL GENE TRANSFER TO THE EXPANSION OF METABOLISM AND ADAPTIVE STRATEGIES[1]

[1] Gao, S., et al. To be submitted to PLOS Genetics.

Abstract

Horizontal gene transfer (HGT), the exchange and stable integration of genetic material between different evolutionary lineages, is believed to shape genomes by facilitating the rapid acquisition of adaptive traits. We predict that the economically important fungus *Fusarium verticillioides* is an excellent candidate for investigating the impact of HGT on the expansion of metabolism and adaptive strategies given its soilborne nature and versatile lifestyle as both a symptomless endophyte as well as a maize pathogen. In this study, we performed a genome-wide identification of HGT events using a phylogenomic pipeline followed by manual curation and found strong support for 117 gene acquisitions via HGT, the majority of which were from bacteria. The functional enrichment of these 117 candidates suggested that those HGT events may enhance several biochemical activities, including lysine biosynthesis and nitrogen metabolism. Further, multiple interesting HGT candidates were found to be narrowly distributed within fungi. For example, the orphan gene FVEG_09873, putatively acquired from plant-associated Proteobacteria, was found only in *F. verticillioides* and encodes a diaminopimelate (DAP) epimerase (EC 5.1.1.7), an enzyme involved in the DAP lysine biosynthesis pathway, which is common in bacteria but has not been found in fungi. Moreover, transcriptional profile analysis revealed HGT candidates that were induced only under the challenge of xenobiotics putatively conferring antimicrobial activities and thus may contribute quantitatively to environmental fitness. FVEG_10494, another strong HGT candidate with orthologs in only a few *Fusarium* species, was highly and specifically up-regulated under nitric oxide (NO) challenge. Functional analysis of FVEG_10494 suggests the gene moderately enhances NO-triggered protective responses and modulates the expression of the *F. verticillioides* secondary metabolism gene cluster responsible for the production of fusarin C. Together, our global analysis of HGT

events in *F. verticillioides* identified a core set of transferred genes favoring expansion of metabolic capabilities and enhancement of adaptive strategies.

Introduction

Horizontal gene transfer (HGT), is the exchange and stable integration of genetic material between different evolutionary lineages [1]. HGT is rampant in prokaryotes and contributes to observed breaks in species boundaries, generates new biological diversity, and shapes genomes and populations [1-4]. In eukaryotes HGT is thought to occur at a lower frequency, likely due to the presence of physical barriers to HGT such as the nuclear envelope, multicellularity (thus separate germline and somatic cells), or RNA interference system [5, 6]. With the rapid increase in publicly accessible eukaryotic genomic data, a growing body of evidence suggests HGT is a factor in the evolution of eukaryotic genomes [6-9]. Several mechanisms have been proposed to explain HGT events in eukaryotes. For example, transposable elements may contribute to HGT by moving or copying genetic material from prokaryotic to eukaryotic genomes [10, 11]. In addition, intimate physical contact, such as plant plasmodesmata [12] and fungal anastomosis [13] may promote exchange of genetic materials between different eukaryotes. An interesting recently proposed hypothesis involves lightning-triggered electroporation and electrofusion [14] as additional natural mechanisms facilitating HGT.

Fungi are one of the eukaryotic groups demonstrating abundant cases of HGT events [14]. The postulated benefits brought to fungi by HGT after functional fixation are the expansion of metabolic networks and osmotrophic capacity [6], promotion of pathogenicity [15], enhanced adaptation to the environment [16-18], and gain of secondary metabolic capacity [19-21]. Recent genome-wide identification of HGT candidates in fungi revealed gene candidates associated with

core metabolic pathways (e.g. amino acid, carbohydrate, nucleic acid), osmotrophic capacity and pathogenesis [6, 22-25]. The gold standard of supporting evidence for HGT is phylogenetic analysis with a gene phylogeny contradicting the established species phylogeny [6]. Phylogeny-independent approaches such as the detection of regions showing atypical genomic characteristics and the identification of biogeographical/ecological co-occurrence [26], are recommended to further support phylogenetically identified putative HGT events.

A study in which 60 fully sequenced fungal genomes were examined showed that prokaryotic-derived HGT are especially enriched in the Pezizomycotina, while scarce cases were identified in the Saccharomycotina [27], leading to the hypothesis that this striking difference might result from distinct lifestyles of these two groups. Consistent with this idea, it has been observed that various lifestyles and occupation of multiple niches may favor horizontal gene acquisition [27], which might be the case for *Fusarium* species. Generally speaking, most *Fusarium* species are considered as soilborne facultative plant pathogens, suggesting more diverse lifestyles compared to obligate pathogens. They can cause plant diseases on many horticultural, field, ornamental and forest crops in various ecosystems with varying host specificity among different species [28]. *Fusarium verticillioides* offers a good model for further evaluation of HGT because it is a soilborne phytopathogen of the economically important crop maize [29], and it can also function as a symptomless endophyte of above and below ground maize tissues as well as being nearly universally seed borne in maize kernels [30]. Although previous studies have revealed the increasing evidence of HGT events in several *Fusarium* species [19, 20, 23, 31-33], such as two horizontally transferred xenobiotic-degrading gene clusters by *Fusarium*, a thorough analysis of how HGT has shaped the genome of *F. verticillioides* has not been carried out.

In this study, we conducted a genome-wide analysis to identify candidates of HGT using a phylogenomic pipeline. This pipeline was previously reported to reveal HGT in pathogenic fungi [22, 34]. From an initial output of 1801 genes, manual curations identified 117 strong HGT candidates, the majority of which were acquired from bacteria. Functional analysis of FVEG_10494, a strong HGT candidate with orthologs in only a few *Fusarium* species and specifically highly expressed under nitric oxide challenge, demonstrated the role of HGT events in providing potential adaptive advantages to *F. verticillioides*.

Materials and Methods

Genome-wide identification of HGT candidates

A phylogenomic pipeline followed by manual evaluation was conducted to globally reveal HGT candidates in *F. verticillioides* (Figure 2.1). All predicted proteins from the *F. verticillioides* genome assembly [32] were BLAST queried (e-value = 1, max target seqs = 1000) against a custom database consisting of NCBI's non-redundant protein database (last updated November 24, 2014) as well as additional protein sequences from 411 fungal and plant genome assemblies. A modified alien index (AI) approach was used to screen the *F. verticillioides* genome for genes with significantly better BLAST hits to distantly related organisms (e.g., bacteria) than to more closely related ones (e.g., other fungi) and thus identify HGT candidates. Two taxonomic lineages were then specified: the recipient lineage into which possible HGT events may have occurred (e.g., *Fusarium*, NCBI taxonomy ID 5506), and a larger ancestral lineage of related taxa (group lineage, e.g., Pezizomycotina, NCBI taxonomy ID 147538). The AI score is given by the formula: $AI = \left(\frac{bbhO}{maxB} - \frac{bbhG}{maxB}\right)$, where *bbhO* is the bitscore of the best BLAST hit to a species outside of the ancestral lineage, bbhG is the bitscore of the best BLAST

hit to a species within the ancestral lineage, and *maxB* is the maximum bitscore possible for the query sequence (i.e., the bitscore of the query aligned to itself). When calculating *bbhG* all hits to the recipient lineage were ignored. AI can range from 1 to -1, and an AI > 0 occurs when the protein has a better BLAST hit to a species outside of the ancestral lineage compared to species within. Seven AI runs using different recipient and ancestral lineage combinations were conducted, which allowed us to identify putative HGT events into different ancestral nodes.

Genes with AI ≥ 0.05 were considered as HGT candidates and were subjected to downstream phylogenetic analysis. Specifically, for each HGT candidate, we used a Perl script to extract up to 300 homologs from the custom database (referenced above) based on: a) BLAST similarity (e-value ≤ $1e^{-3}$), b) allowing up to five orders of magnitude difference between query and subject sequence lengths, and c) permitting the inclusion of up to five sequences per species. Furthermore, to reduce the number of sequences per gene tree, highly similar sequences were collapsed with CD-HIT using default parameters [35]. Sequences were aligned with MAFFT using the E- INS-i strategy [36]. The resulting alignment was trimmed with TRIMAL using the automated1 strategy [37]. Phylogenetic trees were constructed using FASTTREE [38] with a WAG+CAT amino acid model of substitution, 1000 resamples, four rounds of minimum-evolution subtree-prune- regraft moves (-spr 4), and the more exhaustive Maximum Likelihood (ML) nearest-neighbor interchange option enabled (-mlacc 2 –slownni). The BLAST-based Alien Index (AI) screen identified 1801 HGT candidate genes.

Phylogenetic trees were then manually inspected to meet the following criteria in order to be considered strong HGT candidates. First, trees must contain at least 20 sequences since misinterpretation of HGT may arise from limited available data and biased sample collection. Second, because the AI score cannot differentiate between HGT donor and recipient, the gene

phylogeny must contradict the established species phylogeny, and the transfer direction should be from distantly related taxa to fungi. Third, to select for candidates with a strong HGT signal, the topology of the gene tree must meet the following three criteria: containing ≤ 3 fungal monophyletic clades; containing ≤ 3 clusters of fungal genes that are partially resolved but nested with genes in distantly related species; and a star tree (multifurcated phylogeny with many short branches connected at the internal node) including ≤ 30 fungal genes along with abundant genes in distantly related species (Supplemental Figure 2.1). Finally, HGT candidates were further narrowed by BLASTp evaluation to ensure the best hit from the donor group with e-value ≤ $1e^{-30}$ and bitscore > 40% of the query sequence. In total, 117 genes were identified as highly promising HGT candidates. Figure 2.2 shows the number of non-overlapping genes identified from each run. Supplemental Table 2.1 (provided in Supplemental File 1) summarizes detailed information for each of the 117 candidates.

Intron content analysis

To further support the bacterial origin of most HGT candidates, an intron content analysis was performed. The frequency of intron occurrence in the whole genome and in the HGT candidate gene sets was determined by the "exon count" search strategy in FungiDB (http://fungidb.org/fungidb/; for instance, to search for intronless genes, rules were set to exon count ≥ 1 and ≤ 1). The Mann–Whitney-Wilcoxon test was performed using SAS 9.4 (SAS Institute Inc., Cary, NC, USA) to test the difference in frequency of introns between the genome and the HGT candidates.

Transcriptome profile analysis

To examine if identified HGT candidates are likely functional in *F. verticillioides* and explore responsive conditions, the transcriptional profiles of all candidates were checked against

10 expression datasets. These included two RNA sequencing (RNA-seq) datasets extracted from NCBI GEO database (GEO accession numbers: GSE61865 and GSE66044) and an additional eight RNA-seq datasets including seven that are unpublished by us plus one dataset generated in this study, referred to below as NO RNA-seq. Candidates were considered as expressed genes if they had at least one FPKM (Fragments Per Kilobase of exon per Million fragments mapped) or RPKM (Reads Per Kilobase of exon per Million fragments mapped) value that is above two under normal conditions (e.g. wild type in PDB after three days growth) or at least one absolute value of fold change (log 2) greater than 1.5 (p-value < 0.05) under test conditions (e.g. 1.5 mM nitric oxide treatment) compared to the untreated control.

To compare the expression levels of HGT candidates to those of the whole transcriptome, RNA-seq data of the untreated controls were extracted from the GSE66044 and the NO RNA-seq datasets. For each gene in the two samples (HGT candidates and the full transcriptome), corresponding expression values were averaged over all biological replicates. Genes were sorted and collated based on expression levels.

Functional annotation

To reveal the putative function of each of the 117 genes identified as strong HGT candidates, NCBI Conserved Domains (CD) database was employed for putative annotation. For identifying enriched pathways represented among the HGT candidates compared to the frequency of such genes within the whole *F. verticillioides* genome, the MIPS Functional Catalogue (http://mips.helmholtz-muenchen.de/funcatDB/) was used with p-value < 0.05. To search for genes in *F. verticillioides* associated with lysine biosynthesis, genes in *F. graminearum* that were mapped to this pathway in the KEGG PATHWAY Database (http://www.genome.jp/kegg/pathway.html) were extracted and searched for corresponding

orthologs in *F. verticillioides* using FungiDB. The candidates assigned to sub-categories of interest (e.g. nitrogen metabolism, biosynthesis of lysine) were extracted and further characterized. The prediction of the subcellular location of encoded proteins was revealed by the TargetP 1.1 Server (http://www.cbs.dtu.dk/services/TargetP/) and further verified by the TMHMM Server v 2.0 (http://www.cbs.dtu.dk/services/TMHMM/). Two web-based tools, SMURF [39] and antiSMASH [40], were applied to detect the involvement of HGT candidates in secondary metabolism gene clusters. Peroxisomal Targeting Signal 1 prediction was performed using the PTS1 predictor (http://mendel.imp.ac.at/pts1/). To test the potential of FVEG_09873 being a diaminopimelate epimerase, protein sequences and key sites of one reference (WP_001160654 in *Escherichia coli*) and five of the top BLASTp hits in bacteria (WP_017338124 in *Pseudomonas fluorescens* NCIMB 11764, WP_007629306 in *Rhizobium sp.* CCGE 510, WP_059731579 in *Burkholderia cepacia*, WP_059973916 in *B. pyrrocinia*, WP_060148831 in *B. stagnalis*) were extracted from Uniprot (http://www.uniprot.org/). These protein sequences including that of FVEG_09873 were subjected to multiple sequence alignment using Clustal Omega (http://www.ebi.ac.uk/Tools/msa/clustalo/).

Phylogenetic Analyses

Phylogenetic analyses were performed on HGT candidates whose orthologs distribute narrowly in fungi. Protein sequences of the query and corresponding homologs were extracted and aligned using MUSCLE, conducted through Geneious v.8.1.9 (Biomatters Ltd., Auckland, New Zealand). Best-fit maximum likelihood substitution model of each alignment was determined using MEGA v.6.06 [41]. Phylogenies were reconstructed by Maximum Likelihood (ML) and Bayesian Inference (BI) using the best-fit model in the plugin version of PhyML [42] and MrBayes 3.2.6 [43] in Geneious, respectively. The implementation of PhyML was analyzed

with 100 replications of bootstrap branch support. MrBayes was run with the following parameters: 1,100,000 cycles with 4 heated chains, 0.2 heated chain temp, 200 subsampling frequency, 100,000 burn-in length, and 5502 random seed. The two trees were compared manually for consistency.

Fungal and bacterial strains, culture media and growth conditions

Wild-type *F. verticillioides* FRC M-3125 (also known as 7300, the sequenced reference strain) was used for genetic and functional characterization. Strains of *F. verticillioides* were grown routinely on potato dextrose agar (PDA; Neogen Food Safety, Lansing, MI, USA) at 27 °C in the dark or in potato dextrose broth (PDB; Neogen Food Safety) on the shaker incubator at 250 rpm and 27 °C in the dark for three days. For screening for modified strains, PDA was amended with 300 μg/ml geneticin (Life Technologies, Carlsbad, CA, USA) or 150 μg/ml hygromycin B (Invitrogen, Carlsbad, CA, USA). Minimal medium was made according to the *Fusarium* Laboratory Manual (in 1 L: potassium phosphate monobasic, 1 g; magnesium sulfate heptahydrate, 0.5 g; potassium chloride, 0.5 g; trace element solution, 0.2 ml; sucrose, 30 g, bacto agar, 20 g) [44] but without sodium nitrate as nitrogen source. Various nitrogen sources were assessed (see below).

For FVEG_10494 gene deletion plasmid maintenance, *Escherichia coli* (One Shot® MAX Efficiency® DH5α™-T1R, Invitrogen) was grown in or on Luria Bertani (LB) medium amended with 100 μg/ml spectinomycin (Thermo Fisher Scientific, Waltham, MA, USA) at 37 °C in the dark overnight. *Agrobacerium tumefaciens* strain AGL-1 was used for fungal transformation and cultured on LB agar amended with 100 μg/ml spectinomycin at 27 °C in the dark.

Construction of gene deletion mutants and complemented strains

To functionally characterize FVEG_10494, gene deletion mutants as well as complemented strains were created as follows. Deletion plasmid pSG10494_OSCAR was generated for FVEG_10494 using the OSCAR method [45]. Supplemental Table 2.7 and Supplemental Table 2.8 (provided in Supplemental File 2) summarize strains and primers used in this study, respectively. Two pairs of primers were designed to amplify about 1 kb of the 5' (primers P7\25 and P7\26) and 3' flanks (primers P7\27 and P7\28) to the gene's open reading frame (ORF). The deletion construct contains the two flanks surrounding a hygromycin resistance cassette. The ORF of FVEG_10494 was deleted in strain M-3125 via *Agrobacerium*-mediated transformation [46]. Hygromycin-resistant transformants were initially screened by PCR using primers P7\29 and P7\30 for the presence or absence of the FVEG_10494 ORF and using amplification of the Hyg marker gene with primers P1\14 and P1\15 as a positive control. Transformants of interest underwent single-spore purification and were finally screened by PCR for genotype using six pairs of primers (Supplemental Table 2.8, provided in Supplemental File 2): primer pair P1\14 and P1\15 for presence of hygromycin resistance cassette, the primer pair P7\29 and P7\30 for the loss of the FVEG_10494 ORF, the primer pair P7\25 and P1\4 (a primer within the hygromycin resistance cassette) for the presence of 5' flank, the primer pair P7\31 (a primer within the upstream sequence of the 5' flank of FVEG_10494) and P1\4 for confirmation of homologous recombination of the 5' flank, the primer pair P1\3 (a primer within the hygromycin resistance cassette) and P7\28 for the presence of 3' flank, the primer pair P1\3 and P7\32 (a primer within the downstream sequence of the 3' flank of FVEG_10494) for confirmation of homologous recombination of the 3' flank. Deletion strains Δ10494-6.1 and

Δ10494-6.4 (Supplemental Table 2.7, provided in Supplemental File 2) were confirmed by Southern hybridization as noted below.

Complemented strains were constructed via lithium acetate-mediated cotransformation [47]. The wild-type FVEG_10494 amplicon (total length 5059 bp) was generated with primers P7\33 and P7\34 (Supplemental Table 2.8, provided in Supplemental File 2) to include the ORF (2841 bp) and both upstream (911 bp) of the predicted start codon and downstream (1307 bp) of the stop codon. The mixture of the wild-type amplicon and the enzyme digested selection vector pGEN-NOT1 (1 μg) was cotransformed into the competent cells of the deletion strain Δ10494-6.4. Transformants were screened on 300 μg/ml geneticin and 150 μg/ml hygromycin B and further confirmed by PCR with primer pairs P7\29 and P7\30 and P1\37 and P1\38 (Supplemental Table 2.8, provided in Supplemental File 2) for the presence of the FVEG_10494 ORF and the geneticin cassette, respectively.

Southern hybridization

To confirm the loss of the target gene, Southern hybridization was conducted as follows. Total genomic DNA of *F. verticillioides* wild type and transformants was extracted from 4-day-old PDB liquid cultures using the DNeasy Plant Mini Kit (Qiagen Inc., Valencia, CA) following the manufacturer's protocol and then digested with the restriction enzyme *Kpn*I (New England Biolabs, Ipswich, MA, USA). Probes that hybridize to the coding sequence of FVEG_10494 (using primers P7\29 and P7\30) and hygromycin cassette (using primers P1\14 and P1\15), respectively, were amplified using the PCR DIG Probe Synthesis Kit (Roche Diagnostics, Indianapolis, IN, USA). A total of 1.5 μg digested genomic DNA was separated on a 0.8% agarose 0.5X Tris-Borate-EDTA gel and blotted onto a Hybond-N+ nylon membrane (Amersham Biosciences, Buckinghamshire, England). The first round of hybridization was

performed using the FVEG_10494 probe following the DIG application manual (Roche Diagnostics). The probe-target hybrids were detected by chemiluminescent assay and visualized by the Alpha Innotech FluorChem 8000 digital imaging system with a 40-min exposure (Supplemental Figure 2.5.a). The ORF probe was stripped with alkaline buffer and the membrane was reprobed with the hygromycin cassette probe. The probe-target hybrids were detected as described above (Supplemental Figure 2.5.b).

Chemical screening

Since FVEG_10494 contains the type II homoserine kinase (involved in threonine metabolism) and the 4-aminobutyrate aminotransferase (involved in the γ-aminobutyric acid (GABA) metabolism), a chemical screening assay containing compounds associated with either threonine or GABA metabolism was conducted. Strains including M-3125, Δ10494-6.4 and Δ10494-6.4::C3.1 were grown in PDB for three days. The spores were harvested and washed twice with sterile deionized water, followed by dilution to 10^6 per ml. Agar-based nitrogen-limited minimal medium was supplemented with selected compounds, autoclaved and then aliquoted to 6-well culture plates (Corning, NY, USA). The tested compounds (Sigma-Aldrich Chemical Co., Milwaukee, WI, USA) included L-glutamic acid (0.5 mg/ml), GABA (0.5 mg/ml), pyruvic acid (1 mg/ml), L-alanine (0.5 mg/ml), glycine (0.5 mg/ml), succinate (0.5 mg/ml), pyridoxine (10 μg/ml), L-aspartic acid (0.45 mg/ml), L-threonine (0.5 mg/ml), and L-methionine (0.5 mg/ml). Ten μl of a 10^6/ml spore suspension were inoculated at the center of each well and replicated twice for each strain. The plates were parafilm sealed and incubated at 27 °C in the dark.

RNA extraction and qRT-PCR analysis

Transcriptional analysis was used to test the response of FVEG_10494 to nitric oxide (NO). Strains were inoculated into PDB buffered with 0.1 M sodium phosphate and cultured for three days. One ml of culture was transferred to lysing matrix S tubes (MP Biomedicals, LLC, Santa Ana, CA, USA) and then centrifuged at 10,000 x g for 5 min at 4 °C and the supernatant discarded. Lysis buffer (PureLink® RNA Mini Kit, Thermo Fisher Scientific) was immediately added to the fungal pellets and the samples were homogenized using the FastPrep-24™ 5G Instrument (MP Biomedicals) at a speed of 6 m/sec and two segments of homogenization for 30 seconds with 1 min rest in between. The total RNA was extracted following the manufacturer's instructions (PureLink® RNA Mini Kit, Thermo Fisher Scientific). NO treated samples were also cultured in PDB buffered with 0.1 M sodium phosphate for three days followed by 30 min exposure to 1.5 mM diethylenetriamine (DETA) NONOate (Cayman chemical, Ann Arbor, MI, USA) dissolved in 0.01 M NaOH, and the samples were then harvested for RNA extraction as stated above. Three biological replicates were included for each treatment.

For quantitative reverse transcription-PCR (qRT-PCR), RNA samples isolated above were DNase treated (TURBO DNA-free™ Kit, Thermo Fisher Scientific) and checked for quality (RNA integrity number > 6.0) using an Agilent 2100 Bioanalyzer (Agilent Technology, Waldbronn, Germany). Complementary DNA synthesis and qRT-PCR were carried out using a one-step qRT-PCR Kit (SuperScript® III Platinum® SYBR® Green One-Step qRT-PCR Kit, Thermo Fisher Scientific) in triplicate. The data were normalized to the expression level of β-tubulin and calculated via the $2^{-\Delta\Delta CT}$ method [48]. The primers used for this assay are shown in Supplemental Table 2.8 (provided in Supplemental File 2).

RNA sequencing and analysis

Total fungal RNA was isolated and checked for quality as stated above. Twelve libraries (wild type and single mutant Δ10494-6.4 treated with and without 1.5 mM DETA NONOate for 30 min, with three biological replicates each) were prepared and sequenced on an Illumina NextSeq (75 Cycles) High Output Flow Cell (paired end, 75 bp read length) by the Georgia Genomics Facility. Raw RNAseq reads were subject to quality control by fastqc (http://www.bioinformatics.babraham.ac.uk/projects/fastqc/) and then removal of low quality reads (Phred score <20) and Illumina sequencing adapters using Trimmomatic 0.25 [49]. Mapping of the paired-end, filtered reads against *F. verticillioides* 7600 genome [32] (Fusarium verticillioides_7600_3_supercontig, www.fungidb.org) was performed using the align function in the Rsubread package [50] in Bioconductor (www.bioconductor.org). Read counting, normalization and expression level (FPKM) calculations were executed using the featurecount function in Rsubread using the default settings. Differential gene expression analysis was then performed using edgeR [51] and DESeq [52] packages, by applying a false discovery rate threshold of 0.05. The absolute value of log2 fold change threshold was set to 1 to screen for differentially expressed genes (DEGs). The annotations were predicted by the Pedant-Pro (http://pedant.helmholtz-muenchen.de/pedant3htmlview/pedant3view?Method=analysis&Db=p3_p15553_Fus_verti_v31) and the NCBI conserved domains database.

Results

Identification of HGT candidates

The BLAST-based Alien Index (AI) screen initially identified 1801 HGT candidate genes. Subsequent manual inspection using additional criteria reduced the candidates to 117 genes that we consider our strongest representatives for HGT (Supplemental Table 2.1, provided in Supplemental File 1). In most cases, the orthologs of the candidate gene are exclusively distributed within the recipient taxon of fungi. The characterization of putative donors suggests that 115/117 genes were acquired from bacteria. For the other two genes, FVEG_10562 was putatively acquired from oomycetes (phylum Oomycota) to the last common ancestor of Ascomycota, and FVEG_00090 was putatively acquired from green algae (division Chlorophyta) to the last common ancestor of Dikarya.

Given the frequency of bacterial origin of these HGT candidates, we hypothesized they should have fewer introns than the overall *F. verticillioides* genome. In fact, 75% of the identified candidates lacked introns, which is significantly higher compared to the 26% intronless genes in the whole genome (Mann–Whitney-Wilcoxon test, $Z = -2.0499$, $p = 0.0202$, Supplemental Table 2.2, provided in Supplemental File 2). Intriguingly, the genomic distribution shows an enrichment of HGT candidates on chromosome 11, which is the smallest of the 11 mapped *F. verticillioides* chromosomes [32] (Supplemental Figure 2.2). TargetP subcellular location prediction of gene products revealed 6 secreted and 1 mitochondrial-targeted protein (Supplemental Table 2.3, provided in Supplemental File 2). SMURF and anti-SMASH predictions both suggested there are five HGT candidates that are each localized within a putative secondary metabolism gene cluster (Supplemental Table 2.4, provided in Supplemental File 2).

Transcriptome profiling analysis

To test whether these HGT candidates are expressed in *F. verticillioides*, a series of RNA-seq datasets from various physiological and xenobiotic-challenged conditions were screened (Supplemental Table 2.5, provided in Supplemental File 2). Firstly, comparison of the transcriptional levels in untreated controls using two RNA-seq datasets (GSE66044 and the NO RNA-seq) conducted under corresponding optimal conditions (Figure 2.3) showed a similar trend: higher frequency of relatively low-expressed genes (FPKM or RPKM $\leq$ 12) and consistently lower frequency of relatively high-expressed genes. The near identical trend across two independent RNA-seq experiments suggests the identified HGT candidates have a proclivity for low expression levels compared to the whole genome. Secondly, 95 out of 117 HGT candidates were expressed under at least one condition examined (Supplemental Table 2.5, provided in Supplemental File 2), suggesting their potential utility, though perhaps under specific conditions. One-third of the candidates were moderately differentially expressed when exposed to physiological or xenobiotic stresses (Supplemental Table 2.5, provided in Supplemental File 2) among which certain genes (FVEG_09841, FVEG_10494, FVEG_12273, and FVEG_12509) were undetected under non-stressed situations.

HGT candidates are enriched in several amino acid and nitrogen/sulfur metabolic pathways

To gain insight into the functional categories that the horizontally transferred genes are likely involved in, we firstly used the MIPS Functional Catalogue website and identified 62 out of 117 genes involved in the following enriched main functional categories: metabolism, energy, complex cofactor/cosubstrate/vitamin binding, detoxification by degradation, systemic interaction with environment, and biosynthesis of cellular components (Figure 2.4). The

remaining 55 genes not assigned to an enriched category are not discussed further in this section. All 62 candidates are predicted to be involved in Metabolism and 22 of these genes are involved in additional functional categories. Figure 2.4 (lower table) illustrates the distribution of gene candidates in the enriched sub-categories of Metabolism and the degree of their enrichment compared to the genome wide frequency of this category of genes within the *F. verticillioides* genome (numbers in parentheses). Nucleotide metabolism was the most enriched among all subcategories with only two gene candidates. Although carbohydrate metabolism and secondary metabolism contained 38 and 12 candidates, respectively, the degree of fold enrichment compared to the whole genome is only 2.6 and 2.0. Therefore, those enriched subcategories (Supplemental Table 2.6, provided in Supplemental File 2) containing at least 5 genes with fold enrichment of at least 10 within amino acid metabolism (lysine and glycine), nitrogen metabolism, and sulfur metabolism were selected for further characterization. See Table 2.1-2.4 for more details on these genes.

Two distinct pathways are responsible for lysine synthesis in nature: the diaminopimelate (DAP) pathway and the α-aminoadipate (AAA) pathway [53]. While the DAP pathway is commonly found in bacteria and plants, the AAA pathway is almost exclusively limited to higher fungi [54, 55]. To better understand genes that may contribute to lysine biosynthesis in *F. verticillioides*, genes assigned to the biosynthesis of lysine in *F. graminearum* were extracted from the KEGG PATHWAY Database and corresponding *F. verticillioides* orthologs identified using FungiDB (Figure 2.5). Presence of genes required in each step of the fungal-dominant AAA pathway (Figure 2.5, blocks highlighted in green in AAA pathway) suggests the successful exploitation of this pathway for lysine biosynthesis in *F. verticillioides*. Although the DAP pathway is incomplete, three HGT candidates (Figure 2.5, blocks highlighted in yellow and red

in DAP pathway) were associated with this pathway based on EC number and functional annotations (Table 2.1). Two genes, FVEG_00154 (transcriptome analysis did not suggest its expression) and FVEG_05936 (transcribed in tested RNA-seq datasets), both putatively encode dihydrodipicolinate synthase (EC 4.3.3.7). The third gene FVEG_09873 (transcriptome analysis did not suggest its expression) encodes a DAP epimerase (EC 5.1.1.7), catalyzing the stereoinversion of L, L-DAP to D, L-meso-DAP, a precursor to L-lysine in the DAP pathway and peptidoglycan in bacteria [56]. Lastly, in relation to amino acid biosynthesis, five HGT candidates falling into the subcategory metabolism of glycine are summarized in Table 2.2.

Filamentous fungi are capable of metabolizing many nitrogen and sulfur sources, therefore making them resilient colonizers and survivors [57]. The seven HGT candidates (Table 2.3) that are involved in the metabolism of nitrogen may thus confer advantages to *F. verticillioides*. For example, FVEG_00065 and FVEG_01752 are each annotated as a nitrilase, which are enzymes catalyzing the hydrolysis of nitrile compounds to the corresponding carboxylic acid and ammonia and have been implicated in nitrile detoxification and nutrient assimilation in microbes [58]. Sulfur is a critical element for all organisms, including fungi, and soil microbes can convert soil sulfur (mostly present as the sulfate esters) to plant-available inorganic sulfate [59]. The five HGT candidates (Table 2.4) related to sulfur metabolism were annotated as four sulfatases, catalyzing the hydrolysis of sulfate esters, and a sulfotransferase, catalyzing the transfer of a sulfo group from a donor to an acceptor. These genes may play important roles in the synthesis/degradation of sulfate esters in *F. verticillioides* and in sulfur cycling in the environment.

Examination of HGT candidates whose orthologs distribute narrowly in the fungi

Horizontal gene transfer candidates for which orthologs are narrowly distributed within the subphylum Pezizomycotina (Table 2.5) are interesting because they are likely more recently transferred genes. One gene, FVEG_09873, encoding a putative DAP epimerase noted above, amongst the fungi exists solely in *F. verticillioides*. In addition, 5 genes (FVEG_00065, FVEG_10494, FVEG_04320, FVEG_07753 and FVEG_03450) have orthologs only in *Fusarium* species. Another 5 genes (FVEG_11809, FVEG_14084, FVEG_11906, FVEG_06279, FVEG_12509), have orthologs limited within the Pezizomycotina. Phylogenies for the 11 encoded proteins are shown in Figure 2.6 and Supplemental Figure 2.3. All these genes, except for FVEG_09873, are expressed under at least one condition based on the analysis of selected transcriptome datasets (Supplemental Table 2.5, provided in Supplemental File 2).

As mentioned above, encoding a putative DAP epimerase, FVEG_09873 appears only in *F. verticillioides* and has no orthologs in other fungi. Phylogenetic analysis suggests that FVEG_09873 is related to numerous genes derived from Proteobacterial species (Figure 2.6.a), including plant-associated *Rhizobium* species as well as bacteria in the *Burkholderia cepacia* complex whose members demonstrate a widespread distribution in nature and exceptional metabolic versatility [60]. A multiple sequence alignment analysis using protein sequences of one bacterial reference and five top blastp hits in bacteria to FVEG_09873 showed that most of the key sites (e.g. binding site, active site) are conserved (Supplemental Figure 2.4), suggesting FVEG_09873 might still function as a DAP epimerase, despite the lack of expression data.

FVEG_00065 putatively encodes a nitrilase and has orthologs only in *F. fujikuroi* (90% amino acid identity) while having numerous orthologs in bacteria (highest protein identity 59%).

Phylogenetic inference (Supplemental Figure 2.3.a) further supports a transfer event from bacteria. Also having orthologs limited to *Fusarium*, FVEG_03450, FVEG_04320, and FVEG_07753 are all putative hydrolases (Table 2.5) showing strong posterior probability support for their derivation from soil bacteria (Supplemental Figure 2.3.b-d) based on Bayesian analysis.

FVEG_10494, along with its orthologs in the other cereal-infecting *Fusarium* pathogens, contains three conserved domains, namely a type II homoserine kinase, a domain of unknown function (DUF3549), and a 4-aminobutyrate aminotransferase. Its ortholog in *F. pseudograminearum* has been reported as a horizontally acquired gene [23]. Phylogenetic analysis shows FVEG_10494 falls within (Figure 2.6.b) a clade exclusive to cereal-infecting *Fusarium* species nested within *Microbacterium* and other bacterial species. In addition, the GC content of FVEG_10494 (Figure 2.7.a) is distinct compared to its neighboring genes in the *F. verticillioides* genome. Moreover, FVEG_10494 is 76% identical at the amino acid level to the best bacterial protein hit, which is from a bacterial endophyte of corn and sorghum, *M. testaceum* [61]. The reciprocal pBLAST indicates the homologous proteins in *Fusarium* are also the most similar outside *Microbacterium* species. The above evidence strongly suggests a recent horizontal transfer event between *Microbacterium* and *Fusarium,* which may have been facilitated by their similar niche and intimate contact. We chose to particularly focus on functional characterization of FVEG_10494 because of its potential involvement in a predicted secondary metabolism gene cluster (Supplemental Table 2.4, provided in Supplemental File 2) and its previously observed dramatic induction under NO exposure (Figure 2.7.b). More details are presented below.

Among genes whose fungal orthologs are limited to the Hypocreales, FVEG_11809 (predicted to be secreted, Supplemental Table 2.3, provided in Supplemental File 2) and FVEG_14084 putatively encode proteins belonging to the FAD dependent oxidoreductase family (Table 2.5) and share 55 % amino acid sequence identity to each other. In addition, FVEG_11906 and FVEG_06279 encode an epimerase and putatively secreted acetyl esterase/lipase (Supplemental Table 2.3, provided in Supplemental File 2), respectively. FVEG_12509 encodes a salicylaldehyde dehydrogenase and has orthologs limited to an additional three fungal genera beyond *Fusarium* (Supplemental Figure 2.3.h) while grouped with many sequences in Proteobacteria. Intriguingly, this gene contains six introns (bacterial orthologs are intronless) and was suggested to be within a putative secondary metabolism gene cluster (Supplemental Table 2.4, provided in Supplemental File 2). Moreover, FVEG_12509 was induced with exposure to several xenobiotics (Supplemental Table 2.5, provided in Supplemental File 2), including pyrrocidine A, pyrrocidine B, 2-benzoxazolinone, chlorzoxazone, and 2-oxindole, whereas it was barely expressed under control condition (grown in PDB).

Functional characterization of FVEG_10494

Given the limited information on FVEG_10494 and its orthologs, we decided to approach its characterization in two ways: 1) screening mutants on chemical compounds based on the predicted annotation and potentially involved pathways; 2) identifying genes interacting with/influenced by FVEG_10494 via transcriptional analyses.

1. Chemical screening suggests FVEG_10494 may not be related to annotated functions

As already noted, FVEG_10494 encoded protein contains the three conserved domains of a type II homoserine kinase, a domain of unknown function (DUF3549), and a 4-aminobutyrate aminotransferase. Homoserine kinase catalyzes the ATP-dependent phosphorylation of L-

homoserine to L-homoserine phosphate and is important in the biosynthesis of threonine [62]. The enzyme 4-aminobutyrate aminotransferase (also known as GABA transaminase, GABA-T) deaminates GABA, a four-carbon, non-protein amino acid, to succinate semialdehyde. Previous studies indicate that loss of the GABA-T(s) dramatically weaken the ability of the mutants to utilize GABA as the sole nitrogen source [63-65]. To test if FVEG_10494 is actually associated with the above pathways, wild-type strain M-3125, single mutant strain Δ10494-6.4 and complemented strain Δ10494-6.4::C3.1 were grown on nitrogen-limited minimal media amended with selected compounds involved in GABA and threonine metabolism [62, 66] as the sole nitrogen source. We did not observe clear differences among strains grown on any of these compounds (Supplemental Figure 2.6), which suggests that FVEG_10494 may not play a large role in the threonine and GABA pathways or that it is redundant with existing gene(s) under the conditions tested.

2. FVEG_10494 is highly induced under nitric oxide (NO) exposure

A previous unpublished transcriptional study conducted by our group indicated FVEG_10494 as one the most up-regulated genes when *F. verticillioides* was challenged with 1.5 mM DETA NONOate, a NO donor. To validate this observation, qRT-PCR was performed on 3-day-old PDB cultured cells of wild type treated with or without 1.5 mM DETA NONOate. Relative expression analysis suggests that FVEG_10494 in PDB liquid culture was barely transcribed (averaged Ct = 30) but was dramatically increased over 900-fold in samples exposed for 30 min to 1.5 mM DETA NONOate (Figure 2.7.b). The relatively high induction of FVEG_10494 in response to NO indicated a potential role in nitrosative stress.

3. FVEG_10494 impacts expression of the fusarin C biosynthetic gene cluster and strengthens NO-responsive detoxification

To access how FVEG_10494 affects *F. verticillioides* under nitrosative stress, we conducted RNA-seq analysis on wild-type strain M-3125 and the gene deletion mutant Δ10494-6.4 treated with and without 1.5 mM DETA NONOate. A summary of RNA-seq results is shown in Table 2.6. FVEG_10494 was the most up-regulated gene under NO stress in wild type, which is consistent with both the previous transcriptional study and the qRT-PCR analysis described above. Moreover, there were no differentially expressed genes (DEGs) except for FVEG_10494 itself between PDB-grown untreated wild type and the deletion mutant. This was expected since FVEG_10494 is barely expressed in PDB. The transcriptional comparison between the two strains challenged with NO identified 13 upregulated and 16 downregulated genes (including FVEG_10494) in the deletion mutant (Table 2.6; Table 2.7). The absolute value of log2 fold change of all 28 DEGs (removing FVEG_10494) in the NO-exposed deletion mutant when compared to NO-exposed wild type, was mostly below 2 (Table 2.7). The moderate transcriptional change indicates that FVEG_10494, when expressed even at a high level, only moderately impacts the expression of a small number of genes in *F. verticillioides*.

Among the 13 up-regulated genes in the challenged deletion mutant, seven (FVEG_08732, FVEG_09672, FVEG_09673, FVEG_10117, FVEG_10576, FVEG_15200, FVEG_16635) have no annotation or conserved domains and include four small proteins between 100 to 250 amino acids. Five of the up-regulated genes (Table 2.7; FVEG_11078, FVEG_11079, FVEG_11080, FVEG_11085 and FVEG_11086) belong to a secondary metabolite biosynthetic gene cluster for production of fusarin C mycotoxin [67]. This indicates

that FVEG_10494 may play a role in the suppression of the fusarin C biosynthetic gene cluster resulting from NO exposure.

Except for five poorly annotated genes (FVEG_08792, FVEG_09142, FVEG_12249, FVEG_13989, FVEG_15302), those downregulated in the NO-challenged deletion mutant take part in either cellular transportation or nitrosative/oxidative stress based on predicted annotations (Table 2.7). Functional enrichment analysis also suggests that genes related to cellular transportation and detoxification appear more frequently than those in the overall genome (Supplemental Table 2.9, provided in Supplemental File 2). Figure 2.8 shows that for 9 out of 10 downregulated genes in Table 2.7, the absence of FVEG_10494 dampened induction of the genes in the NO challenged mutant compared to the unchallenged mutant. The decreased induction was evident when comparing responses of the genes in wild type when challenged or unchallenged with NO. Overall the data suggest that FVEG_10494 may moderately enhance the efficiency of NO-triggered responses in *F. verticillioides* and thus help the fungus to better overcome such environmental stresses.

Discussion

As a soilborne fungus demonstrating versatile roles in the ecosystem, including as a phytopathogen and a symptomless endophyte of above and below ground plant parts as well as seeds, *F. verticillioides* likely has ample opportunity to develop intimate contact with its host and with other microbes. This diversity of interactions may elevate its susceptibility as a recipient of alien genetic materials. In this study, we implemented an automatic phylogenomic pipeline followed by manual inspection to reveal 117 strong HGT candidates. With our pipeline screening, we performed seven different combinations of recipient and donor scenarios to infer

not only recent transfers (e.g. from bacteria to *Fusarium*) but also more ancient transfers (e.g. from bacteria to Ascomycota). The performance of a series of *in silico* analyses on the 117 candidates, which were putatively acquired independently through the evolution of fungi, allowed us to more confidently reveal shared or enriched features compared to general genome attributes. For instance, the preference of these candidates having a small number of introns is consistent with the intronless attribute of most bacterial genes, and thus supports their bacterial origin.

The semi-automatic phylogenomic pipeline developed here can dramatically accelerate the genome-wide identification of HGT both in speed and quantity. What's more, this pipeline features high flexibility, allowing the users to freely define donor and recipient groups for revealing HGT events of interest and set the threshold of AI score according to the interested number of HGT candidates. Utilizing this pipeline, researchers can explore a full-scale identification of HGT events in one genome via conducting multiple rounds of analyses and combining compatible results. In addition, the application of this pipeline on several evolutionarily related species or species sharing similar niches/hosts can facilitate the study of how HGT shapes genomes and populations. On the other hand, refined small-scale searches, for instance, fungal-to-fungal HGT events, can be quickly done by corresponding assignments of donor and recipient lineages. In this study, we were especially interested in HGT candidates in *F. verticillioides* that were acquired from distant species, such as bacteria, therefore, among six runs out of seven, we defined the donor group being organisms outside of Opisthokont. As a future follow up to this study, we could focus on genes in *F. verticillioides* acquired from other relatively distant fungal lineages, especially those that may be associated with virulence, adaption and secondary metabolite gene clusters. In fact, numerous reports have shown fungal-

to-fungal HGT events conferring potential advantageous traits brought into fungi. For example, the entire pathway consisting of 23 genes for the production of sterigmatocystin (ST), was horizontally transferred from *Aspergillus nidulans* to *Podospora anserine* [21]. Another compelling example is the horizontal transfer of the toxin-encoding gene *ToxA* from the wheat pathogen *Stagonospora nodorum* in the 1940s to another pathogenic fungus, *Pyrenophora tritici-repentis* [68]. In addition, a recent study by our group suggests that two xenobiotic-degrading gene clusters, *FDB1* and *FDB2*, in *F. verticillioides* were horizontally transferred to other fungi independently [19]. Moreover, we could also identify HGT events from distant organisms into other members of the genus *Fusarium* or their ancestors by incorporating additional *Fusarium* genomes, such as *F. graminearum* and *F. oxysporum*.

Based on current case studies of HGT, genes acquired across kingdoms by fungi are largely single genes [69]. In our study, only five HGT candidates out of 117 are putatively localized within secondary metabolite gene clusters as indicated by both SMURF and anti-SMASH. In addition, there are only two pairs of physically neighboring genes, FVEG_09872/ FVEG_09873 and FVEG_14026/FVEG_14027, while orthologs of both of these two neighboring genes demonstrate differential distributions in donor and recipient groups (data not shown) to each other, thus suggesting independent HGT events. In contrast to preferred single genes in cross-kingdom transfer events, intra-kingdom HGT events of whole gene clusters are proposed in fungi [20, 21], partly resulting from a friendlier genomic environment and the use of similar regulatory machineries. Actually, clustering of genes encoding linked metabolic functions has been indicated to be both an evolutionary consequence and driving force of HGT in fungal genomes [70]. Walton proposed the selfish cluster theory, which is analogous to the selfish operon theory [71] that clustering genes confers selective advantage to the cluster itself

because it allows HGT of a network of functionally linked genes in a single step. In return, selection would result in clustering because of the improved chance of co-transfer, leading to the selection for maintenance of the cluster.

The lateral gene transfer and eventually fixation in the recipient's genome is a multi-step process [72], including, 1) the transfer of genes with the genome features typical of the donor lineage, 2) the maintenance and replication of transferred genes, 3) the spread within the population of the recipient, and 4) the amelioration to the genome of the recipient lineage. It is reasonable to assume that the distance between donor and recipient can impact the degree of transferred sequence modification. In the case of prokaryote-to-eukaryote transfer, adjustments of genomic features, including gene promoters, intron-splicing systems [7], or GC content and codon usage, need to be modified to optimize function in the recipient genome (amelioration). This may lead to lower sequence identity of the eukaryote query to the prokaryotic homologs than that in the prokaryote-to-prokaryote HGT (e.g. in our study, the amino acid similarities of the relatively recent transferred candidates to the best bacterial blastp hit are up to 77%).

It is predicted that for retention, the acquired genes should function in the new lineage and preferably contribute advantages to the recipient. Although our analysis indicated 95 of the HGT candidates were expressed under at least one tested condition, these genes had relatively low expression levels compared to the full gene set under optimal conditions based on two independent RNA-seq experiments. Moreover, HGT candidates were identified that are dormant under control conditions but induced moderately or even dramatically upon exposure to various stressed conditions. These observations lead to the hypothesis that some horizontally acquired genes may only be beneficial under challenging environmental conditions and contribute quantitatively to the overall fitness. One example is FVEG_12509, which was only induced with

exposure to several xenobiotics (Supplemental Table 2.5, provided in Supplemental File 2) but was barely expressed under control condition (grown in PDB). Putatively acquired from Proteobacteria, and positioned within a *F. verticillioides* secondary metabolism gene cluster, this gene may confer an adaptive advantage under specific environmental stress. Another example is FVEG_10494, which is the most responsive gene when wild type is treated with NO, but can only moderately enhance the efficiency of the NO-triggered responses in *F. verticillioides* as suggested by the narrow range of genes with affected expression in the NO RNA-seq experiment conducted in this study. In addition, although FVEG_10494 is well annotated, neither bioassays nor RNA-seq studies suggest functions related to type II homoserine kinase or 4-aminobutyrate aminotransferase.

The NO RNA-seq study revealed a small number of DEGs in the mutant when exposed to NO challenge. Five of the up-regulated genes (Table 2.7; FVEG_11078, FVEG_11079, FVEG_11080, FVEG_11085 and FVEG_11086), belonging to the fusarin C biosynthetic gene cluster, appear to be slightly down-regulated in wild type when exposed to NO (data not shown), while they were up-regulated slightly in the NO-treated deletion mutant. A previous study suggested that orthologs in *F. fujikuroi* of FVEG_11078, FVEG_11079, FVEG_11085 and FVEG_11086 are sufficient for the production of fusarin C [73]. In terms of those down-regulated genes in the NO-challenged deletion mutant, predicted annotations suggest their preference in cellular transportation or nitrosative/oxidative stress. For instance, FVEG_04238 is related to *FLR1*, a plasma membrane transporter involved in the efflux of multiple drugs in *Saccharomyces cerevisiae* [74-76]. For another example, FVEG_03830 is related to the bifunctional protein URE2 in *S. cerevisiae* that is associated not only with nitrogen catabolite repression when ample nitrogen sources are available [77], but also oxidative stress [78, 79],

which is likely under NO stress, exhibiting glutathione peroxidase activity *in vitro* [80] and sharing structural similarity to glutathione S-transferases [77].

Consistent with a previous study [6], functional category analysis revealed an enriched number of HGT candidates in amino acid, nitrogen and sulfur metabolisms, suggesting these transfers may benefit the expansion of such processes in *F. verticillioides*. One example may be the putative DAP epimerase encoding gene FVEG_09873. A two-base mechanism relying on a pair of cysteine residues (Cys73 and Cys217, deprotonating the α-carbon and reprotonating the resulting intermediate, respectively) was proposed for the epimerase steroinversion reaction [81]. A multiple sequences alignment analysis (Supplemental Figure 2.4) showed that most of the key sites (e.g. binding site, active site) are conserved in the sequences examined, except for one binding site (position 11 in the *E. coli* sequence) and one active site (position 217 in the *E. coli* sequence), which are different between the reference and the other sequences. Although the second cysteine (C) required in the two-base mechanism is instead a serine (S) in the encoded protein of FVEG_09873, the putative DAP epimerase may still be functional given the following two arguments. Firstly, it has been shown that a protein single mutant C217S in *E. coli* can still remove the α-hydrogen of DAP yet with a noticeable drop in enzyme activity [81]. Secondly, cysteine residues nearing Cys217 may act as the second active site adhering to the two-base mechanism. Previously, a study on the evolution of lysine biosynthesis in eukaryotes [54] suggests that presence of *lysA*, a core gene in the DAP pathway encoding diaminopimelate decarboxylase, in several eukaryotes may have been acquired from eubacteria. Moreover, like the case of *F. verticillioides*, these eukaryotes do not contain a complete set of genes required for the DAP pathway either. It would be interesting to pursue the role of such DAP-pathway genes

in organisms lacking the capability to fully utilize the DAP pathway via the exploration of induced conditions and heterologous expression in model bacteria.

One potential explanation for the existence of incomplete metabolic pathways in fungi is the utilization of certain biochemical components by ectosymbiotic bacteria. Recent studies have shown the impact of ectosymbiotic bacteria on the biology, virulence, the production of secondary metabolites on corresponding fungal hosts. For instance, studies of the ectosymbiotic bacterial-associated nonpathogenic strain of *F. oxysporum* showed that those ectosymbiotic bacteria may alter fungal genes responsible for successful penetration of host plant roots [82], and modulate the production of small volatile organic compounds that protect plants from pathogenic *F. oxysporum* [83, 84]. Additional examples are "mycotoxin" producing endofungal bacteria *Burkholderia rhizoxinica* and *B. endofungorum*, which are both associated with the zygomycete *Rhizopus microspores* and responsible for the production of rhizoxin, the causative agent of rice seedling blight, and rhizonin, a hepatotoxic cyclopeptide, respectively [85]. Therefore, it is reasonable to speculate that ectosymbiotic bacteria may be capable of utilizing certain fungal genetic materials to benefit themselves or both players. More importantly, physically intimate bacterial-fungal associations could facilitate HGT of metabolic genes from bacteria to fungi, which can be supported by the hypothesis of the massive endosymbiotic gene transfer (EGT) occurring during organellar evolution [86, 87].

To summarize our findings, in this study, we revealed the occurrence of HGT candidates in *F. verticillioides* via a flexible and semi-automatic phylogenomic pipeline, and further assessed the functional and genomic attributes. Subsequent studies focusing on functional characterization of interesting HGT candidates may support their contribution to *F.*

verticillioides by conferring adaptive advantages. Together, these findings provide a view of how HGT events have shaped the *F. verticillioides* genome and overall fitness.

References

1. Doolittle, W.F., *Lateral genomics.* Trends Cell Biol, 1999. **9**(12): p. M5-8.
2. Gogarten, J.P., W.F. Doolittle, and J.G. Lawrence, *Prokaryotic evolution in light of gene transfer.* Mol Biol Evol, 2002. **19**(12): p. 2226-38.
3. Jain, R., et al., *Horizontal gene transfer accelerates genome innovation and evolution.* Mol Biol Evol, 2003. **20**(10): p. 1598-602.
4. Polz, M.F., E.J. Alm, and W.P. Hanage, *Horizontal gene transfer and the evolution of bacterial and archaeal population structure.* Trends Genet, 2013. **29**(3): p. 170-5.
5. Aramayo, R. and E.U. Selker, *Neurospora crassa, a model system for epigenetics research.* Cold Spring Harb Perspect Biol, 2013. **5**(10): p. a017921.
6. Richards, T.A., et al., *Gene transfer into the fungi.* Fungal Biology Reviews, 2011. **25**(2): p. 98-110.
7. Keeling, P.J. and J.D. Palmer, *Horizontal gene transfer in eukaryotic evolution.* Nat Rev Genet, 2008. **9**(8): p. 605-18.
8. Schonknecht, G., et al., *Gene transfer from bacteria and archaea facilitated evolution of an extremophilic eukaryote.* Science, 2013. **339**(6124): p. 1207-10.
9. Wijayawardena, B.K., D.J. Minchella, and J.A. DeWoody, *Hosts, parasites, and horizontal gene transfer.* Trends Parasitol, 2013. **29**(7): p. 329-38.
10. Gilbert, C. and R. Cordaux, *Horizontal transfer and evolution of prokaryote transposable elements in eukaryotes.* Genome Biol Evol, 2013. **5**(5): p. 822-32.
11. Walsh, A.M., et al., *Widespread horizontal transfer of retrotransposons.* Proc Natl Acad Sci U S A, 2013. **110**(3): p. 1012-6.
12. Stegemann, S. and R. Bock, *Exchange of Genetic Material Between Cells in Plant Tissue Grafts.* Science, 2009. **324**(5927): p. 649.
13. Mehrabi, R., et al., *Horizontal gene and chromosome transfer in plant pathogenic fungi affecting host range.* FEMS Microbiol Rev, 2011. **35**(3): p. 542-54.
14. Kotnik, T., *Lightning-triggered electroporation and electrofusion as possible contributors to natural horizontal gene transfer.* Physics of Life Reviews, 2013. **10**(3): p. 351-370.
15. de Jonge, R., et al., *Tomato immune receptor Ve1 recognizes effector of multiple fungal pathogens uncovered by genome and RNA sequencing.* Proc Natl Acad Sci U S A, 2012. **109**(13): p. 5110-5.
16. Cheeseman, K., et al., *Multiple recent horizontal transfers of a large genomic region in cheese making fungi.* Nat Commun, 2014. **5**: p. 2876.
17. Garcia-Vallve, S., A. Romeu, and J. Palau, *Horizontal gene transfer of glycosyl hydrolases of the rumen fungi.* Mol Biol Evol, 2000. **17**(3): p. 352-61.
18. Novo, M., et al., *Eukaryote-to-eukaryote gene transfer events revealed by the genome sequence of the wine yeast Saccharomyces cerevisiae EC1118.* Proc Natl Acad Sci U S A, 2009. **106**(38): p. 16333-8.
19. Glenn, A.E., et al., *Two Horizontally Transferred Xenobiotic Resistance Gene Clusters Associated with Detoxification of Benzoxazolinones by Fusarium Species.* PLoS One, 2016. **11**(1): p. e0147486.
20. Proctor, R.H., et al., *Birth, death and horizontal transfer of the fumonisin biosynthetic gene cluster during the evolutionary diversification of Fusarium.* Mol Microbiol, 2013. **90**(2): p. 290-306.
21. Slot, J.C. and A. Rokas, *Horizontal Transfer of a Large and Highly Toxic Secondary Metabolic Gene Cluster between Fungi.* Current Biology, 2011. **21**(2): p. 134-139.
22. Alexander, W.G., et al., *Horizontally acquired genes in early-diverging pathogenic fungi enable the use of host nucleosides and nucleotides.* Proceedings of the National Academy of Sciences, 2016. **113**(15): p. 4116-4121.

23. Gardiner, D.M., et al., *Comparative pathogenomics reveals horizontally acquired novel virulence genes in fungi infecting cereal hosts.* PLoS Pathog, 2012. **8**(9): p. e1002952.
24. Jaramillo, V.D., S.A. Sukno, and M.R. Thon, *Identification of horizontally transferred genes in the genus Colletotrichum reveals a steady tempo of bacterial to fungal gene transfer.* BMC Genomics, 2015. **16**: p. 2.
25. Qiu, H., et al., *Extensive horizontal gene transfers between plant pathogenic fungi.* BMC Biology, 2016. **14**(1): p. 41.
26. Fitzpatrick, D.A., *Horizontal gene transfer in fungi.* FEMS Microbiol Lett, 2012. **329**(1): p. 1-8.
27. Marcet-Houben, M. and T. Gabaldon, *Acquisition of prokaryotic genes by fungal genomes.* Trends Genet, 2010. **26**(1): p. 5-8.
28. Ma, L.J., et al., *Fusarium pathogenomics.* Annu Rev Microbiol, 2013. **67**: p. 399-416.
29. Munkvold, G.P., D.C. McGee, and W.M. Carlton, *Importance of Different Pathways for Maize Kernel Infection by Fusarium moniliforme.* Phytopathology, 1997. **87**(2): p. 209-17.
30. Bacon, C.W. and D.M. Hinton, *Symptomless endophytic colonization of maize by Fusarium moniliforme.* Canadian Journal of Botany, 1996. **74**(8): p. 1195-1202.
31. Campbell, M.A., A. Rokas, and J.C. Slot, *Horizontal transfer and death of a fungal secondary metabolic gene cluster.* Genome Biol Evol, 2012. **4**(3): p. 289-93.
32. Ma, L.J., et al., *Comparative genomics reveals mobile pathogenicity chromosomes in Fusarium.* Nature, 2010. **464**(7287): p. 367-73.
33. Tsavkelova, E., et al., *Identification and functional characterization of indole-3-acetamide-mediated IAA biosynthesis in plant-associated Fusarium species.* Fungal Genet Biol, 2012. **49**(1): p. 48-57.
34. Wisecaver, J.H., et al., *Dynamic Evolution of Nitric Oxide Detoxifying Flavohemoglobins, a Family of Single-Protein Metabolic Modules in Bacteria and Eukaryotes.* Mol Biol Evol, 2016. **33**(8): p. 1979-87.
35. Li, W. and A. Godzik, *Cd-hit: a fast program for clustering and comparing large sets of protein or nucleotide sequences.* Bioinformatics, 2006. **22**(13): p. 1658-9.
36. Katoh, K. and D.M. Standley, *MAFFT multiple sequence alignment software version 7: improvements in performance and usability.* Mol Biol Evol, 2013. **30**(4): p. 772-80.
37. Capella-Gutierrez, S., J.M. Silla-Martinez, and T. Gabaldon, *trimAl: a tool for automated alignment trimming in large-scale phylogenetic analyses.* Bioinformatics, 2009. **25**(15): p. 1972-3.
38. Price, M.N., P.S. Dehal, and A.P. Arkin, *FastTree 2--approximately maximum-likelihood trees for large alignments.* PLoS One, 2010. **5**(3): p. e9490.
39. Khaldi, N., et al., *SMURF: Genomic mapping of fungal secondary metabolite clusters.* Fungal Genet Biol, 2010. **47**(9): p. 736-41.
40. Medema, M.H., et al., *antiSMASH: rapid identification, annotation and analysis of secondary metabolite biosynthesis gene clusters in bacterial and fungal genome sequences.* Nucleic Acids Res, 2011. **39**(Web Server issue): p. W339-46.
41. Tamura, K., et al., *MEGA6: Molecular Evolutionary Genetics Analysis version 6.0.* Mol Biol Evol, 2013. **30**(12): p. 2725-9.
42. Guindon, S. and O. Gascuel, *A simple, fast, and accurate algorithm to estimate large phylogenies by maximum likelihood.* Syst Biol, 2003. **52**(5): p. 696-704.
43. Huelsenbeck, J.P. and F. Ronquist, *MRBAYES: Bayesian inference of phylogenetic trees.* Bioinformatics, 2001. **17**(8): p. 754-5.
44. Leslie, J.F., B.A. Summerell, and S. Bullock, *The Fusarium Laboratory Manual*. 2006: Wiley.
45. Paz, Z., et al., *One Step Construction of Agrobacterium-Recombination-ready-plasmids (OSCAR), an efficient and robust tool for ATMT based gene deletion construction in fungi.* Fungal Genetics and Biology, 2011. **48**(7): p. 677-684.
46. Bundock, P., et al., *Trans-kingdom T-DNA transfer from Agrobacterium tumefaciens to Saccharomyces cerevisiae.* The EMBO Journal, 1995. **14**(13): p. 3206-3214.

47. Bourett, T.M., et al., *Reef coral fluorescent proteins for visualizing fungal pathogens.* Fungal Genet Biol, 2002. **37**(3): p. 211-20.
48. Livak, K.J. and T.D. Schmittgen, *Analysis of Relative Gene Expression Data Using Real-Time Quantitative PCR and the 2−ΔΔCT Method.* Methods, 2001. **25**(4): p. 402-408.
49. Bolger, A.M., M. Lohse, and B. Usadel, *Trimmomatic: a flexible trimmer for Illumina sequence data.* Bioinformatics, 2014. **30**(15): p. 2114-20.
50. Liao, Y., G.K. Smyth, and W. Shi, *The Subread aligner: fast, accurate and scalable read mapping by seed-and-vote.* Nucleic Acids Res, 2013. **41**(10): p. e108.
51. Robinson, M.D., D.J. McCarthy, and G.K. Smyth, *edgeR: a Bioconductor package for differential expression analysis of digital gene expression data.* Bioinformatics, 2010. **26**(1): p. 139-40.
52. Anders, S. and W. Huber, *Differential expression analysis for sequence count data.* Genome Biol, 2010. **11**(10): p. R106.
53. Vogel, H.J., *Lysine Biosynthesis and Evolution.* Evolving Genes and Proteins, 1965: p. 25-40.
54. Torruella, G., et al., *The Evolutionary History of Lysine Biosynthesis Pathways Within Eukaryotes.* Journal of Molecular Evolution, 2009. **69**(3): p. 240-248.
55. Zabriskie, T.M. and M.D. Jackson, *Lysine biosynthesis and metabolism in fungi.* Nat Prod Rep, 2000. **17**(1): p. 85-97.
56. Hor, L., et al., *Dimerization of Bacterial Diaminopimelate Epimerase Is Essential for Catalysis.* Journal of Biological Chemistry, 2013. **288**(13): p. 9238-9248.
57. Tudzynski, B., *Nitrogen regulation of fungal secondary metabolism in fungi.* Front Microbiol, 2014. **5**: p. 656.
58. Howden, A.J.M. and G.M. Preston, *Nitrilase enzymes and their role in plant–microbe interactions.* Microbial Biotechnology, 2009. **2**(4): p. 441-451.
59. Kertesz, M.A. and P. Mirleau, *The role of soil microbes in plant sulphur nutrition.* J Exp Bot, 2004. **55**(404): p. 1939-45.
60. Sousa, S.A., C.G. Ramos, and J.H. Leitao, *Burkholderia cepacia Complex: Emerging Multihost Pathogens Equipped with a Wide Range of Virulence Factors and Determinants.* Int J Microbiol, 2011. **2011**.
61. Zinniel, D.K., et al., *Isolation and characterization of endophytic colonizing bacteria from agronomic crops and prairie plants.* Appl Environ Microbiol, 2002. **68**(5): p. 2198-208.
62. Kingsbury, J.M. and J.H. McCusker, *Homoserine toxicity in Saccharomyces cerevisiae and Candida albicans homoserine kinase (thr1Delta) mutants.* Eukaryot Cell, 2010. **9**(5): p. 717-28.
63. Bonnighausen, J., et al., *Disruption of the GABA shunt affects mitochondrial respiration and virulence in the cereal pathogen Fusarium graminearum.* Mol Microbiol, 2015. **98**(6): p. 1115-32.
64. Ramos, F., et al., *Mutations affecting the enzymes involved in the utilization of 4-aminobutyric acid as nitrogen source by the yeast Saccharomyces cerevisiae.* European Journal of Biochemistry, 1985. **149**(2): p. 401-404.
65. Takahashi, T., et al., *Isolation and characterization of sake yeast mutants deficient in gamma-aminobutyric acid utilization in sake brewing.* J Biosci Bioeng, 2004. **97**(6): p. 412-8.
66. Shelp, B.J., R.T. Mullen, and J.C. Waller, *Compartmentation of GABA metabolism raises intriguing questions.* Trends Plant Sci, 2012. **17**(2): p. 57-9.
67. Brown, D.W., et al., *Identification of gene clusters associated with fusaric acid, fusarin, and perithecial pigment production in Fusarium verticillioides.* Fungal Genet Biol, 2012. **49**(7): p. 521-32.
68. Friesen, T.L., et al., *Emergence of a new disease as a result of interspecific virulence gene transfer.* Nat Genet, 2006. **38**(8): p. 953-956.
69. Gardiner, D.M., K. Kazan, and J.M. Manners, *Cross-kingdom gene transfer facilitates the evolution of virulence in fungal pathogens.* Plant Sci, 2013. **210**: p. 151-8.
70. Walton, J.D., *Horizontal gene transfer and the evolution of secondary metabolite gene clusters in fungi: an hypothesis.* Fungal Genet Biol, 2000. **30**(3): p. 167-71.

71. Lawrence, J.G. and J.R. Roth, *Selfish Operons: Horizontal Transfer May Drive the Evolution of Gene Clusters*. Genetics, 1996. **143**(4): p. 1843.
72. Eisen, J.A., *Horizontal gene transfer among microbial genomes: new insights from complete genome analysis.* Current Opinion in Genetics & Development, 2000. **10**(6): p. 606-611.
73. Niehaus, E.-M., et al., *Genetic Manipulation of the Fusarium fujikuroi Fusarin Gene Cluster Yields Insight into the Complex Regulation and Fusarin Biosynthetic Pathway.* Chemistry & Biology, 2013. **20**(8): p. 1055-1066.
74. Alarco, A.M., et al., *AP1-mediated multidrug resistance in Saccharomyces cerevisiae requires FLR1 encoding a transporter of the major facilitator superfamily.* J Biol Chem, 1997. **272**(31): p. 19304-13.
75. Brôco, N., et al., *FLR1 gene (ORF YBR008c) is required for benomyl and methotrexate resistance in Saccharomyces cerevisiae and its benomyl-induced expression is dependent on Pdr3 transcriptional regulator.* Yeast, 1999. **15**(15): p. 1595-1608.
76. Jungwirth, H., et al., *Diazaborine resistance in yeast involves the efflux pumps Ycf1p and Flr1p and is enhanced by a gain-of-function allele of gene YAP1.* Eur J Biochem, 2000. **267**(15): p. 4809-16.
77. Coschigano, P.W. and B. Magasanik, *The URE2 gene product of Saccharomyces cerevisiae plays an important role in the cellular response to the nitrogen source and has homology to glutathione s-transferases.* Molecular and Cellular Biology, 1991. **11**(2): p. 822-832.
78. Rai, R. and T.G. Cooper, *In vivo specificity of Ure2 protection from heavy metal ion and oxidative cellular damage in Saccharomyces cerevisiae.* Yeast, 2005. **22**(5): p. 343-58.
79. Rai, R., J.J. Tate, and T.G. Cooper, *Ure2, a prion precursor with homology to glutathione S-transferase, protects Saccharomyces cerevisiae cells from heavy metal ion and oxidant toxicity.* J Biol Chem, 2003. **278**(15): p. 12826-33.
80. Bai, M., J.-M. Zhou, and S. Perrett, *The Yeast Prion Protein Ure2 Shows Glutathione Peroxidase Activity in Both Native and Fibrillar Forms.* Journal of Biological Chemistry, 2004. **279**(48): p. 50025-50030.
81. Koo, C.W., et al., *Identification of Active Site Cysteine Residues that Function as General Bases: Diaminopimelate Epimerase.* Journal of the American Chemical Society, 2000. **122**(25): p. 6122-6123.
82. Minerdi, D., et al., *Bacterial ectosymbionts and virulence silencing in a Fusarium oxysporum strain.* Environ Microbiol, 2008. **10**(7): p. 1725-41.
83. Minerdi, D., et al., *Volatile organic compounds: a potential direct long-distance mechanism for antagonistic action of Fusarium oxysporum strain MSA 35.* Environ Microbiol, 2009. **11**(4): p. 844-54.
84. Minerdi, D., et al., *Fusarium oxysporum and its bacterial consortium promote lettuce growth and expansin A5 gene expression through microbial volatile organic compound (MVOC) emission.* FEMS Microbiology Ecology, 2011. **76**(2): p. 342-351.
85. Lackner, G., L.P. Partida-Martinez, and C. Hertweck, *Endofungal bacteria as producers of mycotoxins.* Trends in Microbiology, 2009. **17**(12): p. 570-576.
86. Kurland, C.G. and S.G. Andersson, *Origin and evolution of the mitochondrial proteome.* Microbiol Mol Biol Rev, 2000. **64**(4): p. 786-820.
87. Martin, W., et al., *Evolutionary analysis of Arabidopsis, cyanobacterial, and chloroplast genomes reveals plastid phylogeny and thousands of cyanobacterial genes in the nucleus.* Proc Natl Acad Sci U S A, 2002. **99**(19): p. 12246-51.

Table 2.1: *Fusarium verticillioides* HGT candidates suggesting an enrichment of genes involved in DAP pathway of biosynthesis of lysine as inferred by MIPS Functional Catalogue prediction.

Biosynthesis of lysine, diaminopimelic acid pathway			
Gene ID	FVEG_00154	FVEG_05936	FVEG_09873
Putative Function	Dihydrodipicolinate synthase	Dihydrodipicolinate synthase	Diaminopimelate epimerase
EC number	EC 4.3.3.7	EC 4.3.3.7	EC 5.1.1.7
Run[a]	D	F	A

[a] Run from which the HGT candidate was identified (See Figure 2.2).

Table 2.2: *Fusarium verticillioides* HGT candidates suggesting an enrichment of genes involved in metabolism of glycine as inferred by MIPS Functional Catalogue prediction.

Metabolism of glycine					
Gene ID	FVEG_03408	FVEG_13277	FVEG_08761	FVEG_10494	FVEG_10784
Putative Function	Sarcosine oxidase	Sarcosine oxidase	Glycine/D-amino acid oxidase	Type II homoserine kinase; 4-aminobutyrate aminotransferase	Glycine/D-amino acid oxidase; Glycine cleavage system T protein (aminomethyltransferase)
EC number	EC 1.5.3.1	EC 1.5.3.1	EC 1.4.3.3	EC 2.7.1.39; EC 2.6.1.19	EC 1.4.3.3; EC 2.1.2.10
Run[a]	D	D	D	A	E

[a] Run from which the HGT candidate was identified (See Figure 2.2).

Table 2.3: *Fusarium verticillioides* HGT candidates suggesting an enrichment of genes involved in nitrogen metabolism as inferred by MIPS Functional Catalogue prediction.

Nitrogen metabolism							
Gene ID	FVEG_00065	FVEG_01752	FVEG_08761	FVEG_10494	FVEG_10784	FVEG_12564	FVEG_13277
Putative Function	Nitrilase	Nitrilase	Glycine/D-amino acid oxidase	Type II homoserine kinase; 4-aminobutyrate aminotransferase	Glycine/D-amino acid oxidase; Glycine cleavage system T protein (aminomethyltransferase)	Aspartate aminotransferase	Sarcosine oxidase
EC number	EC 3.5.5.1	EC 3.5.5.1	EC 1.4.3.3	EC 2.7.1.39; EC 2.6.1.19	EC 1.4.3.3; EC 2.1.2.10	EC 2.6.1.1	EC 1.5.3.1
Run[a]	A	F	D	A	E	D	D

[a] Run from which the HGT candidate was identified (See Figure 2.2).

Table 2.4: *Fusarium verticillioides* HGT candidates suggesting an enrichment of genes involved in sulfur metabolism as inferred by MIPS Functional Catalogue prediction.

Sulfur metabolism					
Gene ID	FVEG_08588	FVEG_08652	FVEG_10127	FVEG_11708	FVEG_13201
Putative Function	Arylsulfatase A	Arylsulfatase A	Arylsulfatase A	Arylsulfatase A	Sulfotransferase
EC number	EC 3.1.6.8	EC 3.1.6.8	EC 3.1.6.8	EC 3.1.6.8	EC 2.8.2.-
Run[a]	F	F	E	E	D

[a] Run from which the HGT candidate was identified (See Figure 2.2).

Table 2.5: Summary of *Fusarium verticillioides* HGT candidates distributed narrowly in fungi.

Gene ID	Run[a]	Putative function[b]	Fungal distribution[c]	Protein similarity to the best bacterial hit	Best model for building BI tree[d]
FVEG_09873	A	Diaminopimelate epimerase	*F. verticillioides*	69%	JTT[e]+G[f]
FVEG_00065	A	Nitrilases	*Fusarium*	59%	LG[e]+G
FVEG_03450	G	Glycerophosphodiester phosphodiesterase domain of *Agrobacterium tumefaciens* and similar proteins	*Fusarium*	77%	JTT+G
FVEG_04320	A	Carboxylesterase type B	*Fusarium*	67%	WAG[e]+G+I[g]
FVEG_07753	A	Cellulase	*Fusarium*	66%	WAG+G+I
FVEG_10494	A	Type II Homoserine Kinase; 4-aminobutyrate aminotransferase	*Fusarium*	76%	WAG+G+I
FVEG_11809	B	FAD dependent oxidoreductase	Hypocreales	42%	LG+G
FVEG_11906	B	UDP glucuronic acid epimerase	Hypocreales	64%	LG+G
FVEG_14084	B	FAD dependent oxidoreductase	Hypocreales	43%	LG+G
FVEG_06279	B	Acetyl esterase/lipase	Hypocreales	43%	LG+G
FVEG_12509	D	Salicylaldehyde dehydrogenase	Pezizomycotina	50%	LG+G

[a] Run from which the HGT candidate was identified (See Figure 2.2).
[b] Putative function predicted with the Conserved Domain database of NCBI.
[c] Distribution range of orthologs in fungi based on NCBI BLASTp.
[d] Best amino acid substitution model for building Bayesian Inference (BI) tree.
[e] Amino acid substitution model.
[f] Estimation of gamma distribution.
[g] Estimation of invariable sites.

Table 2.6: Summary of RNA-seq analyses of the *Fusarium verticillioides* wild type and FVEG_10494 gene deletion mutant under Nitric oxide stress[a].

	WT treated vs WT non-treated[b]	Mutant treated vs mutant non-treated[c]	Mutant non-treated vs WT non-treated[d]	Mutant treated vs WT treated[f]
Up-regulated gene count:	330	293	0	13
Down-regulated gene count:	278	246	1	16

[a] Nitric oxide stress exposed on fungal cultures using 1.5 mM DETA NONOate for 30 min.
[b] The comparison between treated wild type (WT) and wild-type control.
[c] The comparison between treated gene deletion mutant and mutant control.
[d] The comparison between gene deletion mutant and wild-type control.
[f] The comparison between treated gene deletion mutant and wild type.

Table 2.7: Summary of differentially expressed genes in the comparison of *Fusarium verticillioides* mutant vs wild type challenged with nitric oxide[a].

FVEG ID	Log FC	Annotation[b]	Conserved domain[c]
FVEG_10834	1.09	NA	Na(+)/urea-polyamine cotransporter DUR3, and related proteins
FVEG_11078	1.04	NA	SAM dependent carboxyl methyltransferase
FVEG_11079	2.11	related to benzoate 4-monooxygenase cytochrome P450	Cytochrome P450
FVEG_11080	1.21	related to aldehyde dehydrogenase (NAD+), mitochondrial	Streptomyces aureofaciens putative aldehyde dehydrogenase AldA (AAD23400)-like
FVEG_11085	1.35	NA	alpha/beta hydrolases
FVEG_11086	1.30	probable polyketide synthase	polyketide synthase
FVEG_04238	-1.65	related to FLR1 - Putative H+ antiporter regulated by yAP-1 and involved in multidrug resistance	Multidrug resistance protein
FVEG_05981	-1.14	related to putative tartrate transporter	Major Facilitator Superfamily
FVEG_11294	-1.34	probable fluconazole resistance protein	Major Facilitator Superfamily
FVEG_12329	-1.59	related to sulfate permease SutB	Sulfate permease or related transporter
FVEG_01376	-1.06	related to flavin oxidoreductase	Old yellow enzyme (OYE) YqjM-like FMN binding domain
FVEG_03830	-.1.19	related to URE2 - nitrogen catabolite repression regulator	Glutathione S-transferase
FVEG_07389	-1.11	NA	Nitroreductase-like family 4
FVEG_11140	-1.83	related to alcohol oxidase	Choline dehydrogenase or related flavoprotein
FVEG_09386	-1.62	NA	classical (c) SDRs
FVEG_01304	-1.11	probable cystathionine gamma-lyase	Cys/Met metabolizm PLP-dependent enzyme

Genes associated with fusarin C biosynthetic gene cluster, cellular transportation, and nitrosative/oxidative are highlighted with orange, blue, and green, respectively.

[a] Nitric oxide stress exposed on fungal cultures using 1.5 mM DETA NONOate for 30 min.

[b] Predicted by Pedant-Pro.

[c] Predicted by Conserved Domain database of NCBI.

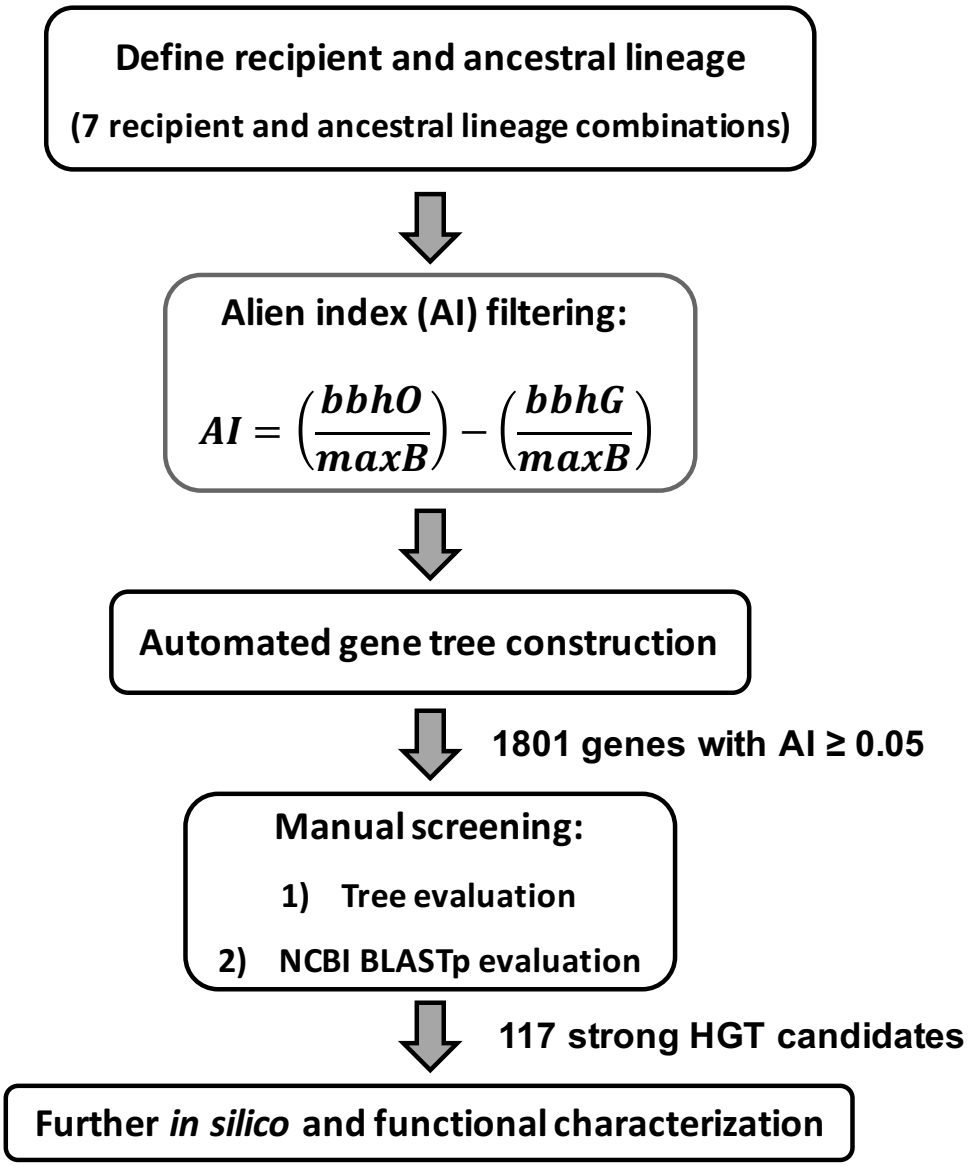

Figure 2.1: Phylogenomic pipeline to identify HGT candidates in *Fusarium verticillioides*. Two taxonomic lineages were first specified: the recipient lineage into which possible HGT events may have occurred, and a larger ancestral lineage of related taxa. Seven runs of global analysis with different recipient and ancestral lineage combinations against all annotated protein sequences of *F. verticillioides* 7600 were conducted using a phylogenomic pipeline, which consisted of the automated filtration modified from the alien index (AI) method [33] and gene tree construction, followed by manual evaluation of both gene trees and NCBI BLASTp results. A total of 117 genes acquired mostly from bacteria were recovered as strong HGT candidates and analyzed further. In the AI formula: bbhO is the bitscore of the best BLAST hit to a species outside of the ancestral lineage, bbhG is the bitscore of the best BLAST hit to a species within the ancestral lineage, and maxB is the maximum bitscore possible for the query sequence.

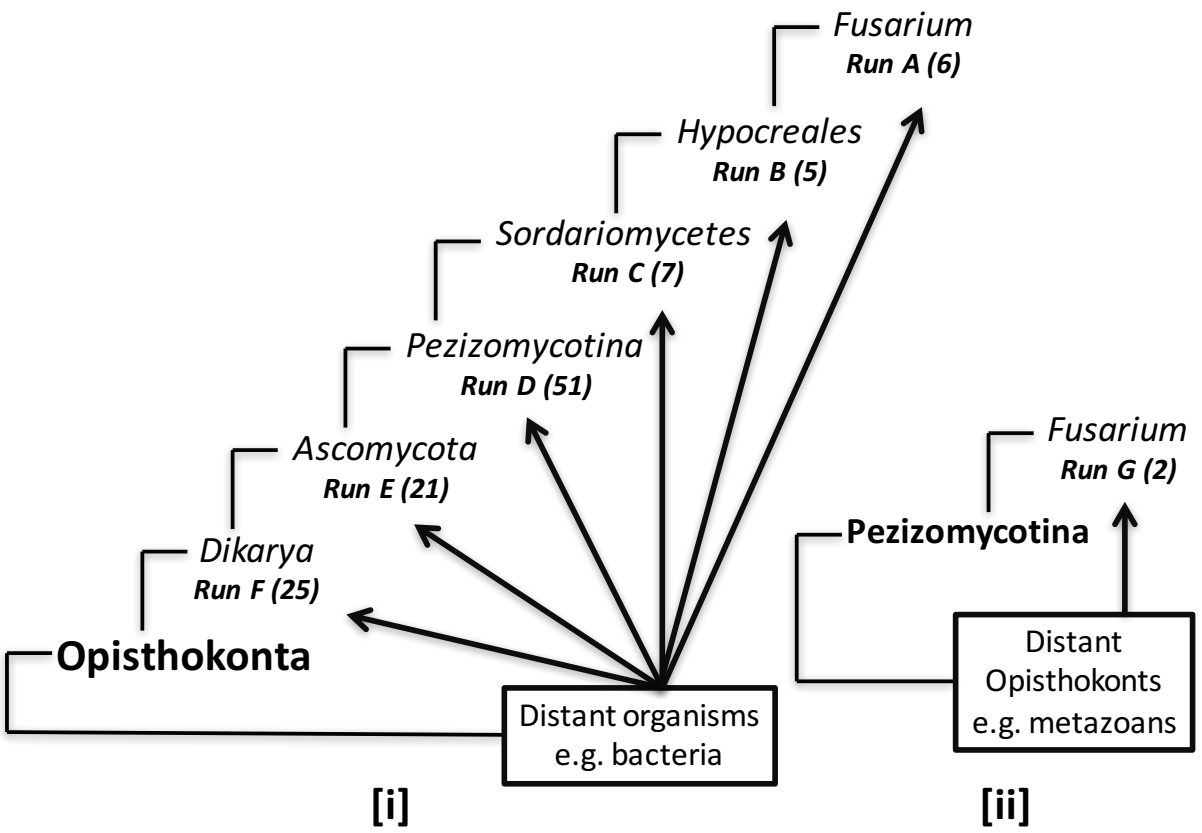

Figure 2.2: *Fusarium verticillioides* HGT candidates recovered from seven runs with different combinations of recipient and donor lineages.

The application of seven runs (A to F [i] and G [ii]) based on different pairs of recipient (arrow) and donor (rectangular frames) lineages revealed non-overlapping sets of HGT candidates (numbers indicated in parentheses). The ancestral lineage is labelled in bold.

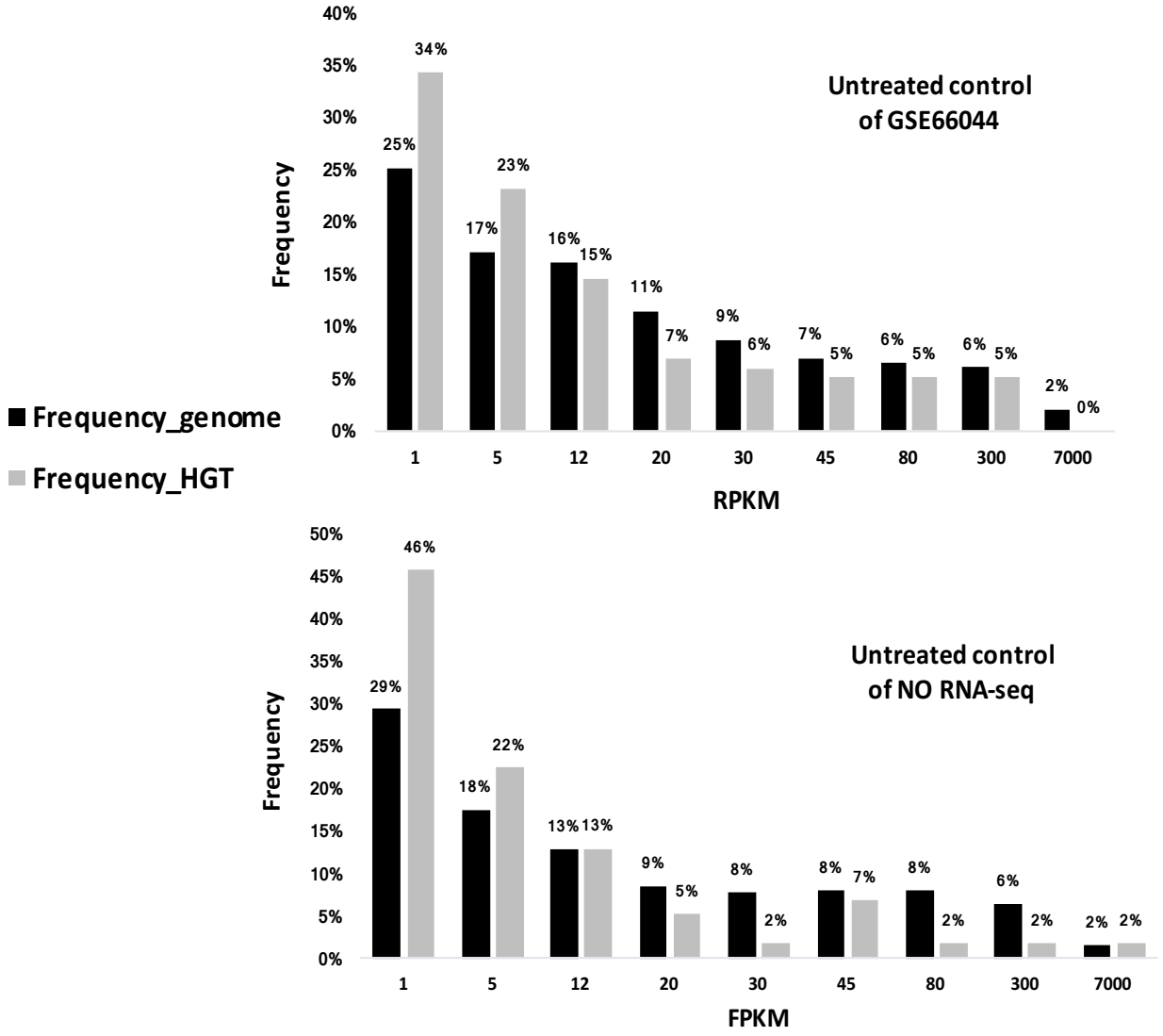

Figure 2.3: Distribution of expression levels of genes in HGT candidates and the genome of *Fusarium verticillioides*.

To compare the expression level of genes between HGT candidates and the full transcriptome, RNA-seq data of untreated control were extracted from the dataset GSE66044 (upper) and the NO RNA-seq data (lower). For each HGT candidate in the two samples (HGT and genome), expression values (RPKM or FPKM) were averaged over all biological replicates and then grouped into a series of range bins (X axis, for instance, x=5 represents expression values that are > 1 and ≤ 5). The number of genes falling into each bin was counted. The percent frequency (Y axis) was then calculated by dividing the gene counts by the total number multiplied by 100 and labeled at the top of each bar.

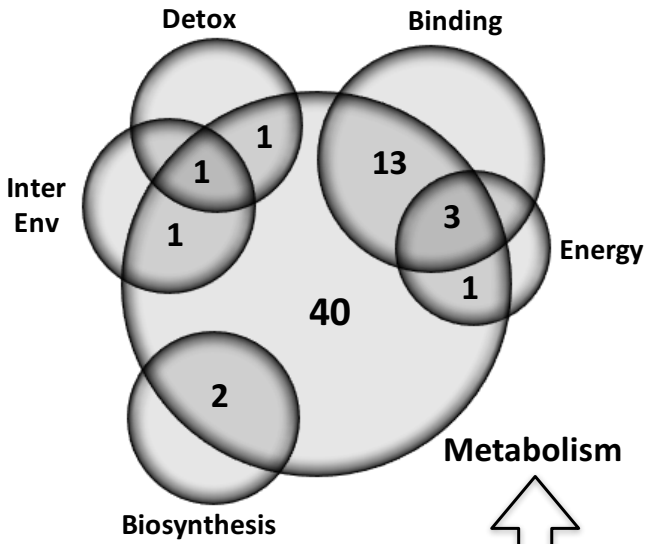

	Amino acid	Nitrogen and sulfur	Nucleotide	Carbohydrate	Secondary
Amino acid	**27 (4.6)**				
Nitrogen and sulfur	**7**	**17 (5.6)**			
Nucleotide	**0**	**0**	**2 (11.5)**		
Carbohydrate	**10**	**10**	**0**	**38 (2.6)**	
Secondary	**7**	**0**	**0**	**8**	**12 (2.0)**

Figure 2.4: Identified functional enrichment of strong HGT candidates in *Fusarium verticillioides*.
The 117 strong HGT candidates were analyzed via the MIPS Functional Catalogue (http://mips.helmholtz-muenchen.de/funcatDB/), and enriched functional categories with p-value < 0.05 are reported. Upper diagram: Distribution of gene candidates (numbers in parentheses) in the enriched main functional categories: 01 Metabolism, 02 Energy, 16.21 Complex cofactor/cosubstrate/vitamine binding, 32.07.09 Detoxification by degradation, 36 Systemic interaction with environment, and 42.19 Biosynthesis of cellular components (peroxisome). Lower table: Distribution of gene candidates in the enriched sub-categories of 01 Metabolism and the degree of fold enrichment compared to the frequency of such genes within the *F. verticillioides* genome (numbers in parentheses).

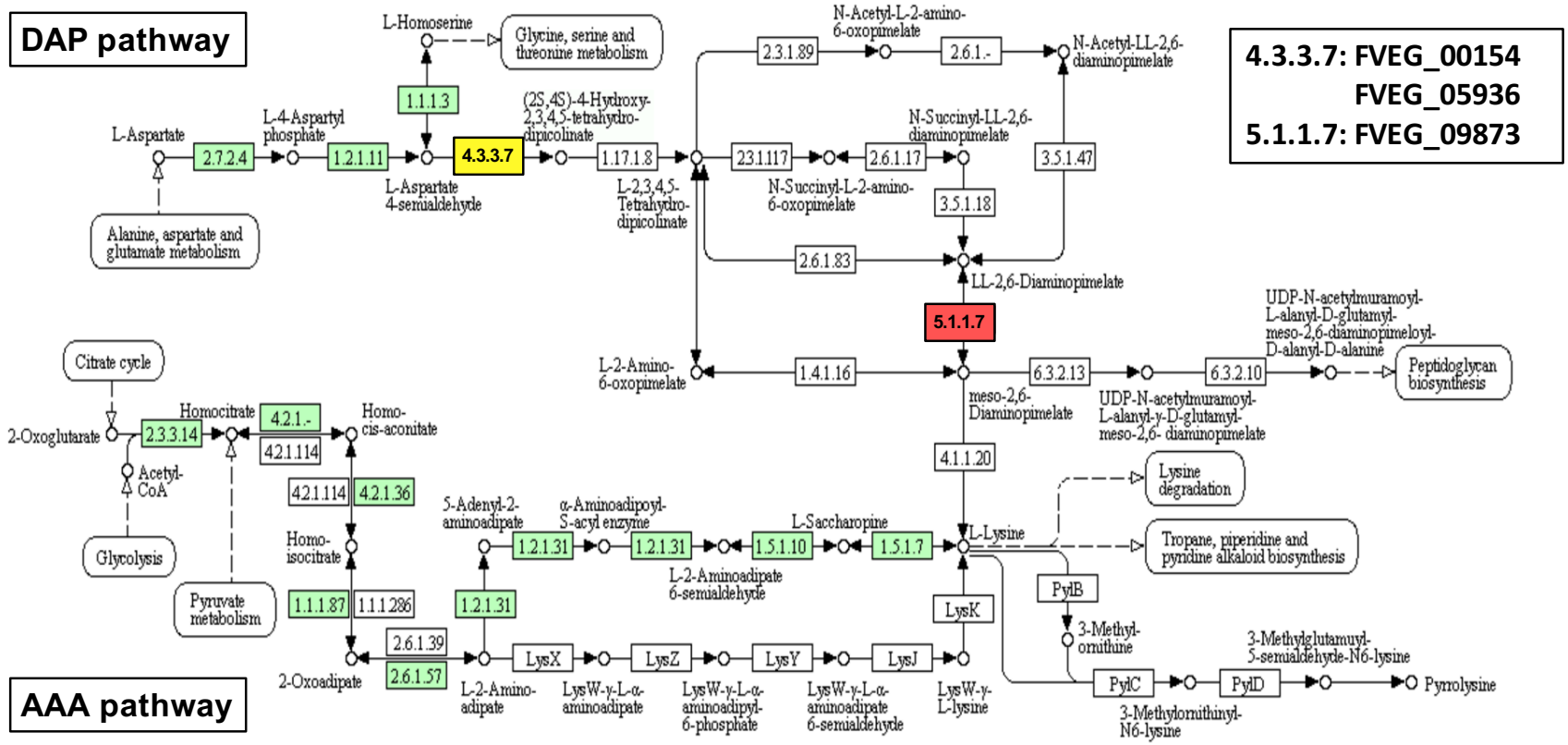

Figure 2.5: Lysine biosynthesis in *Fusarium verticillioides* and HGT candidates mapped to this pathway.

The map of lysine biosynthesis including the diaminopimelate (DAP) pathway (upper branch) and the α-aminoadipate (AAA) pathway (lower branch) was extracted from KEGG PATHWAY Database (http://www.genome.jp/kegg/pathway.html). The figure in each block represents EC number responsible for the corresponding reaction. Genes mapped to this pathway in *F. graminearum* (the reference organism) were extracted from KEGG and all corresponding orthologs (blocks highlighted in green and yellow) in *F. verticillioides* were found.

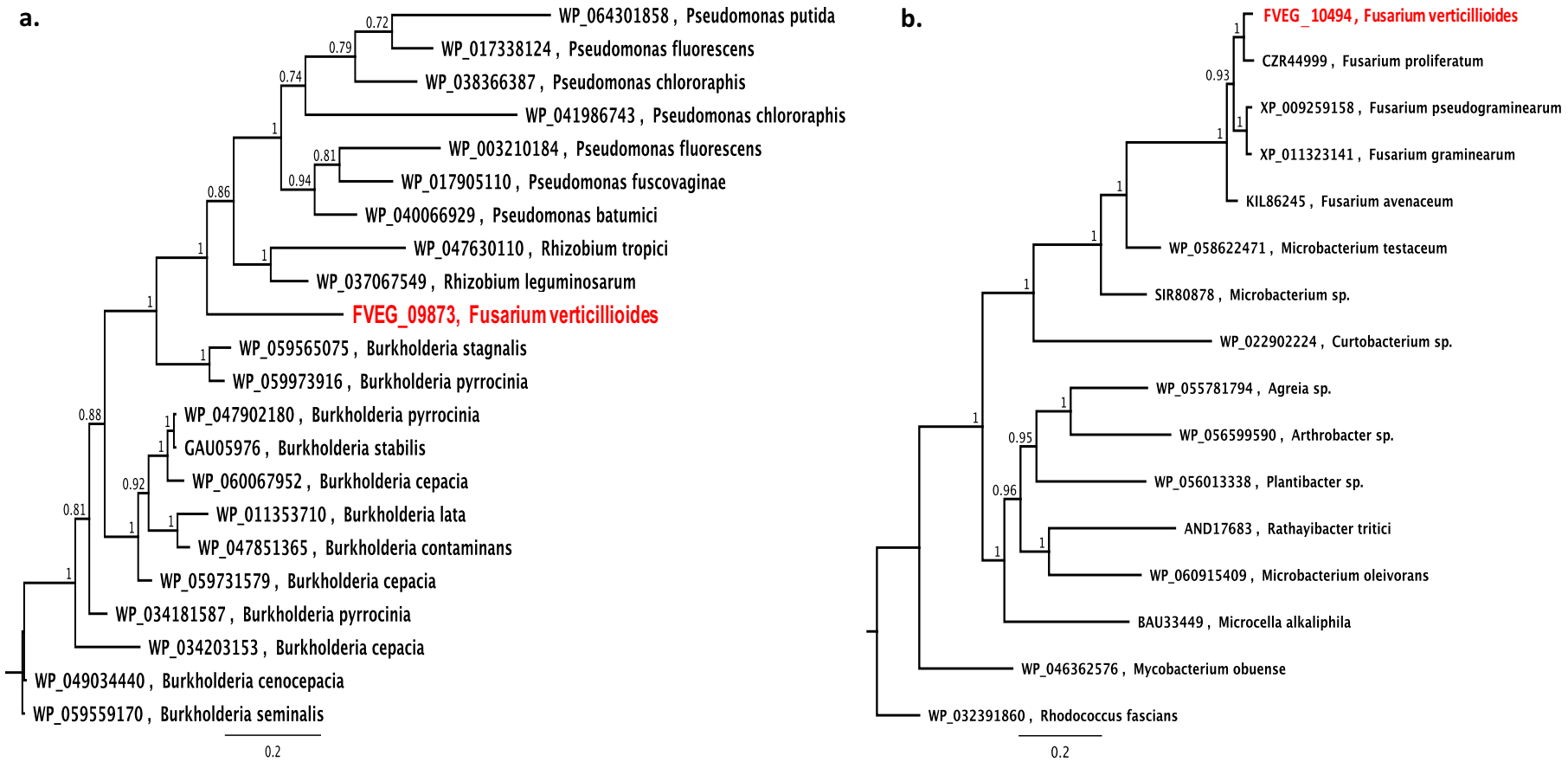

Figure 2.6: Bayesian Inference (BI) of FVEG_09873 (a) and FVEG_10494 (b).

Phylogenies were reconstructed by BI in the plugin version of MrBayes 3.2.6 in Geneious. The analysis was based on the best-fit amino acid substitution models predicted by MEGA v.6.06 (Table 2.5). MrBayes was run with the following parameters: 1,100,000 cycles with 4 heated chains, 0.2 heated chain temp, 200 subsampling frequency, 100,000 burn-in length, and 5502 random seed. Tip labels were displayed as accession number followed by the organism. Genes in *F. verticillioides* are highlighted in red. Branch labels indicate the posterior probability.

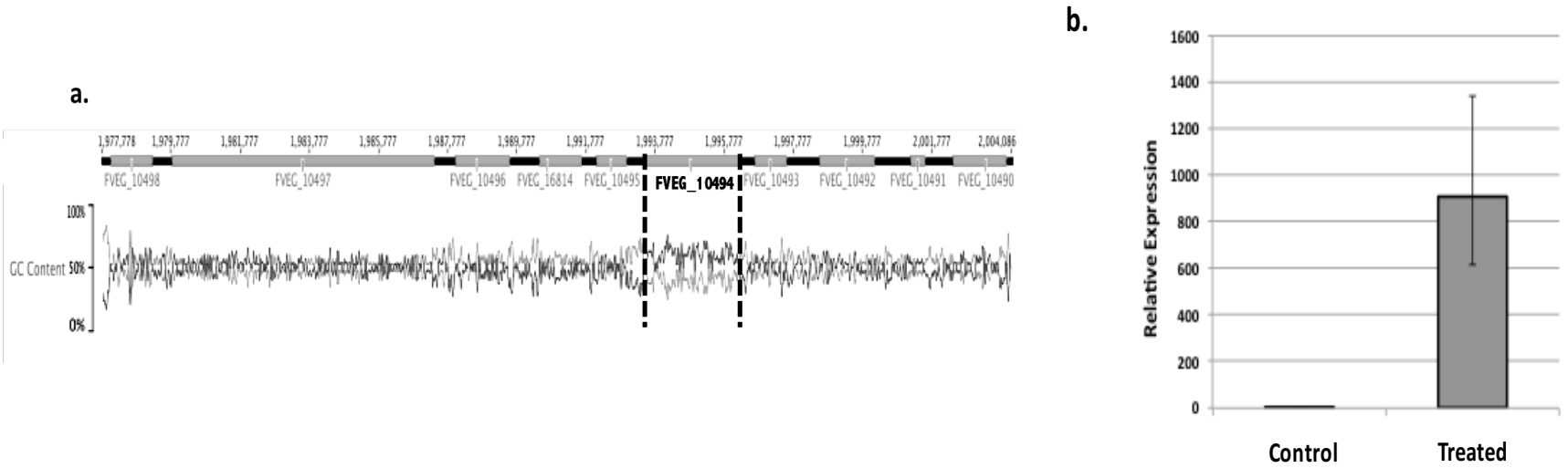

Figure 2.7: Abnormal GC content of FVEG_10494 (a) and its high induction under NO challenge (b).
a. GC content was analyzed using Geneious v.8.1.9. Upper panel shows the schematic genomic region from FVEG_10408 to FVEG_10490. Gray bars indicate genes and black lines indicate the sequence of intergenic regions. The lower panel shows the GC (black line)/AT (gray line) content, the number of which are plotted based on the left percentage scale, of corresponding sequences. FVEG_10494 is highlighted in bold black and its position bound by dashed lines. **b**. Transcriptional analysis of FVEG_10494 under NO stress was performed by challenging three-day-old wild-type culture with 1.5 mM DETA NONOate for 30 min. Complementary DNA synthesis and qRT-PCR analysis were followed with triplicate for each treatment. The $2^{-\Delta\Delta CT}$ method was used to calculate the relative expression levels. Standard deviations were indicated by error bars.

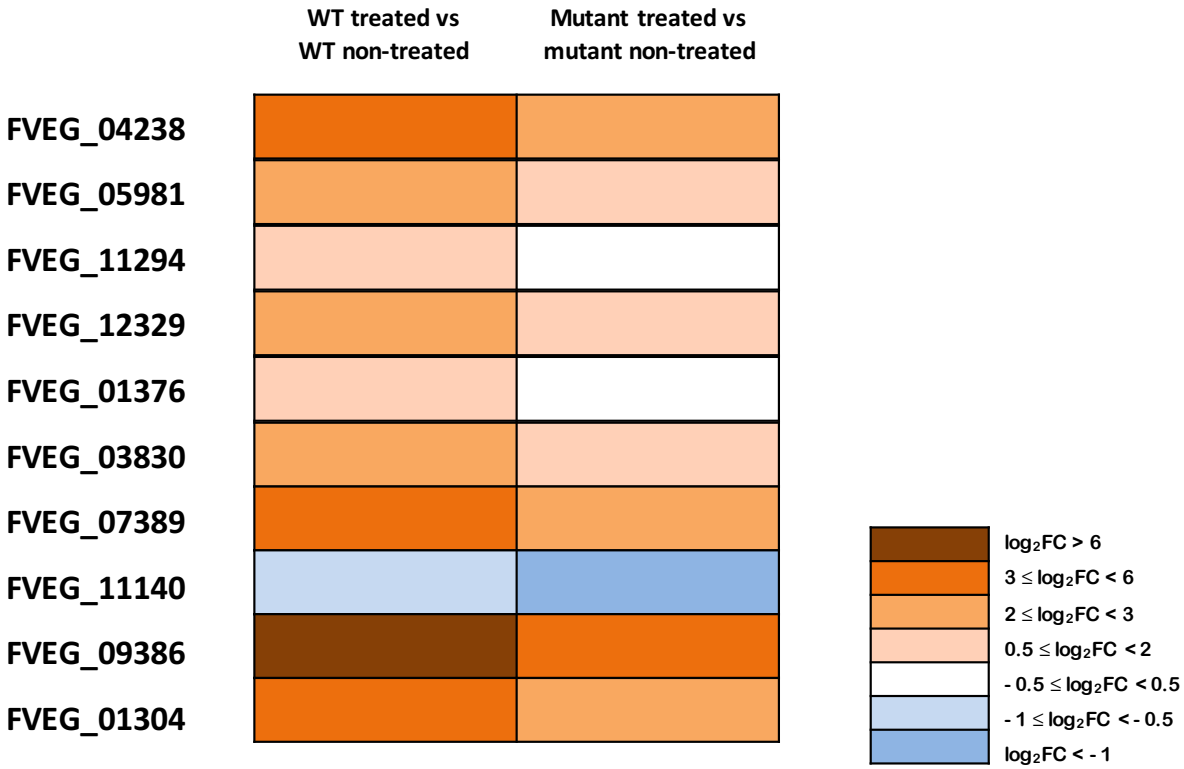

Figure 2.8: Absence of FVEG_10494 weakens expression of selected genes.
The genes down-regulated in the FVEG_10494 mutant compared to wild type when both were treated with NO were examined to compare their expression in wild type treated with NO vs untreated wild type (labeled above, WT treated vs WT non-treated) and in the mutant treated with NO vs untreated mutant (mutant treated vs mutant non-treated). The level of expression for each gene was less in the mutant comparison compared to the wild type comparison. Gene ID is labeled on the left and color scale is shown at the bottom left.

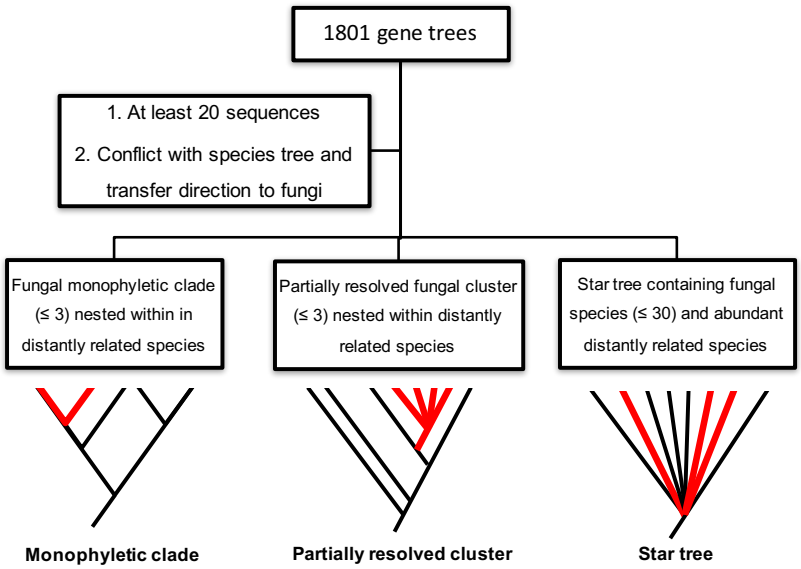

Supplemental Figure 2.1: Criteria of manual curation for detecting strong HGT candidates in *Fusarium verticillioides*.

A total of 1801 genes from the phylogenomic filtering step were manually inspected to meet certain criteria. Firstly, trees should contain at least 20 sequences. Secondly, the gene phylogeny should contradict the established species phylogeny, and the transfer direction is from distantly related species to fungi. Thirdly, to ensure the strong HGT signal, the topology of the gene tree should meet one of the three following scenarios (red lines represent fungal sequences and black lines represent sequences derived from distantly related species): containing ≤ 3 fungal monophyletic clades; containing ≤ 3 clusters of fungal genes that are partially resolved but nested with genes in distantly related species; a star tree (multifurcated phylogeny with many short branches connected at the internal node) including ≤ 30 fungal genes along with other genes in distantly related species.

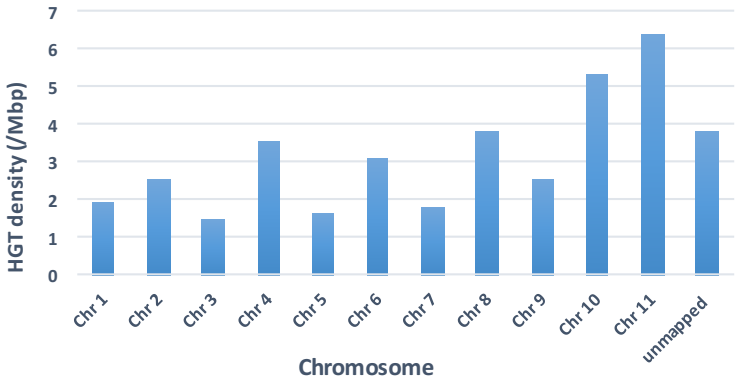

Supplemental Figure 2.2: Distribution of HGT candidates in chromosomes of *Fusarium verticillioides*.

HGT density is calculated by dividing the number of HGT candidates in each chromosome by the size (Mbp) of the corresponding chromosome.

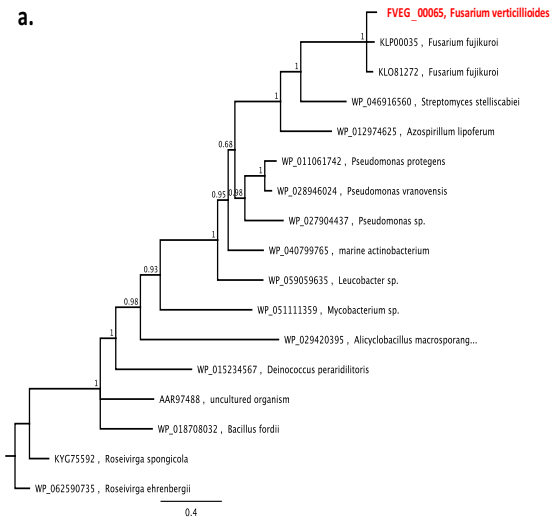
a.
FVEG_00065, Fusarium verticillioides
KLP00035 , Fusarium fujikuroi
KLO81272 , Fusarium fujikuroi
WP_046916560 , Streptomyces stelliscabiei
WP_012974625 , Azospirillum lipoferum
WP_011061742 , Pseudomonas protegens
WP_028946024 , Pseudomonas vranovensis
WP_027904437 , Pseudomonas sp.
WP_040799765 , marine actinobacterium
WP_059059635 , Leucobacter sp.
WP_051111359 , Mycobacterium sp.
WP_029420395 , Alicyclobacillus macrosporang...
WP_015234567 , Deinococcus peraridilitoris
AAR97488 , uncultured organism
WP_018708032 , Bacillus fordii
KYG75592 , Roseivirga spongicola
WP_062590735 , Roseivirga ehrenbergii
0.4

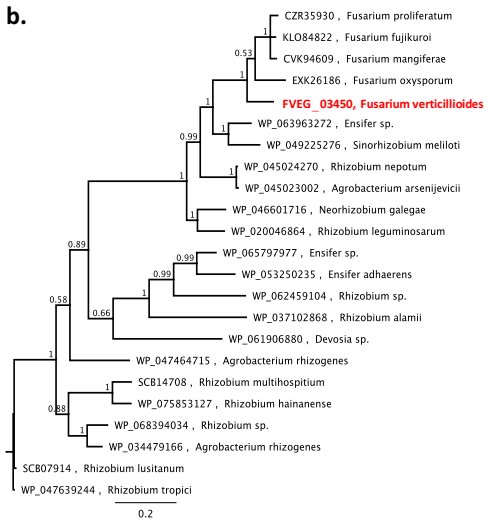
b.
CZR35930 , Fusarium proliferatum
KLO84822 , Fusarium fujikuroi
CVK94609 , Fusarium mangiferae
EXK26186 , Fusarium oxysporum
FVEG_03450, Fusarium verticillioides
WP_063963272 , Ensifer sp.
WP_049225276 , Sinorhizobium meliloti
WP_045024270 , Rhizobium nepotum
WP_045023002 , Agrobacterium arsenijevicii
WP_046601716 , Neorhizobium galegae
WP_020046864 , Rhizobium leguminosarum
WP_065797977 , Ensifer sp.
WP_053250235 , Ensifer adhaerens
WP_062459104 , Rhizobium sp.
WP_037102868 , Rhizobium alamii
WP_061906880 , Devosia sp.
WP_047464715 , Agrobacterium rhizogenes
SCB14708 , Rhizobium multihospitium
WP_075853127 , Rhizobium hainanense
WP_068394034 , Rhizobium sp.
WP_034479166 , Agrobacterium rhizogenes
SCB07914 , Rhizobium lusitanum
WP_047639244 , Rhizobium tropici
0.2

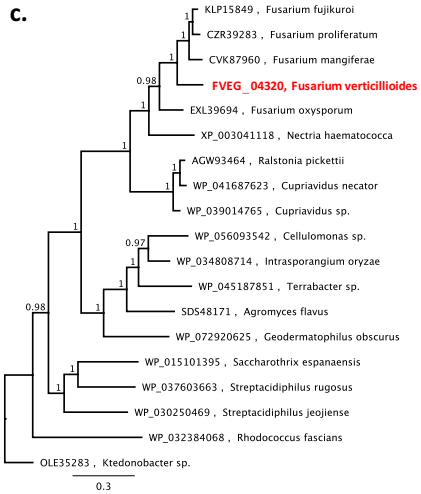
c.
KLP15849 , Fusarium fujikuroi
CZR39283 , Fusarium proliferatum
CVK87960 , Fusarium mangiferae
FVEG_04320, Fusarium verticillioides
EXL39694 , Fusarium oxysporum
XP_003041118 , Nectria haematococca
AGW93464 , Ralstonia pickettii
WP_041687623 , Cupriavidus necator
WP_039014765 , Cupriavidus sp.
WP_056093542 , Cellulomonas sp.
WP_034808714 , Intrasporangium oryzae
WP_045187851 , Terrabacter sp.
SDS48171 , Agromyces flavus
WP_072920625 , Geodermatophilus obscurus
WP_015101395 , Saccharothrix espanaensis
WP_037603663 , Streptacidiphilus rugosus
WP_030250469 , Streptacidiphilus jeojiense
WP_032384068 , Rhodococcus fascians
OLE35283 , Ktedonobacter sp.
0.3

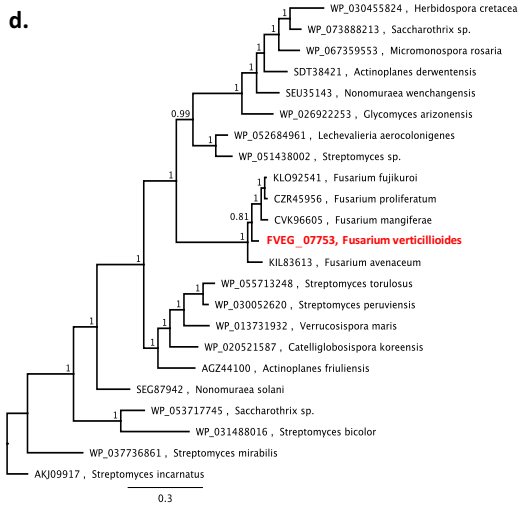
d.
WP_030455824 , Herbidospora cretacea
WP_073888213 , Saccharothrix sp.
WP_067359553 , Micromonospora rosaria
SDT38421 , Actinoplanes derwentensis
SEU35143 , Nonomuraea wenchangensis
WP_026922253 , Glycomyces arizonensis
WP_052684961 , Lechevalieria aerocolonigenes
WP_051438002 , Streptomyces sp.
KLO92541 , Fusarium fujikuroi
CZR45956 , Fusarium proliferatum
CVK96605 , Fusarium mangiferae
FVEG_07753, Fusarium verticillioides
KIL83613 , Fusarium avenaceum
WP_055713248 , Streptomyces torulosus
WP_030052620 , Streptomyces peruviensis
WP_013731932 , Verrucosispora maris
WP_020521587 , Catelliglobosispora koreensis
AGZ44100 , Actinoplanes friuliensis
SEG87942 , Nonomuraea solani
WP_053717745 , Saccharothrix sp.
WP_031488016 , Streptomyces bicolor
WP_037736861 , Streptomyces mirabilis
AKJ09917 , Streptomyces incarnatus
0.3

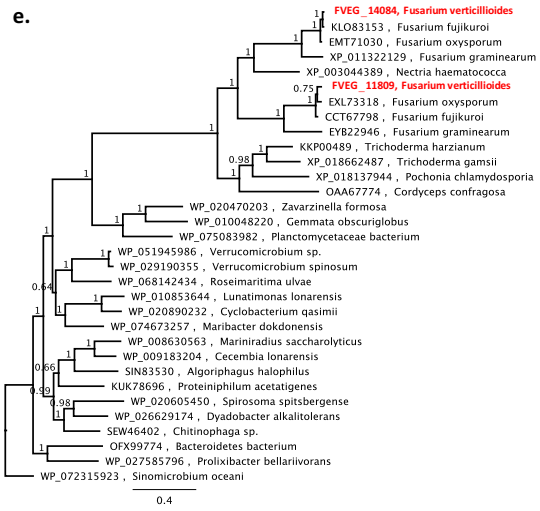
e.
FVEG_14084, Fusarium verticillioides
KLO83153 , Fusarium fujikuroi
EMT71030 , Fusarium oxysporum
XP_011322129 , Fusarium graminearum
XP_003044389 , Nectria haematococca
FVEG_11809, Fusarium verticillioides
EXL73318 , Fusarium oxysporum
CCT67798 , Fusarium fujikuroi
EYB22946 , Fusarium graminearum
KKP00489 , Trichoderma harzianum
XP_018662487 , Trichoderma gamsii
XP_018137944 , Pochonia chlamydosporia
OAA67774 , Cordyceps confragosa
WP_020470203 , Zavarzinella formosa
WP_010048220 , Gemmata obscuriglobus
WP_075083982 , Planctomycetaceae bacterium
WP_051945986 , Verrucomicrobium sp.
WP_029190355 , Verrucomicrobium spinosum
WP_068142434 , Roseimaritima ulvae
WP_010853644 , Lunatimonas lonarensis
WP_020890232 , Cyclobacterium qasimii
WP_074673257 , Maribacter dokdonensis
WP_008630563 , Mariniradius saccharolyticus
WP_009183204 , Cecembia lonarensis
SIN83530 , Algoriphagus halophilus
KUK78696 , Proteiniphilum acetatigenes
WP_020605450 , Spirosoma spitsbergense
WP_026629174 , Dyadobacter alkalitolerans
SEW46402 , Chitinophaga sp.
OFX99774 , Bacteroidetes bacterium
WP_027585796 , Prolixibacter bellariivorans
WP_072315923 , Sinomicrobium oceani
0.4

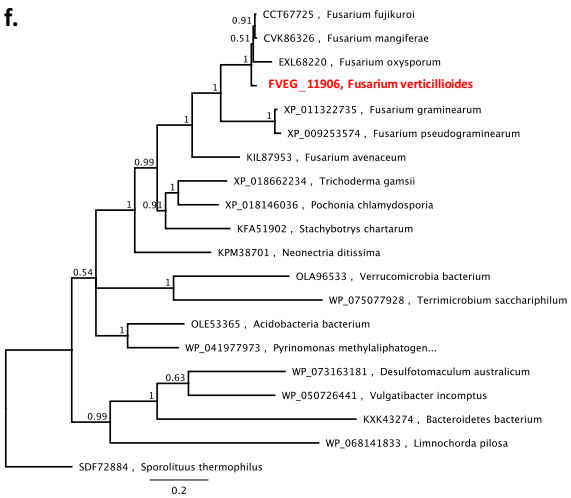
f.
CCT67725 , Fusarium fujikuroi
CVK86326 , Fusarium mangiferae
EXL68220 , Fusarium oxysporum
FVEG_11906, Fusarium verticillioides
XP_011322735 , Fusarium graminearum
XP_009253574 , Fusarium pseudograminearum
KIL87953 , Fusarium avenaceum
XP_018662234 , Trichoderma gamsii
XP_018146036 , Pochonia chlamydosporia
KFA51902 , Stachybotrys chartarum
KPM38701 , Neonectria ditissima
OLA96533 , Verrucomicrobia bacterium
WP_075077928 , Terrimicrobium sacchariphilum
OLE53365 , Acidobacteria bacterium
WP_041977973 , Pyrinomonas methylaliphatogen...
WP_073163181 , Desulfotomaculum australicum
WP_050726441 , Vulgatibacter incomptus
KXK43274 , Bacteroidetes bacterium
WP_068141833 , Limnochorda pilosa
SDF72884 , Sporolituus thermophilus
0.2

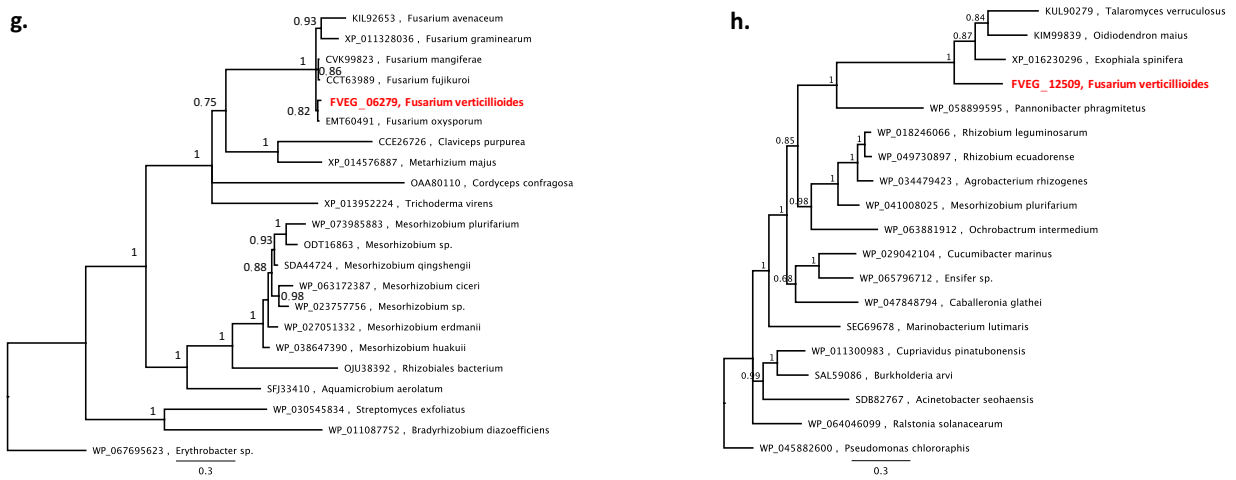

Supplemental Figure 2.3: Bayesian Inference of strong HGT candidates in *Fusarium verticillioides*.

Phylogenies were reconstructed by Bayesian Inference (BI) in the plugin version of MrBayes 3.2.6 in Geneious. The analysis was based on the best-fit amino acid substitution models predicted by MEGA v.6.06 (Table 2.5). MrBayes was run with the following parameters: 1,100,000 cycles with 4 heated chains, 0.2 heated chain temp, 200 subsampling frequency, 100,000 burn-in length, and 5502 random seed. Tip labels were displayed as accession number followed by organism. Genes in *F. verticillioides* are highlighted in red. Branch labels indicate the posterior probability. **a**: FVEG_00065; **b**: FVEG_03450; **c**: 04320; **d**: 07753; **e**: FVEG_11809/FVEG_14084; **f**: FVEG_11906; **g**: FVEG_06279; **h**: FVEG_12509.

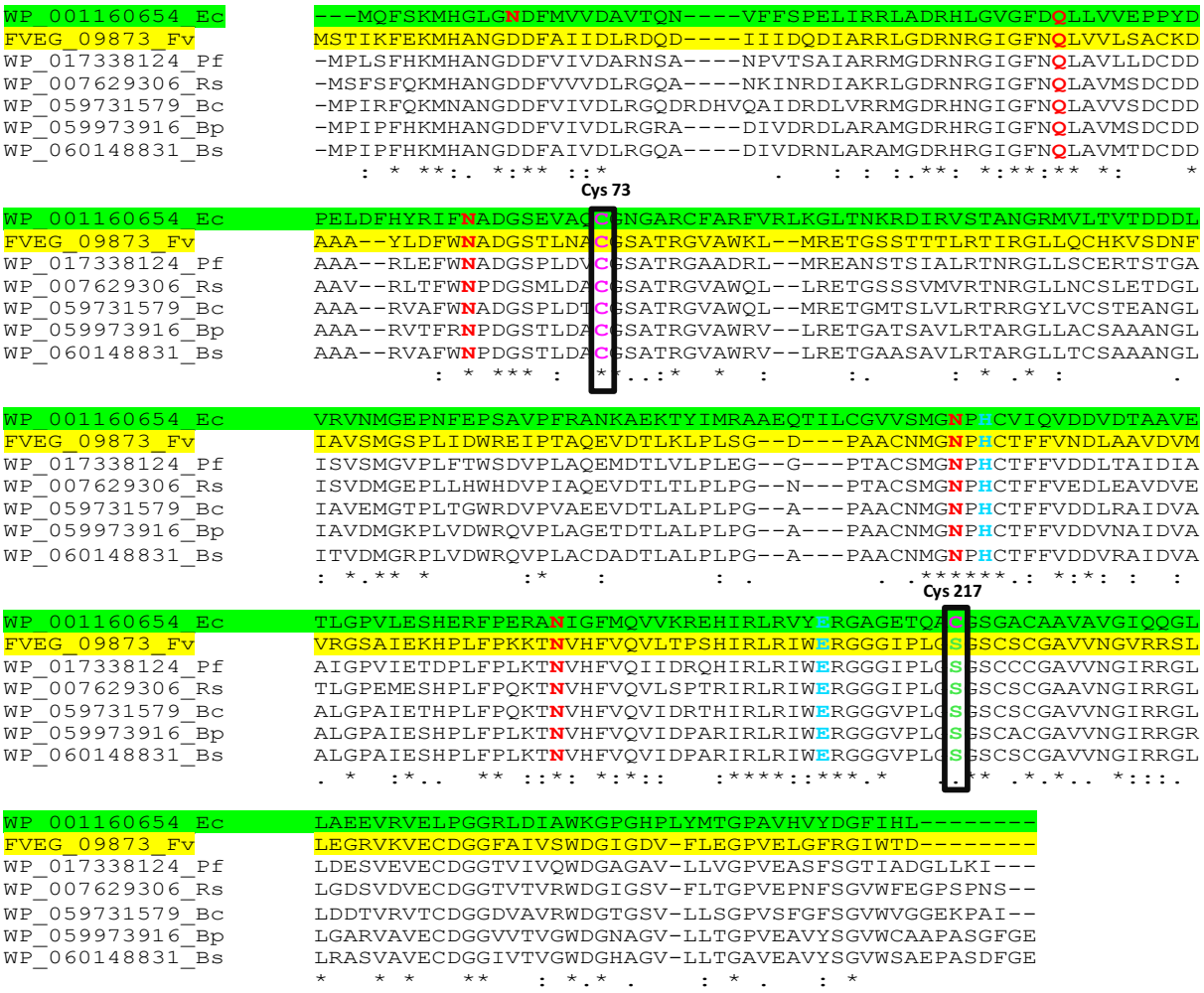

Supplemental Figure 2.4: Multiple sequences alignment of FVEG_09873 for characterizing key sites of being a diaminopimelate epimerase.

Multiple sequences alignment was done using Cluster Omega (http://www.ebi.ac.uk/Tools/msa/clustalo/). Except for FVEG_09873 (Fv), other protein sequences included in this study were WP_017338124 (Pf, organism: *Pseudomonas fluorescens* NCIMB 11764), WP_007629306 (Rs, organism: *Rhizobium sp.* CCGE 510), WP_059731579 (Bc, organism: *Burkholderia cepacia*), WP_059973916 (Bp, organism: *B. pyrrocinia*), WP_060148831 (Bs, organism: *B. stagnalis*) and WP_001160654 (Ec, organism: *Escherichia coli*). Those sequences and key sites were extracted from Uniprot (http://www.uniprot.org/). Sequences of FVEG_09873 and the reference were highlighted with yellow and green, respectively. Key sites for substrate binding (red), proton donor/acceptor (purple), catalytic activity (blue) were labelled with different colors. Two columns of cysteine residues (Cys73 and Cys217 in *E. coli* sequence) required for the two-base mechanism were highlighted in black rectangular frames, and the serine residues in the second column were colored in green. For labels at the bottom, an * (asterisk) indicates positions which have a single, fully conserved residue, a : (colon) indicates conservation between groups of strongly similar properties - scoring > 0.5 in the Gonnet PAM 250 matrix, a . (period) indicates conservation between groups of weakly similar properties - scoring =< 0.5 in the Gonnet PAM 250 matrix.

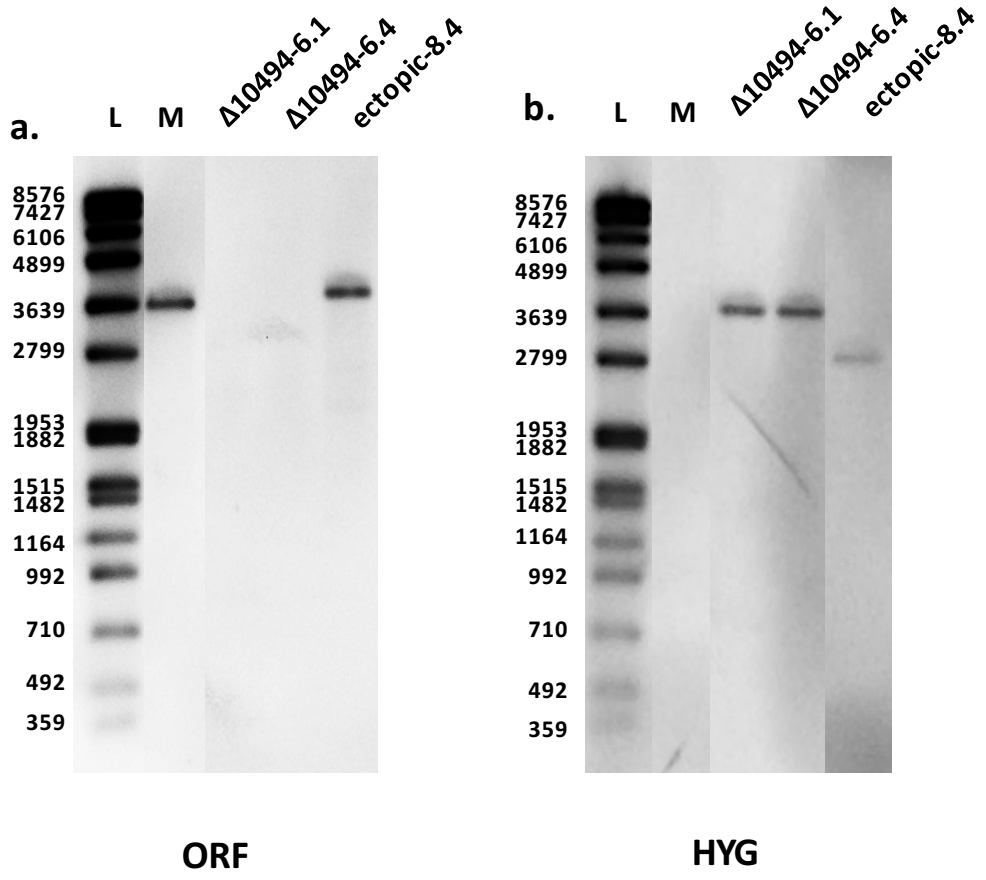

Supplemental Figure 2.5: Southern hybridization of FVEG_10494 gene deletion mutants and ectopic strains.

To confirm the genotype of gene deletion mutants, the whole genomic DNA of wild type (M), gene deletion strains (Δ10494-6.1 and Δ10494-6.4) and ectopic strain (ectopic-8.4) were tested using Southern hybridization. Membrane was visualized by the Alpha Innotech FluorChem 8000 digital imaging system for 40-minutes exposure using the FVEG_10494 ORF probe (**a**) and the hygromycin probe (**b**). DNA Molecular Weight Marker VII (Roche) was used and the size of bands was labelled on the left. Strained tested were labelled at the top. As shown in a, target fragment (size is about 3600 bp) containing the ORF of FVEG_10494 was detected in wild type and ectopic but not in mutants. Oppositely, in b, target fragment (size is about 3900 bp in mutants) containing the hygromycin cassette appeared in mutants and ectopic (with a different size) but not in wild type. Two rounds of southern hybridization support the successful knockout of FVEG_10494 in gene deletion mutates.

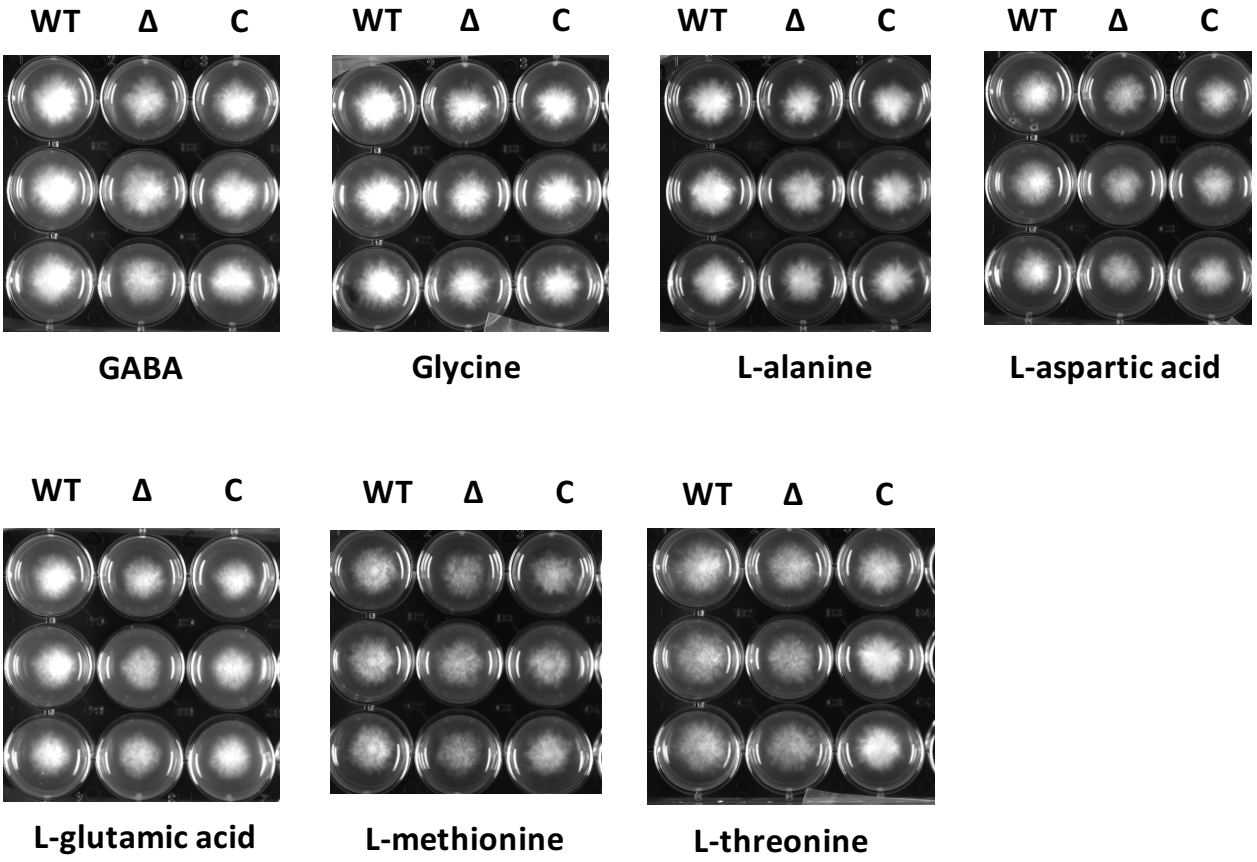

Supplemental Figure 2.6: Chemical screening for characterizing role of FVEG_10494 in γ-aminobutyric acid (GABA) and threonine metabolisms.

For chemicals involved in γ-aminobutyric acid (GABA) and threonine metabolisms, spores of M-3125 (WT), Δ10494-6.4 (Δ) and Δ10494-6.4::C3.1 (C) were inoculated on nitrogen-limited minimal media, which was supplemented with selected chemicals and then aliquoted to 6-well culture plates. Chemicals (Sigma-Aldrich) included are GABA (0.5 mg/ml), glycine (0.5 mg/ml), L-alanine (0.5 mg/ml), L-aspartic acid (0.45 mg/ml), L-glutamic acid (0.5 mg/ml), L-methionine (0.5 mg/ml), L-threonine (0.5 mg/ml), pyruvic acid (1 mg/ml), succinate (0.5 mg/ml), and pyridoxine (10 μg/ml). Pictures were taken 3 days after inoculation. Because the fungal mycelium grown on nitrogen-limited minimal media amended with pyruvic acid, succinate and pyridoxine were hardly visible, pictures were not shown here.

CHAPTER 3

CHARACTERIZATION OF TWO CATALASE-PEROXIDASE ENCODING GENES REVEALS DIFFERENTIAL RESPONSES TO *IN VITRO* VERSUS *IN PLANTA* OXIDATIVE CHALLENGES[2]

[2] Gao, S., et al. To be submitted to Molecular Plant Pathology.

Abstract

Catalase/peroxidases (KatGs) are a superfamily of reactive oxygen species (ROS)-degrading enzymes previously revealed via phylogenetic analysis to be horizontally acquired by ancient Ascomycota from bacteria. A subsequent gene duplication resulted in two KatG paralogues in ascomycetes: the widely distributed, intracellular group (KatG1), and the phytopathogen-dominated, extracellular group (KatG2). To functionally characterize *FvCP01* (KatG1) and *FvCP02* (KatG2) in the maize pathogen, *Fusarium verticillioides*, both single and double gene deletion mutants as well as the corresponding complemented strains were created and subjected to *in vitro* H_2O_2 sensitivity tests and quantitative reverse transcription-PCR (qRT-PCR) analyses under induced and non-induced conditions. We observed that both single mutant *ΔFvCP01* and double mutant *ΔFvCP01/ΔFvCP02*, when compared to the wild type, were much more sensitive to H_2O_2, while *ΔFvCP02* demonstrated moderately impaired tolerance. These results suggest that *FvCP01* is more important than *FvCP02* in alleviating oxidative stress from exogenous H_2O_2 in *F. verticillioides*. The *in vitro* transcriptional analysis of these two genes under H_2O_2 exposure showed induction of *FvCP01* but decreased expression of *FvCP02* in both mycelia and spores in the wild type, which supports the more significant role of *FvCP01* in defense against H_2O_2-derived oxidative stress. However, this transcriptional trend was reversed when the fungus was grown on germinating maize seed. This *in planta* exposure increased the expression of *FvCP02* but not *FvCP01*, indicating *FvCP02* may be responsive to the plant and that *FvCP01* may have a minor role during such interactions with the plant. Yet, in a *ΔFvCP02* mutant grown on the germlings, *FvCP01* was induced by more than three-fold, suggesting that *FvCP01* compensates for the loss of *FvCP02*. Given the differential responses of these two genes to *in vitro* versus *in*

planta challenges, we propose a model to illustrate the differing roles of *FvCP01* and *FvCP02* in the protective response against H_2O_2-derived oxidative stress in *F. verticillioides*.

Introduction

Among reactive oxygen species (ROS), hydrogen peroxide (H_2O_2) is the abundant representative as a by-product of aerobic metabolism [1]. In plants, ROS can be elevated under both abiotic and biotic stresses, such as the infection by phytopathogens [2]. As a diffusible small molecule that can readily cross biological membranes [3], H_2O_2 is heavily involved in fungus-plant interactions [4-6].

For maintaining normal metabolism, living cells need a homeostatically controlled redox potential, which is ensured by antioxidant defense systems consisting of ROS-removing molecules (e.g. glutathione) and various redox enzymes (e.g. superoxide dismutase and peroxidases) [4, 7]. Catalase/peroxidases (commonly abbreviated as KatGs) are bifunctional heme b-containing peroxidases with both efficient catalase and peroxidase activities [8]. Phylogenetic reconstruction suggested that the fungal KatG genes were horizontally acquired from the bacterial phylum Bacteroidetes to ancient Ascomycota [9]. Those fungal KatG genes were further duplicated [1], resulting in two distinct groups, KatG1 and KatG2 [8]. Representatives of KatG1 are intracellular proteins and distribute widely in fungi. Organelle separation and immunofluorescence microscopy have indicated that KatG1 encoded proteins are peroxisome-localized in several fungal species examined [10]. In contrast, members of the KatG2 group are likely to be extracellular proteins, indicated by the occurrence of an N-terminal signal sequence for secretion [8]. In addition, KatG2 genes, because they are mostly limited to fungal phytopathogens, are inferred to play a potential role in host-pathogen interactions. Evidence based on the functional characterization of the KatG2 in *Magnaporthe oryzae*

suggested a moderate contribution to defense against H_2O_2 produced by the host during the early stages of infection [11].

Fusarium verticillioides is an economically important maize pathogen causing stalk rot, ear rot and seedling blight [12]. Beyond its pathogenic nature, *F. verticillioides* may also colonize maize as a symptomless intercellular endophyte [13]. A major concern regarding this fungus is its capacity to produce the fumonisin class of mycotoxins, which threaten humans and animal health upon consumption of contaminated maize products [14]. In *F. verticillioides*, FVEG_10866 and FVEG_12888 encode KatG1 and KatG2, respectively. A previous report showed that both FVEG_10866 and FVEG_12888 were induced under H_2O_2 stress *in vitro* and deletion of FVEG_12888 weakened fungal oxidative resistance [15].

To functionally characterize FVEG_10866 and FVEG_12888 (referred to here as *FvCP01* and *FvCP02*, respectively) in *F. verticillioides*, we generated both single and double gene deletion mutants as well as the corresponding complemented strains. Through H_2O_2 sensitivity and quantitative reverse transcription-PCR (qRT-PCR) analyses, we observed distinct contributions made by *FvCP01* and *FvCP02* to *in vitro* versus *in planta* challenges and further propose a model to describe their roles in defending *F. verticillioides* against environmental H_2O_2 oxidative stress.

Materials and Methods

Fungal and bacterial strains, culture media and growth conditions

All strains of *F. verticillioides* created for this study are listed in Table 3.1. Wild-type strains FRC M-3125 and JFL A00999 were used for genetic modification and functional characterization. Strains were grown routinely on potato dextrose agar (PDA; Neogen Food

Safety, Lansing, MI, USA) at 27 °C in the dark or in potato dextrose broth (PDB; Neogen Food Safety) on the shaker incubator at 250 rpm and 27 °C in the dark for three days. For screening of transformed strains, PDA amended with 300 μg/ml geneticin (Life Technologies, Carlsbad, CA, USA) or 150 μg/ml hygromycin B (Invitrogen, Carlsbad, CA, USA) was used. Water agar (3 %) was used for single spore isolation of conidia and ascospores. Sexual crosses were carried out on carrot agar [16] at 27 °C with 16 h of light and 8 h of dark cycles. For H_2O_2 sensitivity tests, PDA was amended with a commercial 3 % H_2O_2 solution (0.88 mol/L; CVS pharmacy) to make final concentrations of 0, 2, 2.8, and 3.3 mM.

To construct gene deletion mutants, *Escherichia coli* (One Shot® MAX Efficiency® DH5α™-T1R, Invitrogen) was routinely grown in or on low Na (0.5 g/L) Luria Bertani (LB) medium amended with 100 μg/m spectinomycin (Thermo Fisher Scientific, Waltham, MA, USA) at 37 °C overnight. *Agrobacterium tumefaciens* strain AGL-1 was used for fungal transformation and cultured on Luria Bertani (LB) medium amended with 100 μg/m spectinomycin at 27 °C.

Construction of gene deletion mutants and complemented strains

Plasmids pSG10866_OSCAR and pSG12888_OSCAR were created as the gene deletion constructs for FVEG_10866 (*FvCP01*) FVEG_12888 (*FvCP02*) using the OSCAR method [17], respectively. Table 3.2 summarizes primers used in this study. Two pairs of primers for each gene were designed to amplify about 1 kb of the 5' (primers P7\1 and P7\2 for *FvCP01*; primers P7\13 and P7\14 for *FvCP02*) and 3' flanks (primers P7\3 and P7\4 for *FvCP01*; primers P7\15 and P7\16 for *FvCP02*) of the corresponding open reading frames (ORF). Each gene deletion construct contains the two flanks separated by a hygromycin resistance cassette, all between the T-DNA borders. By transformation and homologous recombination with the gene deletion

construct, the gene-coding sequences of both genes were deleted in wild-type strain M-3125. Hygromycin-resistant transformants were initially screened for the presence of the hygromycin resistance cassette (primers used: P1\14 and P1\15) and loss of the ORF of the corresponding target gene (primers P7\5 and P7\6 for *FvCP01*; primers P7\17 and P7\18 for *FvCP02*) to identify potential gene deletion mutants, which were further subjected to single-spore purification and confirmation PCR screening. The following criteria were used during PCR screening: 1) presence of hygromycin resistance cassette and the loss of ORF of corresponding target gene as described above; 2) presence of 5' flank of corresponding target gene (primers P7\1 and P1\4, a primer within the hygromycin resistance cassette, for *FvCP01*; primers P7\13 and P1\4 for *FvCP02*); 3) presence of integrated outer sequence upstream of the 5' flank (primers P1\4 and P7\7, a primer within the upstream sequence of the 5' flank of *FvCP01*; primers P1\4 and P7\19, a primer within the upstream sequence of the 5' flank of *FvCP02*); 4) presence of the 3' flank of the corresponding target gene (primers P7\4 and P1\3, a primer within the hygromycin resistance cassette, for *FvCP01*; primers P7\16 and P1\3 for *FvCP02*); 5) presence of integrated outer sequence downstream of the 3' flank (primers P1\3 and P7\8, a primer within the downstream sequence of the 3' flank of *FvCP01*; primers P1\3 and P7\20, a primer within the downstream sequence of the 3' flank of *FvCP02*. Deletion strains of each gene were confirmed by Southern hybridization as noted in the following section. The construction of the double mutant is described below.

Complemented strains were constructed via lithium acetate-mediated cotransformation [18]. The wild-type amplicon of *FvCP01* (total length 5116 bp) was generated with primers P7\9 and P7\10 to include the ORF (2787 bp) and the sequences both upstream, containing 1067 bp 5' of the predicted start codon, and downstream, containing 1262 bp 3' of the stop codon. The wild-

type amplicon of *FvCP02* (total length 4693 bp) was generated with primers P7\21 and P7\22 to include the ORF (2538 bp) and both upstream (985 bp) of the predicted start codon and downstream (1170 bp) of the stop codon. The mixture of the two wild-type amplicons and the linearized selection vector pGEN-NOT1 (1 µg, digested by *Not*I; New England Biolabs, Ipswich, MA, USA) was used to cotransform the competent cells of the double deletion mutant. Transformants were selected on 300 µg/ml geneticin. Complemented transformants were identified by PCR for the reintroduction of one or both target genes (primers P7\5 and P7\6 for *FvCP01*; primers P7\17 and P7\18 for *FvCP02*) and geneticin resistance cassette (primers P1\37 and P1\38). Strains that were singly complemented (with *FvCP01* or *FvCP02* only) and doubly complemented (with both *FvCP01* and *FvCP02*) were obtained.

Southern hybridization

Genomic DNA of *F. verticillioides* strains was extracted from four-day-old PDB liquid cultures using a DNeasy Plant Mini Kit (Qiagen Inc., Valencia, CA) following the manufacturer's protocol and digested with the restriction enzyme *Kpn*I. Probes that hybridized to the ORFs of the target genes (primers P7\5 and P7\6 for *FvCP01*; primers P7\17 and P7\18 for *FvCP02*) and the hygromycin cassette (primers P1\14 and P1\15), were amplified using the PCR DIG Probe Synthesis Kit (Roche Diagnostics, Indianapolis, IN, USA). A total of 1.5 µg digested genomic DNA was separated on a 0.8% agarose 0.5X Tris-Borate-EDTA gel and further blotted onto a Hybond-N+ nylon membrane (Amersham Biosciences, Buckinghamshire, England). After overnight blotting, the gel was post-stained (GelRed Nucleic Acid Stain, Phenix Research Products, Candler, NC, USA) and visualized to confirm the successful transfer of DNA. A mixture, containing *FvCP01* and *FvCP02* ORF probes, was used in the first round of hybridization following the DIG application manual (Roche Diagnostics). The probe-target

hybrids were detected by a chemiluminescent assay and visualized on an Alpha Innotech FluorChem 8000 digital imaging system for 30 min exposure (Supplemental Figure 3.1.a). The previous probe was stripped by alkaline buffer and the membrane was reprobed with the hygromycin probe. The probe-target hybrids were detected and visualized as above (Supplemental Figure 3.1.b).

Sexual crosses and double mutant construction

Female strains were grown on carrot agar at 27 °C for 7 days in the dark. One ml of 3-day-old PDB culture of the male strain was spread gently and evenly over the female growth. Crosses were carried out in triplicate. The fertilized plates were incubated at 27 °C with 16 h of light and 8 h of dark. After 2 to 3 weeks, the cirrhi (spore exudate) were visible at the tip of the perithecia and were transferred with an inoculation needle into 700 µl of sterile water to disperse the ascospores. A 50 µl aliquot of ascospore suspension was plated onto 3% water agar for single spore isolation of progeny.

Double mutants of *FvCP01* and *FvCP02* were obtained by two rounds of sexual crosses as described above (Supplemental Figure 3.2) in which *MAT1-1* and *MAT1-2* strains were used as male and female, respectively. A first cross was done by mating the single mutant of Δ*FvCP01 (Δfvcp01/MAT1-1)* with the wild-type strain A00999 (*MAT1-2*). From this cross a progeny strain, *F1-ΔFvCP01* (*Δfvcp01*/*MAT1-2*), was isolated and crossed in round two with the single mutant of Δ*FvCP02* (*Δfvcp02*/*MAT1-1*). Progeny obtained from this second round cross were PCR-screened for hygromycin resistance and loss of *FvCP01* and *FvCP02* to obtain verified double deletion mutants. One such progeny was used in subsequent experimentation.

H_2O_2 sensitivity test

For mycelial inoculum, an agar plug (created using a 4-mm cork borer) was taken from a one-week-old PDA culture of tested strains and inverted onto 100 mm Petri plates containing PDA or MM amended with 0, 5, 10 and 15 mM H_2O_2. Triplicate plates were inoculated for each treatment. The diameters of fungal colonies were measured routinely three and five days after incubation at 27 °C in the dark. This experiment was repeated two and three times on PDA and MM, respectively. Statistical differences between strains and treatments were estimated by ANOVA using SAS 9.4 (SAS Institute Inc., Cary, NC, USA).

For conidial inoculum, spores of all tested strains were harvested from three-day-old PDB liquid cultures by filtering and washing and further diluted to 10^6 conidia ml. For each strain, triplicate 3 µl spore suspension drops were spotted onto 100 mm Petri plates containing PDA amended with 0, 2, 2.8 and 3.3 mM H_2O_2. Colony diameters were measured four days after incubation at 27 °C in the dark. This experiment was repeated three times. Statistical differences between strains treated were estimated by ANOVA using SAS 9.4 (SAS Institute Inc., Cary, NC, USA).

Copy number characterization

To characterize the copy number of *FvCP01* and *FvCP02* in three complemented strains, genomic DNA was extracted from three-day-old PDB liquid culture using the DNeasy Plant Mini Kit following the manufacturer's protocol. Wild type (positive control) and double mutant (negative control) were also extracted as above. Quantitative PCR (qPCR) was conducted using the Platinum® Taq DNA Polymerase (Thermo Fisher Scientific) and SYBR® Green I dye (Thermo Fisher Scientific). Primers for detecting the ORFs of target genes (primers P7\11 and

P7\12 for *FvCP01*; primers P7\23 and P7\24 for *FvCP02*) were used. The data were normalized to β-tubulin as a reference gene and calculated via $2^{-\Delta\Delta CT}$ method [19].

Virulence assay and fumonisin (FB)/ergosterol extraction

Seeds of sweet corn Silver Queen (W. Atlee Burpee & Co., Warminster, PA, USA) were surface sterilized, imbibed, and heat shocked as previously described [20]. For each fungal strain, 50 seeds were placed in a 100 x 15 mm petri dish with 10 mL of $1x10^4$ spores/mL spore suspension. For uninoculated control, 10 mL of sterile water was added to the seeds. After overnight incubation in the dark at 27 ℃, seeds were planted in autoclaved potting mix (Fafard 2 Mix, Agawam, MA, USA) in 4-inch azalea pots. Three pots of 10 seed per pot were included for each treatment. Pots were placed in plastic saucers and watered from below on days 2, 4, and 6 after planting. All subsequent watering was as needed and added to the soil from below. Plants were grown for 14 days in a growth chamber with 16 hour days at 30 ℃ and 8 hour nights at 20 ℃. Upon harvesting, above-ground plant tissues were collected by cutting the stem at the soil line. Plant height and fresh weight were measured for each seedling from each pot. Symptoms were visually inspected and evaluated according to the symptom severity scale (Supplemental Figure 3.4). This experiment was repeated three times.

The roots of seedlings were collected for the extraction of fumonisin and ergosterol. Root system of seedlings was carefully removed from the soil and washed in ice-water bath to remove any remaining soil. The root masses obtained from one pot were grouped as one replicate for each treatment and freeze-dried. The lyophilized tissue was grounded into a fine powder using a coffee grinder. A total of 10 mg of each sample material was weighed for the fumonisin extraction. The leftover was saved for ergosterol extraction. For extracting fumonisin, each sample was immersed in 1mL of acetonitrile:water (1:1) with 5% formic acid and shaken for 3

hours. Supernatants were filtered (0.22 μm), diluted 10-fold in acetonitrile:water (3:7) with 1% formic acid and analyzed by liquid chromatography-mass spectrometry for fumonisin B1, B2, and B3. For extracting ergosterol, each sample was immersed in 5 mL of 0.07M potassium hydroxide in methanol and shaken at 250 rpm for 1 hour. Followed by sonication and filtration, the extracts obtained were neutralized with 150 μl of 0.1M hydrogen chloride. The neutralized samples were loaded on C18 Sep-Pak Cartridges (Waters) and eluted with 1 ml of isobutanol. All eluted samples were stored at 4 ℃ and analyzed by liquid chromatography-mass spectrometry for ergosterol within 24 hours to prevent degradation. These experiments were repeated twice.

***In vitro* and *in planta* qRT-PCR analysis**

For control *in vitro* samples, three-day-old PDB cultures were filtered through cheesecloth to separate the spores and mycelia which were processed and analyzed separately. The spore suspension was pelleted by centrifugation at 10,000 g for 5 min at 4 °C and resuspended in lysis buffer (PureLink® RNA Mini Kit, Thermo Fisher Scientific) and transferred to the lysing matrix D tubes (MP Biomedicals, LLC, Santa Ana, CA, USA). Mycelia were transferred from the cheesecloth to the lysing matrix D tubes and resuspended in lysis buffer. Samples were homogenized using a FastPrep-24™ 5G Instrument (MP Biomedicals) at 6 m/sec with two pulses of 30 seconds and a one min pause between pulses. Total RNA was then extracted according to the manufacturer's instructions (PureLink® RNA Mini Kit, Thermo Fisher Scientific). For treated *in vitro* samples, three-day-old PDB cultures were challenged in 2 mM H_2O_2 for 2 h followed by RNA extraction as stated above. Extractions were carried out with 3 biological replicates for each treatment.

For *in planta* analysis, the control samples were extracted by adding one ml of three-day-old PDB cultures to lysing matrix D tubes (MP Biomedicals) and then centrifuged at 10,000 x g

for 5 min at 4 °C and the supernatant discarded. Lysis buffer (PureLink® RNA Mini Kit) was immediately added to the fungal pellets and the samples were homogenized using the FastPrep-24™ 5G Instrument (MP Biomedicals) at a speed of 6 m/sec and two segments of homogenization for 30 seconds with 1 min rest in between. Total RNA was extracted with the PureLink kit as described above. Three biological replicates were included for each strain. For *in planta* samples, seeds of sweet corn Silver Queen (W. Atlee Burpee & Co.) were surface sterilized, imbibed, and heat shocked as previously described [20]. A total of 50 seeds were placed in a 100-mm petri dish for each strain. Ten mL of 10^4 spores/mL suspension prepared from three-day-old PDB cultures of wild-type strain M-3125 or single deletion mutants, Δ*FvCP01* or Δ*FvCP02*, were added to their respective seeds. After 18 h incubation at 27 °C in the dark, germinated seeds were transferred onto wet filter membrane for additional 72 h incubation under the same conditions. After 90 h post inoculation (hpi), germinated seedlings with observable fungal mycelium were ground in liquid nitrogen. Total RNA was extracted with the PureLink kit as described above. Four biological replicates were included for each strain.

For quantitative reverse transcription-PCR (qRT-PCR), RNA samples were digested with DNase (TURBO DNA-free™ Kit, Thermo Fisher Scientific) and checked for quality (RNA integrity number > 6.0) using an Agilent 2100 Bioanalyzer (Agilent Technology, Waldbronn, Germany). Complete DNA digestion was confirmed by conventional PCR targeting the reference gene β-tubulin. Complementary DNA synthesis and qRT-PCR were carried out using a one-step qRT-PCR Kit (SuperScript® III Platinum® SYBR® Green One-Step qRT-PCR Kit, Thermo Fisher Scientific) in triplicate. The data were normalized to the expression level of β-tubulin and calculated via $2^{-\Delta\Delta CT}$ method. The primers used for this assay are shown in Table 3.2.

Results

Both *FvCP01* and *FvCP02* contribute to *in vitro* H_2O_2 tolerance but differential trends among strains were observed using mycelial and conidial inocula.

Given the predicted function of *FvCP01* and *FvCP02,* we evaluated their individual and combined effects on H_2O_2 sensitivity via the *in vitro* bioassays using both mycelial and spore inocula. As shown in Figure 3.1 and Figure 3.2, growth differences among strains were progressively more obvious with increasing H_2O_2 concentrations. When using the mycelia as the initial inoculum on both MM (Figure 3.1 A and B) and PDA (Figure 3.1 C), regardless of medium, both single mutants showed moderately impaired tolerance (Δ*FvCP01* is more resistant than Δ*FvCP02*) to H_2O_2 *in vitro* compared to wild type, while the double mutant was dramatically sensitive to H_2O_2, suggesting that these two genes confer resistance to exogenous H_2O_2. In addition, the growth rate of complemented strains on PDA showed recovered H_2O_2 resistance comparable to the corresponding strains of similar genotype: the partially complemented double mutant strain ΔΔ::*FvCP02* was similar to Δ*FvCP01*, the partially complemented double mutant strain ΔΔ::*FvCP01* was similar to Δ*FvCP02*, and the double complemented strain ΔΔ::*FvCP01/FvCP02* was similar to wild type (Figure 3.1 C).

For a more homogeneous inoculum and to avoid the transfer of media in the agar plugs, we then used spores as the initial inoculum. As shown in Figure 3.2 A and B, the most impacted strains were the single mutant Δ*FvCP01*, the partially complemented double mutant strain ΔΔ::*FvCP02*, and the double mutant Δ*FvCP01*Δ*FvCP02*, all three of which were barely able to grow on medium with 3.3 mM H_2O_2. In addition, Δ*FvCP02* and ΔΔ::*FvCP01* were almost as resistant as wild type to 2.4 mM and 2.8 mM H_2O_2, yet on 3.3 mM these two strains grew significantly worse than M-3125 and the double complemented strain ΔΔ::*FvCP01/FvCP02*.

Thus we found *in vitro* H_2O_2 tolerance to rank as follows: ΔΔ::*FvCP01/FvCP02* > M-3125 > Δ*FvCP02* ≈ ΔΔ::*FvCP01* > Δ*FvCP01* ≈ ΔΔ::*FvCP02* ≈ Δ*FvCP01*Δ*FvCP02*. These results suggest that although both genes contribute to H_2O_2 tolerance, *FvCP01* is more important than *FvCP02* in alleviating oxidative stress resulting from exogenous H_2O_2.

Given the enhanced growth of the double complemented strain ΔΔ::*FvCP01/FvCP02* compared to M-3125 on ≥ 2.8 mM H_2O_2, we hypothesized that multiple copies of wild-type amplicons might have been incorporated into the genome of ΔΔ::*FvCP01/FvCP02* during transformation. We therefore determined the copy number of *FvCP01* and *FvCP02* in the three complemented strains using qPCR. Results (Supplemental Figure 3.3) show the presence of one copy of wild-type target gene in the corresponding singly complemented strains ΔΔ::*FvCP01* and ΔΔ::*FvCP02*. In contrast, two copies of *FvCP01* and one copy of *FvCP02* were found in the double complemented strain ΔΔ::*FvCP01/FvCP02*. This result suggests that the additional resistance observed in the double complemented strain is due to the extra copy of *FvCP01*.

FvCP01* and *FvCP02* may play a minor role in virulence of *F. verticillioides

In order to determine the impact of *FvCP01* and *FvCP02* on virulence in *F. verticillioides*, the pathogenicity of deletion strains as well as their corresponding complemented strains were tested by inoculating seeds of the susceptible maize cultivar “Silver Queen”. Seedling fresh shoot length and weight were measured 14 days after planting (dap). Symptoms were visually inspected and evaluated according to a symptom severity scale (Supplemental Figure 3.4). Statistical analyses suggest the fresh shoot length is the most robust parameter. Among the three independent experimental repeats (Figure 3.3), A00999 seems to be less virulent than M-3125. In addition, we did not observe consistent significantly reduced virulence of the two single-gene mutants compared to M-3125, while the fresh shoot length of the double

mutant Δ*FvCP01*Δ*FvCP02* was moderately and significantly longer than that of M-3125 (Figure 3.3.A and 3.3.B). Although the weakened virulence of the double mutant can result from the loss of two genes, its mixed genotype (75% from M-3125 and 25% from A00999) can't be fully ruled out. To address this issue, we also included the three complemented strains (derived from the double mutant) in the virulence assays but did not obtain a consistent disease severity trend across those strains. The inconsistency may be caused by biological variance of maize seeds and the unclear influence of mixed genotype on the fungus. In addition, fumonisin content, an indicator of virulence [20], and ergosterol content, a measure of fungal mass, were extracted from root tissues inoculated with tested strains. Again, we did not find consistent decreased fumonisins production or ergosterol content (data not shown) in mutants for these two genes individually or in combination.

***FvCP01* was moderately induced *in vitro* under H_2O_2 challenge**

Since *FvCP01* and *FvCP02* differ in their efficacy to counter *in vitro* exogenous H_2O_2 oxidative stress, we determined the *in vitro* transcriptional response of both genes under H_2O_2 exposure in two different fungal structures. Figure 3.4 summarizes results obtained from mycelia (left) and spores (right) of wild-type strain M-3125 that were treated with or without 2 mM H_2O_2 for 2 h. The same trend of differential transcription was observed from mycelia and spores. *FvCP01* demonstrated moderate transcriptional increase upon H_2O_2 treatment. However, the transcriptional level of *FvCP02* was reduced by H_2O_2 exposure. The opposing transcriptional responses of these two genes suggests that *FvCP01* but not *FvCP02* is primarily responsible for degrading exogenous H_2O_2. This observation is consistent with the major role of *FvCP01* in countering *in vitro* H_2O_2-derived oxidative stress.

In planta transcriptional analysis shows a reversed trend of *FvCP01* and *FvCP02* expression

The fungal KatG2 extracellular protein-encoding genes are mostly found in phytopathogens [8], so we hypothesized that the KatG2 *FvCP02* would be more protective of host derived oxidative challenge. *In planta* transcriptional analysis (Figure 3.5) of *FvCP01* and *FvCP02* were conducted on 90 hpi germlings inoculated with either wild-type strain M-3125 or single deletion mutants Δ*FvCP01* or Δ*FvCP02*. In M-3125-inoculated germlings, contrary to the trend of the *in vitro* study (Figure 3.4), *FvCP02* showed elevated transcription while *FvCP01* showed reduced transcription compared to PDB growth control. This reversed phenomenon supports the hypothesis that *FvCP02* is more responsive to the *in planta* oxidative stress compared to *in vitro* conditions. A similar degree of up-regulation of *FvCP02* was also observed in the germlings inoculated with Δ*FvCP01*, indicating the loss of *FvCP01* had minimal, if any, impact on *FvCP02* response *in planta*. However, as shown in germlings inoculated with Δ*FvCP02*, when *FvCP02* was deleted, *FvCP01* was instead transcribed at a higher level than seen in wild type, supporting that *FvCP01* may compensate for the lack of *FvCP02 in planta*.

Discussion

In this study, we functionally characterized two catalase-peroxidase-encoding genes by an *in vitro* H_2O_2 sensitivity assay and through *in vitro*/*in planta* qRT-PCR analyses. Firstly, inferred by differing tolerance of wild-type and modified strains on H_2O_2 amended medium using different types of inocula, we concluded that both *FvCP01* and *FvCP02* contribute to H_2O_2 detoxification although differential trends among strains were observed using mycelia and spores as the initial inocula. Secondly, two sets of qRT-PCR analyses conducted *in vitro* and *in planta*

suggest differential reactions of these two genes to *in vitro* and *in planta* H_2O_2 oxidative stress. We therefore propose a model illustrating roles of *FvCP01* and *FvCP02* in the battle against H_2O_2 oxidative stress in conidial inoculum (Figure 3.6). The prerequisites of this model are that the protein encoded by *FvCP01*, designated as FvCP01, and the protein encoded by *FvCP02*, designated as FvCP02, are intracellular and extracellular catalase-peroxidases, respectively. Under a normal condition of low ROS activity (Figure 3.6.A), the proteins FvCP01 (yellow diamond) and FvCP02 (red triangle) are constitutively expressed as suggested by transcriptional analysis (Supplemental Figure 3.5). Upon *in vitro* exogenous H_2O_2 oxidative stress in wild type (Figure 3.6.B), the limited abundance of extracellular FvCP02 presumably can only degrade a portion of the added large pool of H_2O_2. The remaining H_2O_2 is expected to diffuse into the cell, leading to the overexpression of the intracellular FvCP01, and is therefore fully degraded. While the wild-type fungus infects the susceptible germinated corn germlings (Figure 3.6.C), *FvCP02* is induced due to the perception of plant-derived H_2O_2 and/or a currently unknown host signal, resulting in the generation of adequate FvCP02 to eliminate H_2O_2, resulting in decreased production of FvCP01. However, in the *ΔFvCP02* gene deletion mutant (Figure 3.6.D), owing to the loss of extracellular protection, plant-derived H_2O_2 enters the cell and *FvCP01* is accordingly up-regulated to guarantee efficient H_2O_2 scavenging.

Differential H_2O_2 resistance trends of tested strains were observed using both mycelial and conidial inocula. Firstly, spores appear to be more sensitive to H_2O_2 than mycelia based on our data, which supports the more dramatic transcriptional change in spores exposed to *in vitro* H_2O_2. Secondly, *FvCP01* seems to be less important than *FvCP02* using the mycelial inoculum while a reversed trend appears using the conidial counterpart. The same conclusion is also suggested by the response of double complemented strain which harbors two and one copy of

FvCP01 and *FvCP02*, respectively. In the test using conidial inoculum, an extra copy of *FvCP01* makes the double complemented strain even more tolerant than wide type but negligibly contributes to enhanced resistance in the mycelial inoculum test. An explanation of the stated inconsistencies is the differential capability in exploiting *FvCP02* in degrading exogenous H_2O_2 between mycelia and spores. Although *FvCP01* and *FvCP02* can be constitutively transcribed in both types of structures, *FvCP02* may be more readily translated and secreted for ROS scavenging by mycelia in comparison to spores. To address this possibility, a fluorescent fusion protein may be able to elucidate the localization of *FvCP02* under different developmental stages and even relatively quantify the amount of this enzyme secreted. On the other hand, without help from the secreted FvCP02, spores heavily rely on FvCP01 for alleviating oxidative stress. When the spores are struggling with H_2O_2 challenge, spore germination and subsequent growth were heavily compromised if *FvCP01* is deleted. The primary susceptibility of spores to H_2O_2 may be carried over until the formation of a colony, therefore reflecting the roles of these two proteins in protecting the fungus from oxidative stress.

Previously, it was reported [15] that the deletion of FVEG_12888 (*FvCP02*) in *F. verticillioides* reduced tolerance to H_2O_2, which agrees with our *in vitro* H_2O_2 sensitivity test (Figure 3.1 and Figure 3.2). In addition, the authors report that both FVEG_10866 (*FvCP01*) and FVEG_12888 were induced in both mycelia and spores under exogenous H_2O_2 stress (challenged with 1.96 mM H_2O_2 for 2 h in yeast extract-peptone-glycerol (YPG) medium). This result differs from our observation of *in vitro* transcriptional analysis (treated with 2 mM H_2O_2 for 2 h in PDB) in that 1) FVEG_12888 showed reduced transcriptional level under oxidative stress and 2) FVEG_10866 was upregulated when treated with H_2O_2 but with a much lower degree of induction in both mycelia and spores. We observed a fold change of < 3 for FVEG_10866 in our

study versus > 20 fold-change by Lan et al., 2014. To explore this inconsistency, we repeated the same experiment in YPG. In addition, we tested two incubation periods (15 min and 2 h), and four H_2O_2 concentrations (2, 4, 5 and 10 mM). We also tested additional target genes (FVEG_08420, encoding a glutathione transferase, and FVEG_05591, encoding a catalase). All these results are shown in Supplemental Figure 3.6. However, we still did not obtain similar fold change trends as previously reported. This variation may result from lab conditions or perhaps the source of the strains.

According to our *in vitro* and *in planta* transcriptional analyses, *FvCP01* appears largely involved in non-host-mediated H_2O_2 stress while *FvCP02* is mainly responsible for effective response to oxidative challenge derived from the host. This result is consistent with the predominant distribution of KatG2 genes in phytopathogens. In addition, the unexpected induction of *FvCP01* in the *ΔFvCP02* mutant grown on the maize germlings suggests that *FvCP01* compensates for the loss of *FvCP02* during host-associated growth. Those conclusions further imply that *FvCP01* and *FvCP02* may function as main players in two independent but coordinated redox pathways, perhaps targeting endogenous versus exogenous, and plant-specific oxidative stress responses, respectively. When necessary, *FvCP01* can, at least partially, compensate for the loss of *FvCP02*. These pathways are plausibly part of the "ROS gene network", consisting of ROS-degrading and ROS-producing proteins. This ROS gene network has been described in *Arabidopsis* with more than 150 genes potentially involved [21] and in some microorganisms on a smaller scale [22]. Additionally, we observed upregulation of these two genes in three FVEG_02853 (*FvStuA*) single gene deletion mutants (unpublished data) in liquid GYAM medium [23]. The gene *FvStuA* encodes a putative transcription factor belonging to the APSES (ASM-1, Phd1, StuA, EFG1, and Sok2) protein family, which contains

transcription factors regulating various cellular development and biological processes in fungi [24-26]. This suggests the *FvCP01* and *FvCP02* or even the "ROS gene network" may be fine-tuned by "universal" gene regulators, such as *FvStuA*, in *F. verticillioides*.

The contrary roles of ROS in some fungal phytopathogens, depending on their lifestyles, have been observed [4, 27]. It has been reported that the biotrophic pathogens are suppressed by H_2O_2 accumulation [28, 29], while necrotrophic pathogens may stimulate and/or even benefit from the oxidative burst, the massive ROS production response upon pathogen ingress [30-32]. In our study, the up-regulation of *FvCP02* in *F. verticillioides* grown on germlings suggests defense against *in planta* ROS during a potential necrotrophic stage. In addition, a previous study showed that the infiltration of catalase led to reduced ROS accumulation in the host during the necrotrophic stage of *Septoria tritici* and improved growth of the pathogen [33]. The above reveal that fungi can live in plants under oxidative stress, especially in the case of necrotrophs, but may not depend on the production of ROS to infect the hosts [33].

In many cases, ROS-scavenging systems are not essential for fungal virulence. For example, in the biotrophic pathogen *Claviceps purpurea*, deletion of genes encoding a putatively secreted catalase and a superoxide dismutase, only slightly decreased fungal virulence [34, 35]. Similarly, loss of an extracellular catalase in the necrotrophic fungal pathogens *Botrytis cinerea* and *Cochliobolus heterostrophus* did not demonstrate reduced virulence on hosts even though corresponding mutants were less resistant than the wild-type strain to H_2O_2 *in vitro* [32, 36]. Another example is the characterization of the KatG2 representative in *M. oryzae* indicating that this gene plays a role in oxidative stress resistance *in planta* at the early stages of infection but not in overall fungal virulence [11]. In the assay conducted in this study, we did not observe consistently significant weakened virulence of both single mutants compared to the wild type,

although two out of three independent results showed moderately reduced virulence of the double mutant. In addition, fumonisin content analysis did not suggest consistent decreased fumonisins production (data not shown) in mutants for these two genes individually or in combination, suggesting *FvCP01* and *FvCP02* contribute mildly to the seedling disease and fumonisins biosynthesis in *F. verticillioides*. Given the correlation of severity of above-ground symptoms with fumonisin content in roots [37], the lack of effect of *FvCP01* or *FvCP02* on fumonisin production may obscure their roles in virulence toward maize seedlings.

In summary, we revealed the distinct but coordinated functions of two *F. verticillioides* catalase-peroxidases-encoding genes *in vitro* and *in planta*. Consistent with their phylogenetic and subcellular localization attributes, *FvCP01* and *FvCP02* are possibly two major players in the "ROS gene network" with preferential and spatially differentiated oxidative stress responses.

References

1. Zamocky, M., et al., *Molecular evolution of hydrogen peroxide degrading enzymes.* Arch Biochem Biophys, 2012. **525**(2): p. 131-44.
2. Apel, K. and H. Hirt, *Reactive oxygen species: metabolism, oxidative stress, and signal transduction.* Annu Rev Plant Biol, 2004. **55**: p. 373-99.
3. Gadjev, I., J.M. Stone, and T.S. Gechev, *Chapter 3: Programmed Cell Death in Plants: New Insights into Redox Regulation and the Role of Hydrogen Peroxide*, in *International Review of Cell and Molecular Biology*. 2008, Academic Press. p. 87-144.
4. Heller, J. and P. Tudzynski, *Reactive oxygen species in phytopathogenic fungi: signaling, development, and disease.* Annu Rev Phytopathol, 2011. **49**: p. 369-90.
5. Lehmann, S., et al., *Reactive oxygen species and plant resistance to fungal pathogens.* Phytochemistry, 2015. **112**: p. 54-62.
6. Nanda, A.K., et al., *Reactive oxygen species during plant-microorganism early interactions.* J Integr Plant Biol, 2010. **52**(2): p. 195-204.
7. Breitenbach, M., et al., *Oxidative stress in fungi: its function in signal transduction, interaction with plant hosts, and lignocellulose degradation.* Biomolecules, 2015. **5**(2): p. 318-42.
8. Zamocky, M., P.G. Furtmuller, and C. Obinger, *Two distinct groups of fungal catalase/peroxidases.* Biochem Soc Trans, 2009. **37**(Pt 4): p. 772-7.
9. Zamocky, M., P.G. Furtmuller, and C. Obinger, *Evolution of structure and function of Class I peroxidases.* Arch Biochem Biophys, 2010. **500**(1): p. 45-57.
10. Zamocky, M., et al., *Intracellular targeting of ascomycetous catalase-peroxidases (KatG1s).* Arch Microbiol, 2013. **195**(6): p. 393-402.
11. Tanabe, S., et al., *The Role of Catalase-Peroxidase Secreted by Magnaporthe oryzae During Early Infection of Rice Cells.* Molecular Plant-Microbe Interactions, 2010. **24**(2): p. 163-171.
12. Munkvold, G.P., D.C. McGee, and W.M. Carlton, *Importance of Different Pathways for Maize Kernel Infection by Fusarium moniliforme.* Phytopathology, 1997. **87**(2): p. 209-17.
13. Bacon, C.W. and D.M. Hinton, *Symptomless endophytic colonization of maize by Fusarium moniliforme.* Canadian Journal of Botany, 1996. **74**(8): p. 1195-1202.
14. Bacon, C.W., A.E. Glenn, and I.E. Yates, *Fusarium verticillioides: managing the endophytic association with maize for reduced fumonisins accumulation.* Toxin Reviews, 2008. **27**(3-4): p. 411-446.
15. Lan, N., et al., *Coordinated and distinct functions of velvet proteins in Fusarium verticillioides.* Eukaryot Cell, 2014. **13**(7): p. 909-18.
16. Klittich, C.J.R. and J.F. Leslie, *Nitrate Reduction Mutants of Fusarium Moniliforme (Gibberella Fujikuroi).* Genetics, 1988. **118**(3): p. 417-423.
17. Paz, Z., et al., *One step construction of Agrobacterium-Recombination-ready-plasmids (OSCAR), an efficient and robust tool for ATMT based gene deletion construction in fungi.* Fungal Genet Biol, 2011. **48**(7): p. 677-84.
18. Bourett, T.M., et al., *Reef coral fluorescent proteins for visualizing fungal pathogens.* Fungal Genet Biol, 2002. **37**(3): p. 211-20.
19. Livak, K.J. and T.D. Schmittgen, *Analysis of Relative Gene Expression Data Using Real-Time Quantitative PCR and the 2−ΔΔCT Method.* Methods, 2001. **25**(4): p. 402-408.
20. Glenn, A.E., et al., *Transformation-Mediated Complementation of a FUM Gene Cluster Deletion in Fusarium verticillioides Restores both Fumonisin Production and Pathogenicity on Maize Seedlings.* Molecular Plant-Microbe Interactions, 2007. **21**(1): p. 87-97.
21. Mittler, R., et al., *Reactive oxygen gene network of plants.* Trends Plant Sci, 2004. **9**(10): p. 490-8.

22. Passardi, F., et al., *Phylogenetic distribution of catalase-peroxidases: Are there patches of order in chaos?* Gene, 2007. **397**(1–2): p. 101-113.
23. Brown, D.W., et al., *The Fusarium verticillioides FUM Gene Cluster Encodes a Zn(II)2Cys6 Protein That Affects FUM Gene Expression and Fumonisin Production.* Eukaryotic Cell, 2007. **6**(7): p. 1210-1218.
24. Doedt, T., et al., *APSES proteins regulate morphogenesis and metabolism in Candida albicans.* Mol Biol Cell, 2004. **15**(7): p. 3167-80.
25. Nishimura, M., et al., *Mstu1, an APSES Transcription Factor, Is Required for Appressorium-Mediated Infection in Magnaporthe grisea.* Bioscience, Biotechnology, and Biochemistry, 2009. **73**(8): p. 1779-1786.
26. Ramirez-Zavala, B. and A. Dominguez, *Evolution and phylogenetic relationships of APSES proteins from Hemiascomycetes.* FEMS Yeast Res, 2008. **8**(4): p. 511-9.
27. Barna, B., et al., *The Janus face of reactive oxygen species in resistance and susceptibility of plants to necrotrophic and biotrophic pathogens.* Plant Physiol Biochem, 2012. **59**: p. 37-43.
28. Mellersh, D.G., et al., *H2O2 plays different roles in determining penetration failure in three diverse plant–fungal interactions.* The Plant Journal, 2002. **29**(3): p. 257-268.
29. Vanacker, H., T.L. Carver, and C.H. Foyer, *Early H(2)O(2) accumulation in mesophyll cells leads to induction of glutathione during the hyper-sensitive response in the barley-powdery mildew interaction.* Plant Physiol, 2000. **123**(4): p. 1289-300.
30. Able, A.J., *Role of reactive oxygen species in the response of barley to necrotrophic pathogens.* Protoplasma, 2003. **221**(1-2): p. 137-43.
31. Govrin, E.M. and A. Levine, *The hypersensitive response facilitates plant infection by the necrotrophic pathogen Botrytis cinerea.* Curr Biol, 2000. **10**(13): p. 751-7.
32. Schouten, A., et al., *Functional analysis of an extracellular catalase of Botrytis cinerea.* Mol Plant Pathol, 2002. **3**(4): p. 227-38.
33. Shetty, N.P., et al., *Role of hydrogen peroxide during the interaction between the hemibiotrophic fungal pathogen Septoria tritici and wheat.* New Phytologist, 2007. **174**(3): p. 637-647.
34. Garre, V., U. Muller, and P. Tudzynski, *Cloning, characterization, and targeted disruption of cpcat1, coding for an in planta secreted catalase of Claviceps purpurea.* Mol Plant Microbe Interact, 1998. **11**(8): p. 772-83.
35. Moore, S., O.M.H. De Vries, and P. Tudzynski, *The major Cu,Zn SOD of the phytopathogen Claviceps purpurea is not essential for pathogenicity.* Molecular Plant Pathology, 2002. **3**(1): p. 9-22.
36. Robbertse, B., et al., *Deletion of all Cochliobolus heterostrophus Monofunctional Catalase-Encoding Genes Reveals a Role for One in Sensitivity to Oxidative Stress but None with a Role in Virulence.* Molecular Plant-Microbe Interactions, 2003. **16**(11): p. 1013-1021.
37. Williams, L.D., et al., *Fumonisin disruption of ceramide biosynthesis in maize roots and the effects on plant development and Fusarium verticillioides-induced seedling disease.* J Agric Food Chem, 2007. **55**(8): p. 2937-46.

Table 3.1. *Fusarium verticillioides* strains used in this study.

Index	Strain	Genotype	Description
3\1	FRC M-3125[a]	Wild type, mating type *MAT1-1*	Strain used for gene deletion, also known as 7600, the sequenced strain
3\8	JFL A00999[b]	Wild type, mating type *MAT1-2*	Strain used for sexual cross
12\17	Δ*FvCP01*	*Δfvcp01/MAT1-1*	*FvCP01* deletant derived from M-3125
12\18	Δ*FvCP02*	*Δfvcp02/MAT1-1*	*FvCP02* deletant derived from M-3125
12\19	F1-Δ*FvCP01*	*Δfvcp01/MAT1-2*	F1 progeny generated by crossing Δ*FvCP01* with the A00999
12\20	Δ*FvCP01*Δ*FvCP02*	*Δfvcp01/Δfvcp02*	*FvCP01* and *FvCP02* double deletant derived by sexual crosses
12\21	ΔΔ::*FvCP01*	*Δfvcp01/Δfvcp02::FvCP01*	Double deletant complemented with *FvCP01*
12\22	ΔΔ::*FvCP02*	*Δfvcp01/Δfvcp02::FvCP02*	Double deletant complemented with *FvCP02*
12\23	ΔΔ::*FvCP01/FvCP02*	*Δfvcp01/Δfvcp02::FvCP01/FvCP02*	Double deletion strain complemented with both *FvCP01* and *FvCP02*, containing 2 copies of *FvCP01*

[a]FRC, *Fusarium* Research Center, Pennsylvania State University.
[b]JFL, John F. Leslie, Kansas State University.

Table 3.2. Primers used in this study.

Index	Primer name	Primer sequence	Purpose
P7\1	FVEG_10866 O1	GGGGACAGCTTTCTTGTACAAAGTGGAACCCTCATGTATGTGGATAGTGAAT	PCR 5' flank of *FvCP01*
P7\2	FVEG_10866 O2	GGGGACTGCTTTTTTGTACAAACTTGTGAAACTTATGCCGGATTTGTCAAC	
P7\3	FVEG_10866 O3	GGGGACAACTTTGTATAGAAAAGTTGTTGTCCAAATTCATCATCTGGGAATG	PCR 3' flank of *FvCP01*
P7\4	FVEG_10866 O4	GGGGACAACTTTGTATAATAAAGTTGTCAAATCGTACCCTGATCTCTACTG	
P7\13	FVEG_12888 O1	GGGGACAGCTTTCTTGTACAAAGTGGAATTGGTGATGACTTGTTGAGAATTG	PCR 5' flank of *FvCP02*
P7\14	FVEG_12888 O2	GGGGACTGCTTTTTTGTACAAACTTGTAGTTACAGTGCATCTTAGTCTAGC	
P7\15	FVEG_12888 O3	GGGGACAACTTTGTATAGAAAAGTTGTTGATGCGACCTTAATCCTGTACATA	PCR 3' flank of *FvCP02*
P7\16	FVEG_12888 O4	GGGGACAACTTTGTATAATAAAGTTGTTCTCGGTAAGTAATCCACCATTTC	
P1\14	HygMarker_For	TGTTTATCGGCACTTTGCATCGGC	PCR part of hygromycin resistance cassette; Southern probe
P1\15	HygMarker_Rev	AGCTGCATCATCGAAATTGCCGTC	
P7\5	FVEG_10866_F	GGTTAGTACTCCCAAAGCCAATAA	PCR part of the CDS of *FvCP01;* Southern probe
P7\6	FVEG_10866_R	GGAACCAGCAAGAACAATAACATC	
P7\7	FVEG_10866_5'-outer	CTGAGTTTAGTGATGCGTGTATTT	For testing the integrity of outer sequences flanking the 5' flank and 3' flank of *FvCP01*, respectively
P7\8	FVEG_10866_3'-outer	TAGTCCTCCAAGCTAACCAATCTA	
P7\17	FVEG_12888_F	CTACAACGGTAGCACAGACATTTA	PCR part of the CDS of *FvCP02;* Southern probe
P7\18	FVEG_12888_R	AGTAGACAGGATAGTGGACTTGAG	
P7\19	FVEG_12888_5'-outer	CCTACTGATAGAGCGTCGATAAAG	For testing the integrity of outer sequences flanking the 5' flank and 3' flank of *FvCP02*, respectively
P7\20	FVEG_12888_3'-outer	CCTTCATGAGATCCGTGAGTAAAT	
P1\4	HygRev	GCCGATGCAAAGTGCCGATAAACA	For testing the integrity of outer sequences flanking the 5' flank and 3' flank of target gene, respectively
P1\3	HygFor	AGAGCTTGGTTGACGGCAATTTCG	
P7\9	FVEG_10866_CP_F	GCGATCATCCACCTCCATTTA	PCR *FvCP01* for complementation
P7\10	FVEG_10866_CP_R	TCTACGTCCCTTGGGTCTATT	
P7\21	FVEG_12888_CP_F	GTAATCGGGAACTTGGGAAGAG	PCR *FvCP02* for complementation
P7\22	FVEG_12888_CP_R	GAGTGAGAGTGAGGCTGTTATG	
P1\37	Geneticin marker_for	GATCGCTGCTGTTCTCCTATC	PCR part of geneticin resistance cassette
P1\38	Geneticin marker_rev	CTGATCTGACCAGTTGCCTAAA	
P7\11	qPCR_10866_F	CTCTTCTACAGACCGTGTCAAG	PCR *FvCP01* for qPCR and qRT-PCR
P7\12	qPCR_10866_R	GAGCCGTCATAGTTGGTGTT	
P7\23	qPCR_12888_F	CCTTGCTGATGGTTTCCGTA	PCR *FvCP02* for qPCR and qRT-PCR
P7\24	qPCR_12888_R	GGGAGGAGTAAGGGTAAGAAGA	
P1\50	TUB2-F	CAGCGTTCCTGAGTTGACCCAACAG	PCR β-tubulin for qPCR and qRT-PCR
P1\51	TUB2-R	CTGGACGTTGCGCATCTGATCCTCG	
P1\42	GF_mat1a	GTTCATCAAAGGGCAAGCG	For verification of mating type MAT1-1
P1\43	GF_mat1b	TAAGCGCCCTCTTAACGCCTTC	
P1\44	GF_mat2c-CC	AGCGTCACCATTCGATCAAG	For verification of mating type MAT1-2
P1\45	GF_mat2d	CTACGTTGAGAGCTGTACAG	

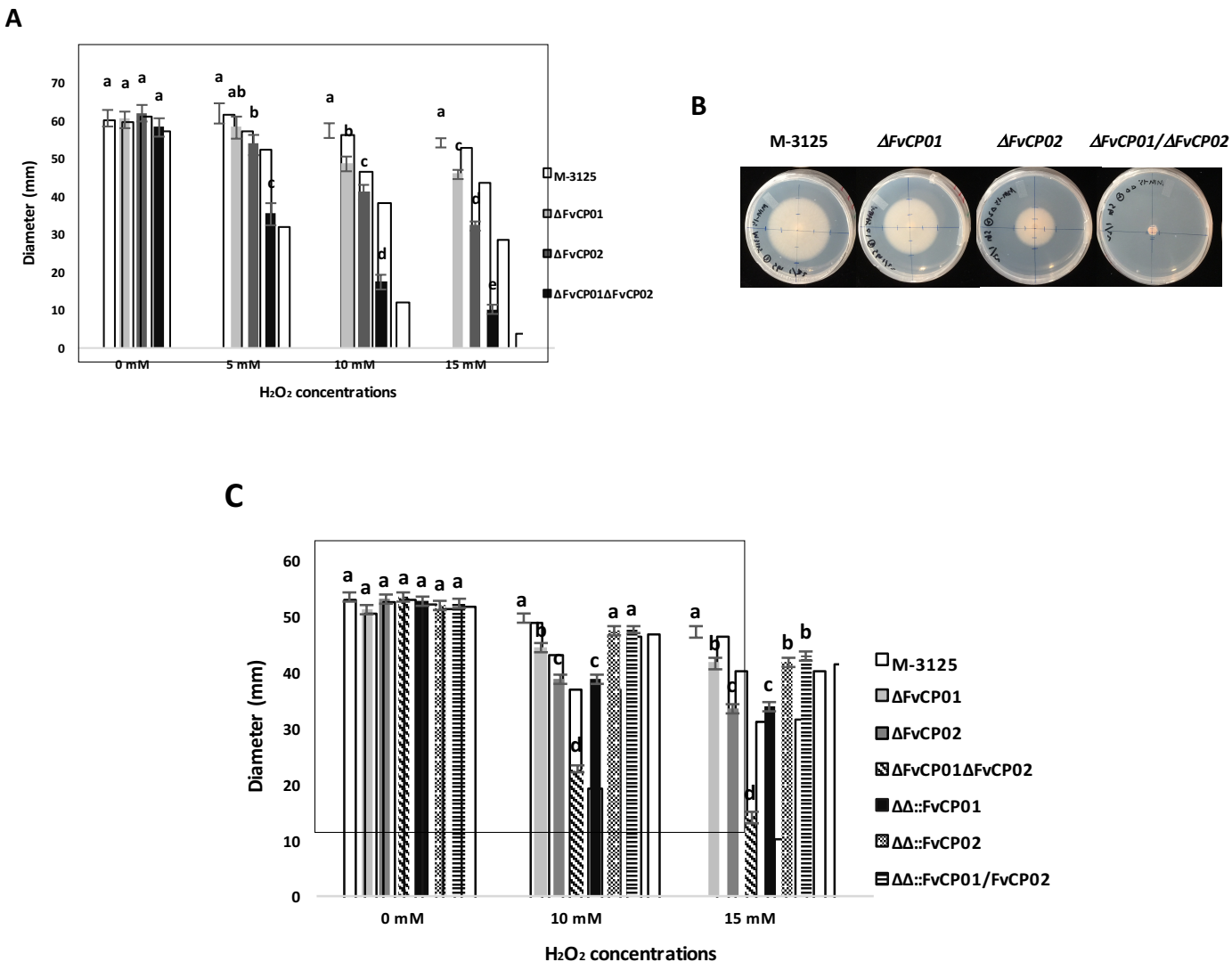

Figure 3.1: H_2O_2 sensitivity analysis of *Fusarium verticillioides* strains using mycelial inoculum.

A 4-mm cork borer was used to remove agar plugs from colony margins. Plugs were inverted on MM or PDA media. The diameter of the fungal colonies was measured 5 days post inoculation (DPI). **A**. Colony growth on MM amended with 0, 5, 10 and 15 mM H_2O_2 5 DPI. **B**. Representatives of tested strains grown on MM amended with 15 mM H_2O_2 5 DPI. **C**. Colony growth on PDA amended with 0, 10 and 15 mM H_2O_2 5 DPI. Data of MM and PDA were collected from three independent experiments and one representative, respectively. Bars represent means of colony diameters of each strain and were marked with standard error. The significant differences ($P<0.05$) between strains treated with the same concentrations of H_2O_2 were estimated by ANOVA with the software SAS and marked with the letters.

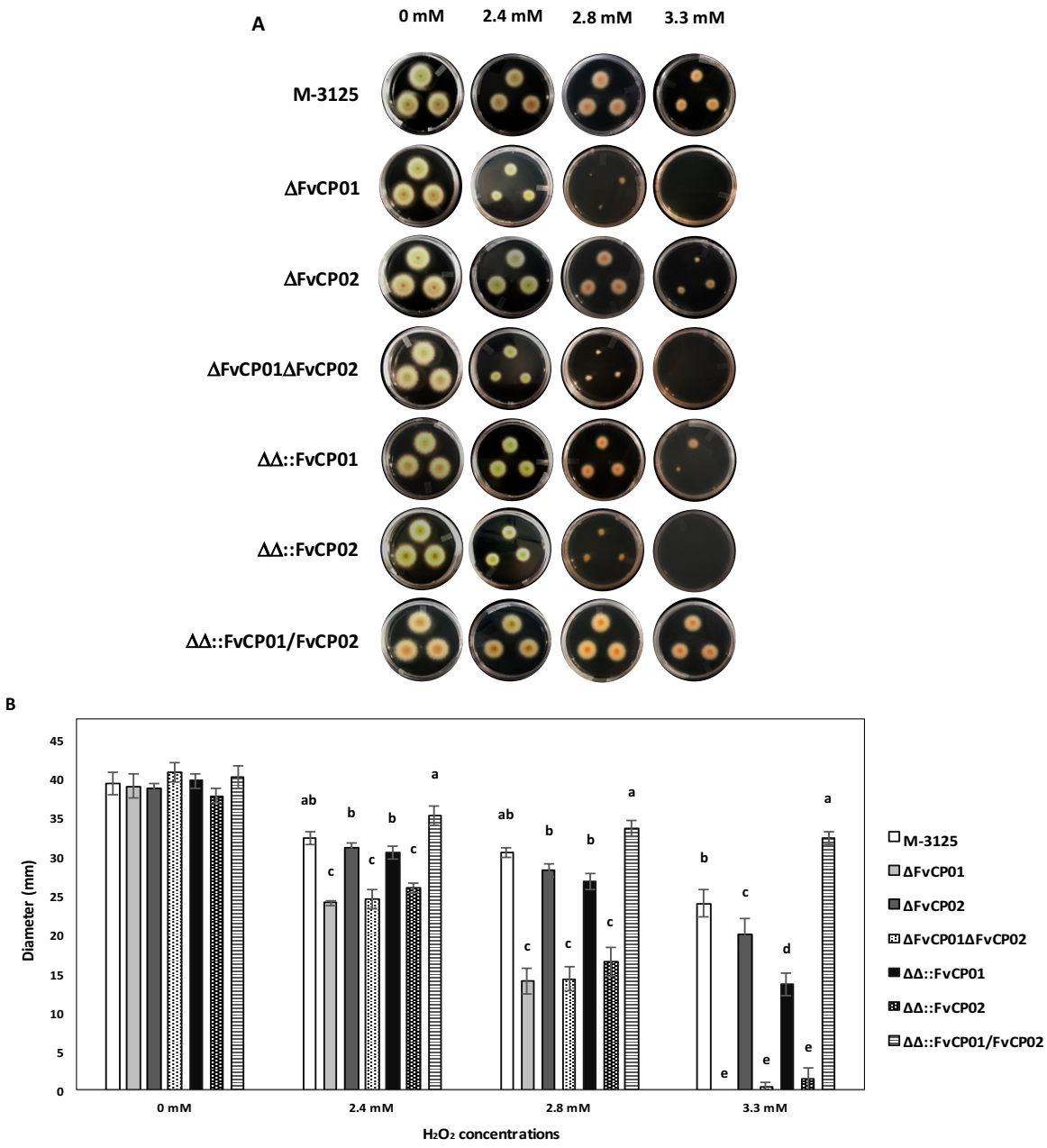

Figure 3.2: H_2O_2 sensitivity analysis of *Fusarium verticillioides* strains using conidial inoculum.

A. Wild-type M-3125, deletion mutants and complemented strains were inoculated onto plates supplemented with 0, 2.4, 2.8, 3.3 mM H_2O_2. Triplicate 3 µl of 10^6 spores were inoculated on each plate. Photos were taken 4 days after inoculation. **B**. Colony growth (indicated by diameter) of strains was measured for each treatment 4 days after inoculation. Data collected and statistically analyzed from 3 independent experiments with three measured colonies (data were taken twice for each colony) for each treatment. Bars represent means of colony diameters of each strain. Error bars represent standard error. Statistical differences ($P<0.05$) of strains treated were estimated by ANOVA with the software SAS. Strains sharing letters are not significantly different.

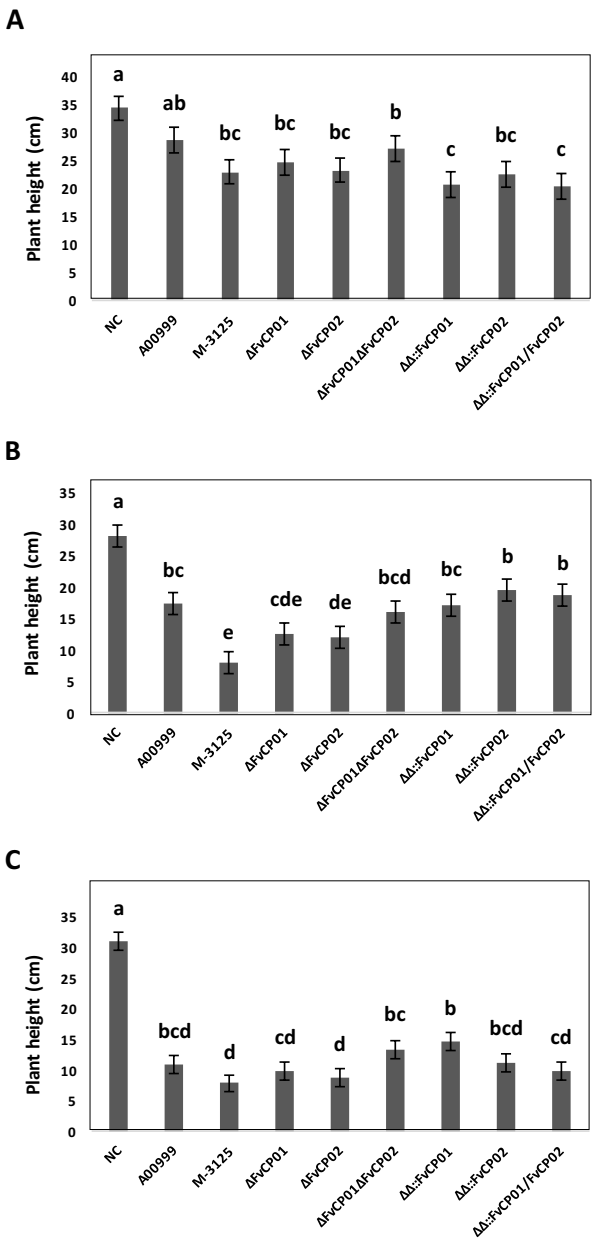

Figure 3.3: Data of virulence assays collected from three independent experiments.
Seeds of sweet corn Silver Queen were inoculated with tested strains and grown for 14 days with 16 hours at 30 ℃ and 8 hours at 20 ℃. Data were collected from 3 independent experiments and shown in **A**, **B**, **C**, respectively. Bars represent means of plant height and bars indicate standard error. The significant differences ($P<0.05$) between treatments were estimated by ANOVA with the software SAS and marked with the letters.

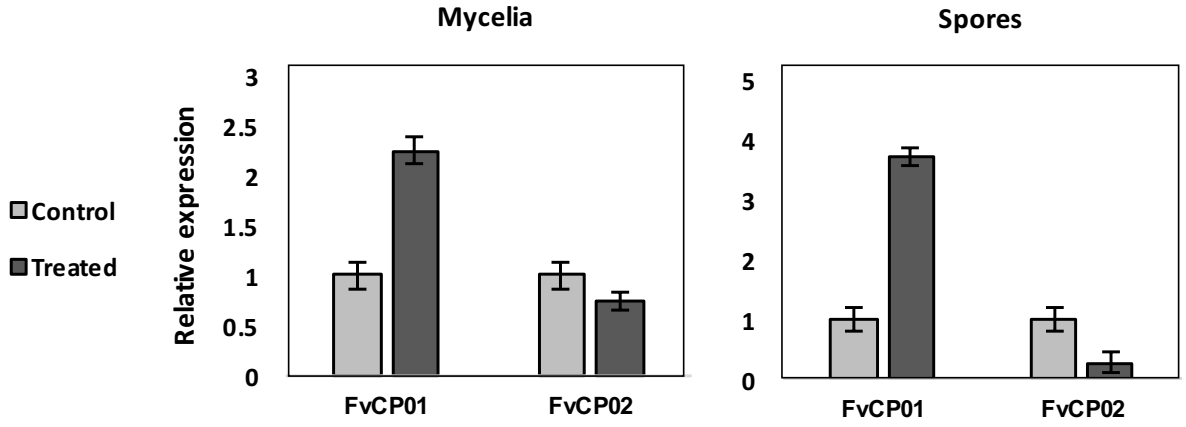

Figure 3.4: *In vitro* qRT-PCR transcription analysis of *FvCP01* and *FvCP02* under H_2O_2 exposure.

Results were obtained from mycelia (left) and spores (right) of wild-type strain M-3125 treated with (Treated) or without (Control) 2 mM H_2O_2 for 2 h. Relative expression was calculated via the $2^{-\Delta\Delta CT}$ method by comparing the transcriptional level of Treated to those of Control and normalizing to expression of β-tubulin. Values shown here were results averaged over three technical replicates from two independent trials. Standard errors are indicated as error bars.

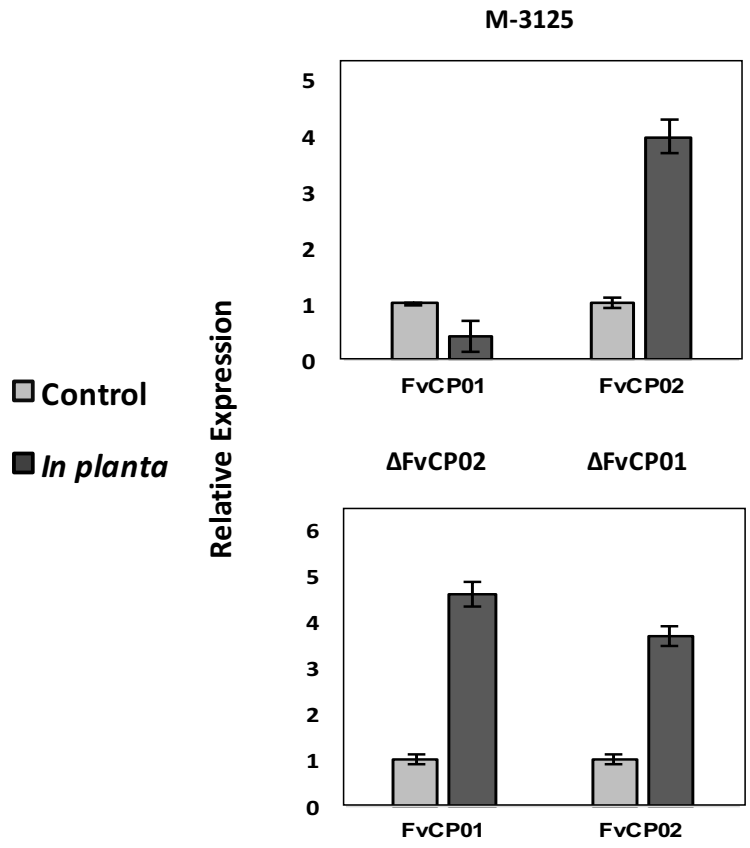

Figure 3.5: *In planta* qRT-PCR transcription analysis of *FvCP01* and *FvCP02*.
Strains included in this study were wild-type strain M-3125 (upper graph), and single deletion mutants Δ*FvCP01* and Δ*FvCP02* (lower graph). Results were obtained from three-day-old PDB culture (Control) and 90 hpi germlings (*In planta*). Relative expression was calculated via the $2^{-\Delta\Delta CT}$ method by comparing the transcriptional level of *In planta* to those of Control and normalizing to expression of β-tubulin. Values shown here were results averaged over three technical replicates (Control samples) or four technical replicates (*In planta* samples) from three independent trials. Standard errors are indicated as error bars.

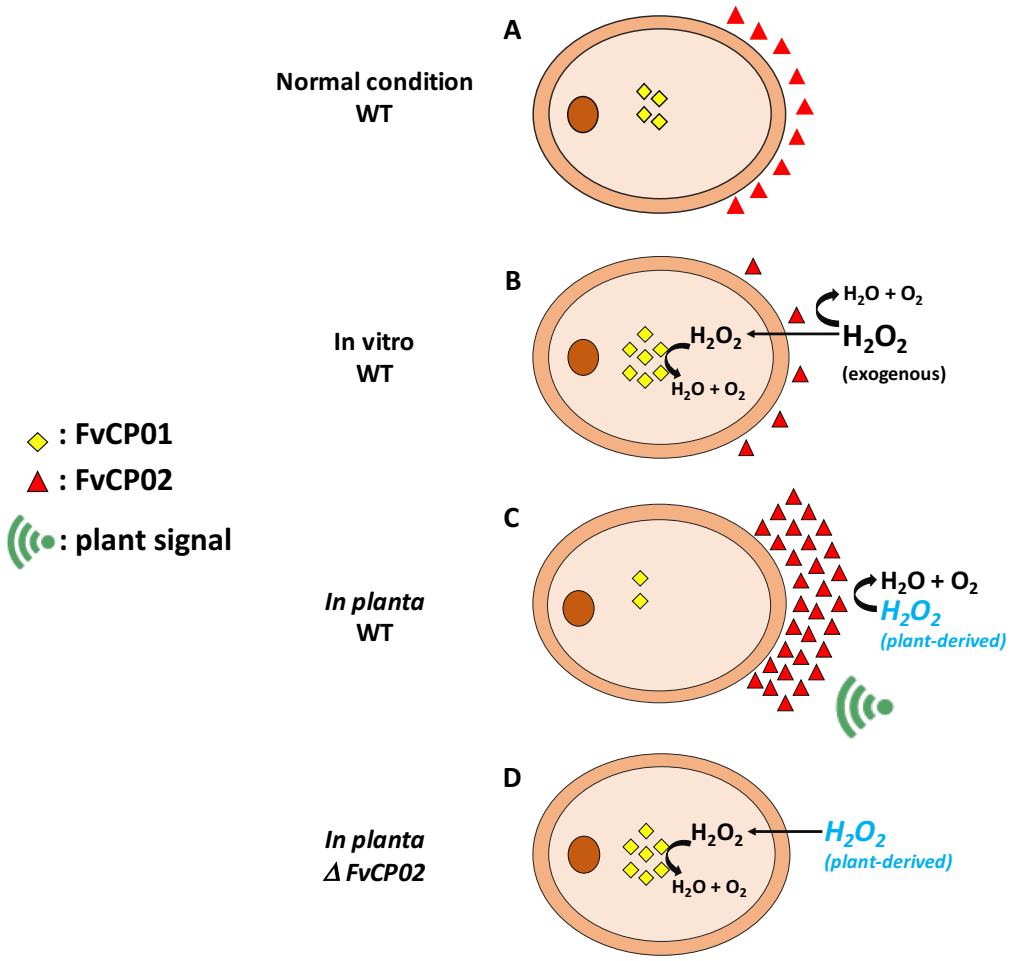

Figure 3.6: Proposed model for differential roles of *FvCP01* and *FvCP02* in oxidative stress protection.

A. Under low H_2O_2 stress, the proteins FvCP01 (yellow diamond) and FvCP02 (red triangle) are constitutively expressed. **B**. Under excessive oxidative stress in wild type, the limited amount of extracellular FvCP02 can only degrade a portion of the H_2O_2 and the excess would then diffuse into the cell, leading to the increased intracellular FvCP01. **C**. When wild type infects the susceptible maize germlings, *FvCP02* is induced due to the perception of plant-derived H_2O_2 and/or other plant signals, leading to the generation of adequate FvCP02 to eliminate H_2O_2 and the decreased production of FvCP01. **D**. However, in the Δ*FvCP02* gene deletion mutant, owing to the loss of the extracellular protection, plant-derived H_2O_2 enters the fungal cell. *FvCP01* is accordingly up-regulated to alleviate the oxidative stress.

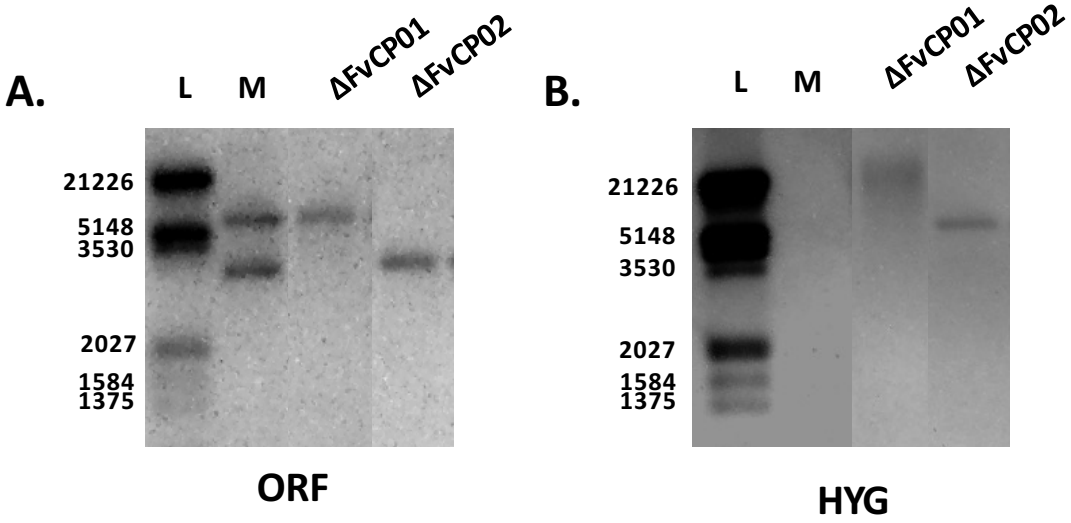

Supplemental Figure 3.1: Southern hybridization of single gene deletion mutants Δ*FvCP01* and Δ*FvCP02*.

To confirm the genotype of gene deletion mutants, genomic DNA (digested with *Kpn*I) of wild-type M-3125 (M) and gene deletion mutants Δ*FvCP01* and Δ*FvCP02* were tested using Southern hybridization. Blots were probed for **A**. a combination of *FvCP01* and *FvCP02* ORF and **B**. the hygromycin resistance cassette. Lanes contain: L, DNA Molecular Weight Marker Ⅲ (Roche) with band lengths labeled at left; M, wild-type M3125; ΔFvCP01, single mutant Δ*FvCP01*; ΔFvCP02, single mutant Δ*FvCP02*. **A**. The target fragment of *FvCP01* and *FvCP02* are 3400 bp and 6000 bp, respectively. Wild type hybridizes to ORF probes for both genes while Δ*FvCP01* only hybridizes to the ORF probe of *FvCP02*, and Δ*FvCP02* only hybridizes to the *FvCP01* ORF probe. **B**. The hygromycin-containing target fragments for generating Δ*FvCP01* and Δ*FvCP02* are 30,000 and 5,000 bp, respectively. Two rounds of southern hybridization support the successful knockout of these two genes in corresponding single deletion mutants.

Cross round one:

Male: Δ*FvCP01* (*Δfvcp01/MAT1-1*) × Female: A00999 (*MAT1-2*)

F1 (*Δfvcp01/MAT1-2*)

Cross round two:

Male: Δ*FvCP02* (*Δfvcp02/MAT1-1*) × Female: F1 (*Δfvcp01/MAT1-2*)

F2 (*Δfvcp01/Δfvcp02*)

Supplemental Figure 3.2: Δ*FvCP01*/Δ*FvCP02* double mutant construction by sexual crosses.

The double mutant used in this study was constructed by two rounds of sexual crosses in which *MAT1-1* and *MAT1-2* strains were used as male and female, respectively. The first mating was between the single mutant Δ*FvCP01 (*Δ*fvcp01/MAT1-1*) and the wild-type strain A00999 (*MAT1-2*). A single mutant F1 progeny with mating type *MAT1-2* (Δ*fvcp01/MAT1-2*) was then crossed with the single mutant Δ*FvCP02* (Δ*fvcp02/MAT1-1*). A double mutant progeny of the genotype Δ*fvcp01*/Δ*fvcp02* was identified from the second cross progeny and used for subsequent experiments including generation of single and double complemented strains. The double mutant genetic background is thus 75% M3125 and 25% A00999.

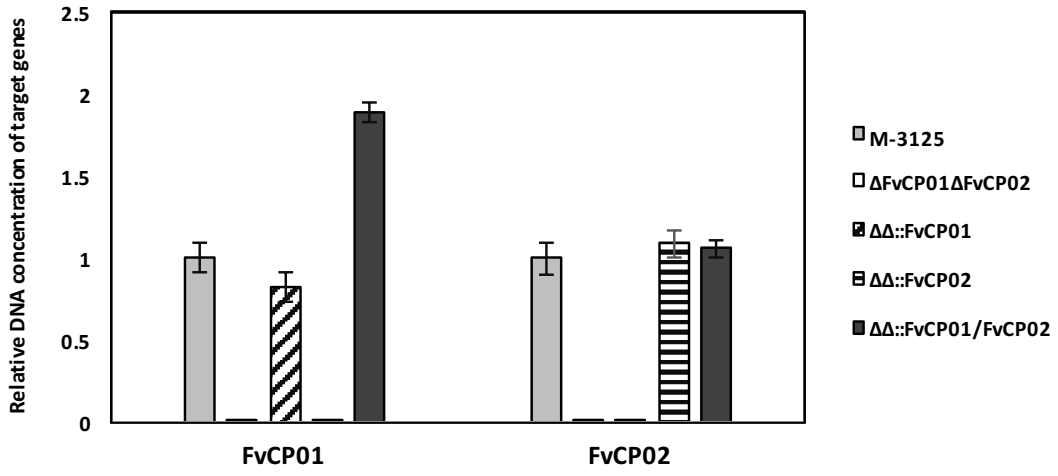

Supplemental Figure 3.3: Copy number determinization of complemented double mutant. The copy number of *FvCP01* and *FvCP02* in the double deletant was determined by qPCR of extracted genomic DNA. M3125 and Δ*FvCP01*/Δ*FvCP02* served as single and null copy controls, respectively. The data were normalized to the reference gene β-tubulin and calculated via the $2^{-\Delta\Delta CT}$ method. Standard error is indicated as error bars.

Scale	Stunting level	Chlorotic lesion/deformation
0	Normal height	None
1	Normal height	Few obscure lesions or clearing vein, near to health
2	Slightly short (~20 cm)	More lesions and/or clearing vein and/or leaf distortion
3	Moderately short (~15cm)	Lesions and/or clearing vein and/or leaf distortion
4	Very short (~10cm)	Lesions and/or clearing vein and/or leaf distortion
5	Extremely short (~5cm)	Near to death and/or dense lesions

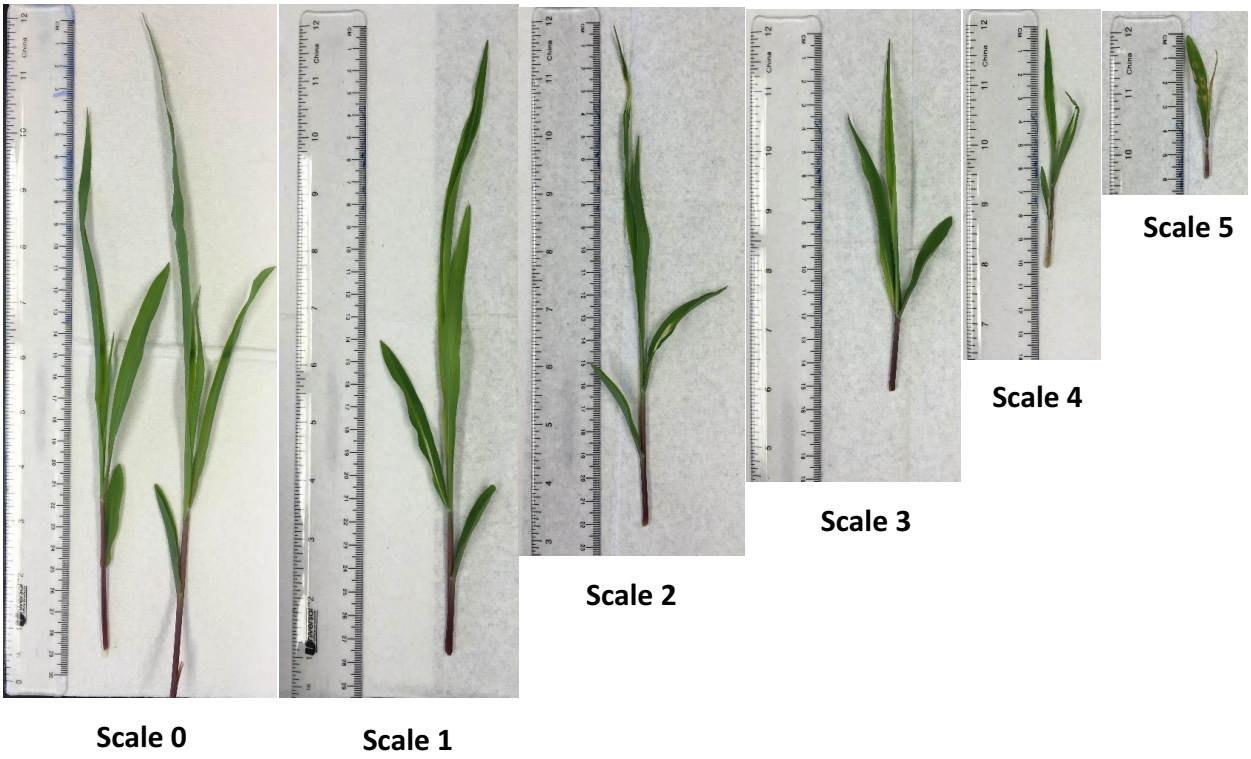

Supplemental Figure 3.4: Symptom severity scale for 14 days after planting seedling virulence assay.

Severity scale, arranging from 0 to 5, was determined by visual checking for symptoms including stunted growth, chlorotic lesions, and deformation. The standards for determination (upper table) and corresponding representatives (lower images) for each scale are shown.

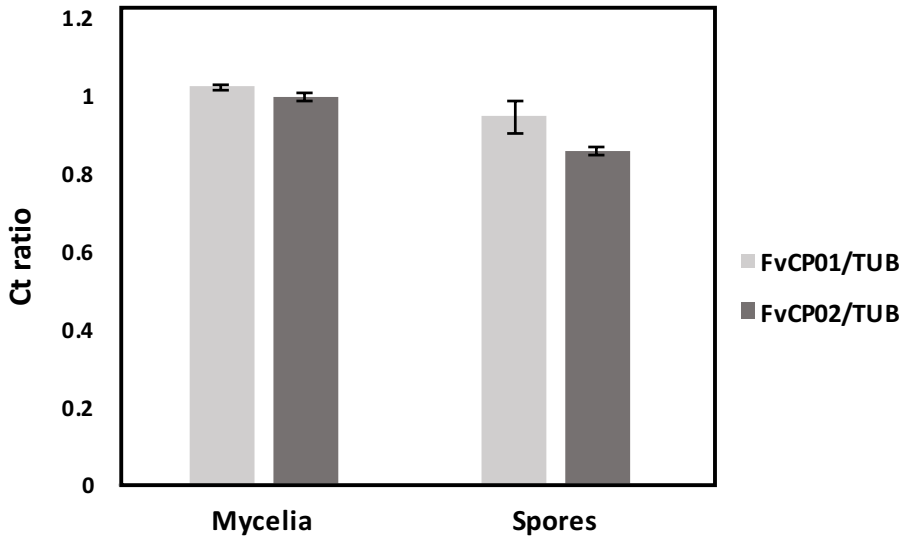

Supplemental Figure 3.5: C_t ratio of *FvCP01* and *FvCP02* compared to reference gene β-tubulin.

The C_t values of *FvCP01* and *FvCP02* were divided by the C_t values of the reference gene β-tubulin based on data obtained from *in vitro* qRT-PCR analysis of mycelia and spores of wild-type strain M-3125 grown under control conditions (three-day-old PDB culture). Data represent two biological replicates, each with three technical replicates. A ratio <1 means the gene had a lower C_t value, suggesting a higher expression, than that of β-tubulin. Similarly, a ratio >1 means the gene had a higher C_t value, suggesting a lower expression, than that of β-tubulin. Results reveal that the expression level of *FvCP01* and *FvCP02* are comparable to that of β-tubulin in mycelia and slightly higher in spores. These data suggest *FvCP01* and *FvCP02* are constitutively expressed at a level equal to or even higher than β-tubulin. Standard error is indicated as error bars.

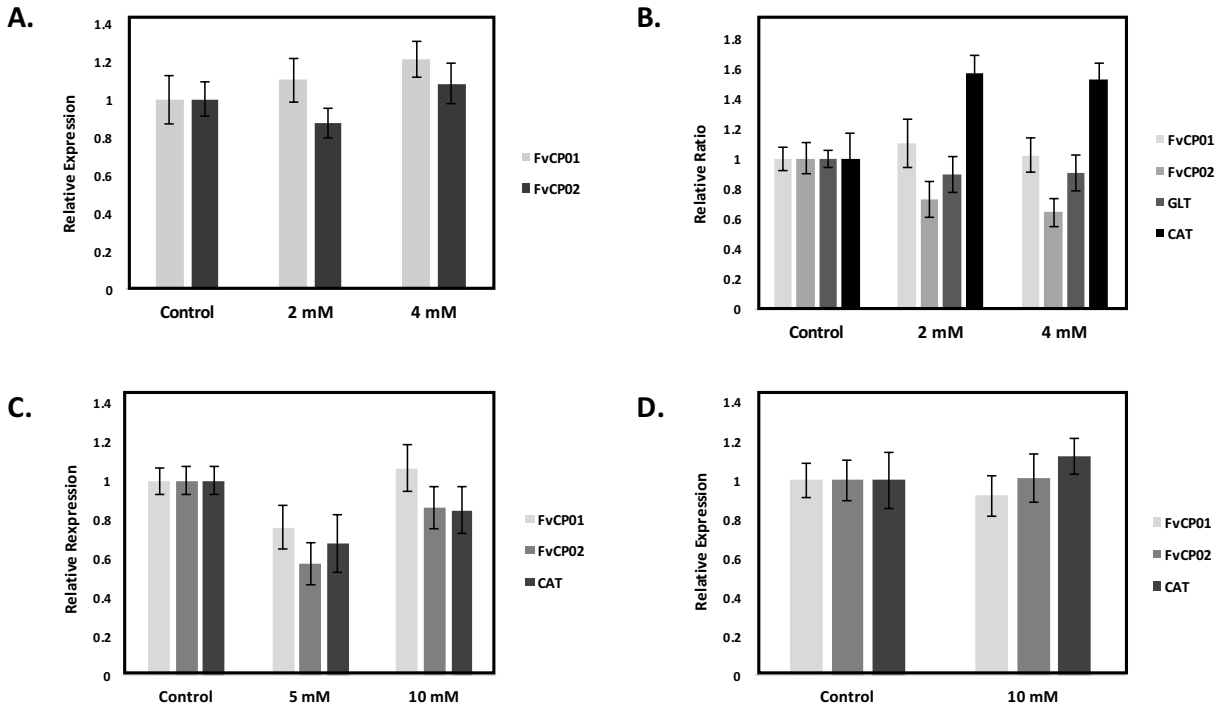

Supplemental Figure 3.6: *In vitro* qRT-PCR transcription analyses under various H_2O_2 exposure conditions in YPG medium.

Transcriptional analyses of *FvCP01*, *FvCP02*, a glutathione transferase (GLT), and a catalase (CAT) conducted on 3-day-old YPG culture of wild-type strain M-3125 treated with various concentrations of H_2O_2 for different exposure times. **A**. Relative expression of *FvCP01* and *FvCP02* under 2 and 4 mM H_2O_2 for 2 h. **B**. Relative expression of *FvCP01*, *FvCP02*, GLT and CAT under 2 and 4 mM H_2O_2 for 2 h. **C**. Relative expression of *FvCP01*, *FvCP02* and CAT under 5 and 10 mM H_2O_2 for 2 h. **D**. Relative expression of *FvCP01*, *FvCP02* and CAT under 5 and 10 mM H_2O_2 for 15 min. Data were collected from one experiment with three technical replicates. Relative expression was calculated via the $2^{-\Delta\Delta CT}$ method by comparing the transcriptional level of H_2O_2-treated samples to those of Control and normalized to β-tubulin. Standard errors are indicated as error bars.

CHAPTER 4

DEVELOPMENT OF AN INDUCIBLE FUNGAL GENE EXPRESSION VECTOR

Introduction

One effective way to study gene function is to establish regulatable gene expression systems of either transgenes or native genes in organisms. Although in many cases a strong constitutive promoter is used to drive a target gene, inducible promoters, which can be temporally and spatially controlled, are desirable for studies requiring stringent expression control. Advantages of employing inducible expression systems include 1) quantitative gene expression at a given developmental stage for a specific duration of time and even in a specific type of cell [1, 2]; 2) ability to study genes whose constitutive expression is deleterious or lethal to the host [3]. Unlike the development of various well-established chemical-inducible promoters and their extensive use in plants [4, 5], only a limited number of inducible expression systems regulated by chemicals have been developed for fungi, among which most have been studied in ascomycetous fungi. For example, efforts have been made to develop metabolically independent and accurately adjustable expression systems by adopting the transcriptional activation of the human estrogen receptor (hERα) in *Aspergillus* [6], and the thiamine promoter system (P*thiA*) in *Aspergillus oryzae* [7].

However chemical-inducible expression systems are categorized, two functional components are critical for all systems. The first component (activator or repressor protein) uses a constitutive promoter to express a chemical-responsive transcription factor, while the second

component (target promoter) employs multiple copies of the transcription factor binding site linked to a minimal promoter to drive the expression of a target gene [3]. Zuo and colleagues [1] developed an estrogen receptor (ER)-based inducible system for use in plants by constructing a chimeric transcriptional activator, the XVE protein, which contains the DNA-binding domain (DBD) of the bacterial repressor *LexA* (X), the acidic transactivation domain of *VP16* (V) and the regulatory region of human ER. Without the hormone ligand, the fusion protein is expressed under the control of a constitutive promoter, G10-90, and is anchored in the cytosol. After addition of the inducer, β-estradiol, association of the ligand with XVE leads to the translocation of this ligand-receptor complex into the nucleus. Subsequently, XVE binds to a chimeric promoter consisting of eight copies of the *LexA*-binding sites upstreaming from a 35S minimal promoter, which results in the expression of a target gene. The vector containing both transactivator and target promoter was named pER8. Demonstrating high efficiency and specificity, the expression of a *GFP* reporter gene is rapidly (in 30 min) induced at rates strongly correlated with a wide range of inducer concentration in transgenic *Arabidopsis* and tobacco plants (from 8 nM to 5 μM).

In this study, we aimed to construct a chemically-inducible and metabolism-independent expression systems for *Fusarium verticillioides* genes *in planta* by adopting this XVE-based inducible system. In addition, the efficiency of cloning target gene into the modified vector and fungal transformation would be enhanced by introducing the Gateway® system and employing *Agrobacterium tumefaciens*-mediated transformation, respectively. Theoretically, this system is generally applicable to other ascomycetous fungi, most interestingly to phytopathogens, providing a promising way to study the interaction between phytopathogenic fungi and their hosts.

Materials and Methods

Fungal and bacterial strains, culture media and growth conditions

Wild-type strain FRC M-3125 was used for genetic modification and functional characterization. *F. verticillioides* strains were grown routinely on potato dextrose agar (PDA; Neogen Food Safety) at 27 °C in the dark or in potato dextrose broth (PDB; Neogen Food Safety) on a shaker incubator at 250 rpm and 27 °C in the dark. For selection of fungal transformants, PDA amended with 150 μg/ml hygromycin B was used. Water agar (1.5 %) was used for single spore isolation for conidia. To test the effect of β-estradiol on fungal growth or the induction of target gene in the transformants, PDA or PDB amended with noted amounts of DMSO or β-estradiol dissolved in DMSO (described below) were used, respectively.

During the construction of the XVE-based inducible vector, *Escherichia coli* (One Shot® MAX Efficiency® DH5α™-T1R, Invitogen) was routinely grown in or on Luria Bertani (LB) medium amended with 100 μg/m spectinomycin (Thermo Fisher Scientific) at 37 °C overnight. The *Agrobacterium tumefaciens* strain AGL-1 was used for fungal transformation and cultured on Luria Bertani (LB) medium amended with 100 μg/m spectinomycin at 27 °C in the dark.

In vitro β-estradiol sensitivity assay

The inducer β-estradiol was prepared as a 10 mM stock solution in dimethyl sulfoxide (DMSO) and stored at -20 ℃ in small aliquots. To test the effect of β-estradiol on growth rate of *F. verticillioides*, a total of 50 mL Potato Dextrose Agar (PDA) medium amended with 0, 5 μL, 25 μL, 50 μL, 0.125 mL, 0.25 mL and 0.5 mL DMSO only or β-estradiol stock solution (the concentration of β-estradiol in media is 0, 1 μM, 5 μM, 10 μM, 25 μM, 50 μM and 100 μM, respectively) were thoroughly mixed and poured onto two plates. A 4-mm cork borer agar from a

one-week-old M-3125 PDA culture plate was inverted onto the tested plates. The diameters of fungal colonies were measured each day for seven days after inoculation.

Construction of an XVE-based inducible vector pOSHG and fungal transformation

Primers used are listed in Table 4.1. To construct the targeting vector pOSXHG, the following steps were performed (Figure 4.2). 1) Design a starting DNA fragment, SynDNA-XVE, based on the vector pER8 [1]. The starting sequence is 2747 bp and consists of two transcription units. The first transcription unit contains a *ToxA* gene promoter from *Pyrenophora tritici-repentis* [8], the fusion protein XVE, and a transcription terminator from the glucoamylase gene in *A. awamori* [9]. In the second transcription unit, eight copies of *LexA* operator sequences fused to the *Saccharomyces cerevisiae URA3* minimal promoter [10] was intended to inducibly control the transcription of target genes. Sequence of the restriction enzyme, I-Ceu-I, was added between this two units for the latter insertion of hygromycin resistance cassette (*hyg*R). Sequence of the restriction enzyme, I-Sce-I, was placed downstream of the *URA3* minimal promoter for the latter insertion of target genes. In addition, attachment (att) sites for Gateway® cloning, attB3 and attB2r were added to the 5' and 3' end of the starting DNA fragment, SynDNA-XVE, respectively. This DNA fragment was synthesized and cloned in pUC57 by GenScript, giving rise to the starting vector 2) Insertion of *hyg*R as the antibiotic marker. A *hyg*R sequence with terminal I-Ceu-I sites was amplified (using primers P7/37 and P7/38) from vector pDONR-A-Hyg, which contains *hyg*R under the control of the *A. nidulans Trp*C promoter and terminator. Both *hyg*R fragment and the starting vector were digested with I-Ceu-I followed by ligation after the vector dephosphorylation. Candidates of the modified vector were propagated in *E. coli* and confirmed by sequencing. The obtained core sequence was named as synDNA-XVE-HYG 3) Modification of the backbone vector pOSCAR [11]. To utilize the I-Sce-I site in the latter step

for the introduction of target genes, an I-Sce-I site present in the backbone vector pOSCAR was destroyed creating pOSCAR-S$^-$. Bacteriophage T4 DNA polymerase (New England Biolabs) was used to remove protruding nucleotides from the 3' termini of the digested pOSCAR (by I-Sce-I), therefore eliminating I-Sce-I sites. Vector candidates were propagated and confirmed as stated in step 2. 4) Cloning target sequence synDNA-XVE-HYG into modified pOSCAR from step 3. The core sequence synDNA-XVE-HYG was PCR amplified (using primers P7/39 and P7/40) and cloned into the modified pOSCAR via BP clonase (Invitrogen), resulting in pOXH. Vector candidates were propagated and confirmed as stated in step 2. 5) Target gene synthetic *GFP* (sGFP) insertion. A sGFP sequence with the nos terminator [12] flanked with the I-Sce-I sites was amplified (using primers P7/41 and P7/42) from vector pCM56 [13]. Both sGFP-nos fragment and the vector obtained in step 4 were digested with I-Sce-I followed by ligation after the dephosphorylation of the vector, resulting in the final vector pOXHG (Figure 4.3).

The verified final vector pOXHG was transformed into wild-type strain M-3125. Hygrormycin-resistant fungal transformants were isolated and initially PCR-screened for 1) *hyg*R amplified by primers P1/14 and P1/15; 2) sGFP amplified by primers P7/41 and P7/42; 3) the complete insertion (including the two transcription units, hygR and sGFP sequences) amplified by primers P7/39 and P7/40. Potential positive transformants were single-spore isolated. The same PCR screening process as above was performed again on those purified transformants candidates to finally obtain the fungal transformants harboring the intact components of the inducible expression system. One fungal transformant was used in the transcriptional analysis.

RNA extraction and qRT-PCR analysis

Fungal transformant M3125-OXHG-1 was inoculated in triplicate treatment replicates in 50 ml PDB amended with nothing, 0.25 ml DMSO or 50 μM β-estradiol (in 0.25 ml DMSO). Cultures were incubated for three days and one ml was harvested in the lysing matrix S tubes (MP Biomedicals) and then centrifuged at 10,000 g for 5 minutes at 4 degree to get the fungal pellets. Lysis buffer PS (RapidPure™ RNA Plant Kit, MP Biomedicals) was immediately added and samples were lysed using the FastPrep-24™ 5G Instrument (MP Biomedicals) at 6 m/sec, 30 seconds twice, with a one min pause between pulses. The manufacturer's manual (RapidPure™ RNA Plant Kit, Thermo Fisher Scientific) was followed to extract total RNA.

For quantitative reverse transcription-PCR (qRT-PCR), RNA samples were digested by DNase (RQ1 RNase-Free DNase, Promega) and checked for quality (RNA integrity number > 6.0) using the Agilent 2100 Bioanalyzer. Complementary DNA synthesis and qRT-PCR were carried out using a one-step qRT-PCR Kit (SuperScript® III Platinum® SYBR® Green One-Step qRT-PCR Kit, Thermo Fisher Scientific) with technical triplicates for each sample. The data were normalized to the expression level of β-tubulin and calculated via $2^{-\Delta\Delta CT}$ method. The primers used for this assay are shown in Table 4.1.

Results

Effect of β-estradiol on *F. verticillioides* morphogenesis

One criterion of an ideal chemical-inducible expression system is that the inducer should not be toxic and have no, or minimal, physiological effects in targeted organisms [3, 14]. Therefore, we firstly tested the effect of the inducer β-estradiol and the corresponding solvent DMSO on growth rate of *F. verticillioides*. As shown in Figure 4.1, no effect of DMSO on

fungal growth was detected. However, a dose effect of the application of β-estradiol was observed on the growth rate of wild-type strain M-3125 growth rate. According to Zuo et al. [1], the expression level of the XVE-based system in plants seems to be saturated at the 5 μM β-estradiol, which barely influences the colony growth when compared to the DMSO only control. In addition, no visible morphological damage of both spores and mycelia owing to the addition of DMSO only or β-estradiol was observed (data not shown). Bringing all this together, β-estradiol concentrations that are less than 5 μM are expected to strongly induce gene expression and have little to no physiological impact and will be applied for further assay.

Construction of an XVE-based inducible promoter

A five-step methodology (Figure 4.2) was applied to generate the final inducible vector pOXHG (Figure 4.3). The details were summarized in the Materials and Methods. The verified final vector pOXHG was transformed into wild-type strain M-3125 via *A. tumefaciens*-mediated transformation. Confirmed fungal transformant M3125-OXHG-1 was used in the following experiment.

Transcriptional analysis of XVE and sGFP in the fungal transformant

The expected *GFP* fluorescence upon induction of M3125-OXHG-1 by β-estradiol was not observed, promoting us to further analyze plasmid function. To determine if the XVE fusion protein can be constitutively expressed and the target gene sGFP can be specifically induced by β-estradiol, a transcriptional analysis was performed by comparing the expression of XVE and sGFP in the fungal transformant M3125-OXHG-1 treated with 0.25 ml DMSO (in 50 ml PDB) or 50 μM β-estradiol (in 0.25 ml DMSO) to those of control after three-day culturing. Given the constant induction (up to four days) of the target gene under 2 μM β-estradiol, the above induction condition was expected to result in adequate transcripts of target gene to allow

detection. Although XVE was constitutively expressed in all three treatments, addition of DMSO or 50 μM β-estradiol lead to transcriptional increase by 0.8 and 1.5 times, respectively. Moreover, transcripts of sGFP were barely detected in all treatments. In summary, the transcriptional analysis suggests that despite the fact that fusion protein XVE was constitutively expressed as expected, the target gene sGFP was unable to be induced even when exposing to a high β-estradiol concentration which should have triggered strong gene expression.

Discussion

The purpose of this project was to construct an *in planta* chemical-inducible and metabolism-independent expression system for *F. verticillioides* by adopting the XVE-based system, which demonstrate high efficiency and specificity in plants. Fungal transformants harboring core components for inducible expression were successfully obtained using the five-step methodology and *A. tumefaciens*-mediated transformation. Transcriptional analysis supports expression of the chimeric transcriptional activator XVE but not the inducible expression of the target gene when the inducer was applied.

To explore why the vector constructed for this study failed to execute inducible expression of the target gene (*GFP*) in *F. verticillioides*, the following trouble-shooting plan was proposed based on the expected results. The responsive induction of the target gene when triggered with the inducer, β-estradiol, relies on 1) constitutive expression of the chimeric transcriptional activator XVE in the cytosol; 2) successful association of XVE with the inducer; 3) translocation of the XVE-inducer complex into the nucleus; 4) ability of the complex to bind to the target promoter (consisting of eight copies of *LexA*-binding sites and a *URA3* minimal promoter); 5) functioning of the chimeric target promoter in transcribing the target gene; 6)

successful translation and detection of target gene. The transcriptional analysis of XVE expression in verified fungal transformant when treated with or without the inducer support its constitutive expression. To address the lack of expected performance described above additional work is required. For example, to address points 2) and 3) above, we could create an XVE-GFP fusion protein to detect the *in vivo* localization of XVE by fluorescence microscopy. This proposed fusion protein should be cytosolic until addition of the inducer upon which it should translocate to the nucleus. Since 2) is prerequisite to 3), the visualization of XVE in the nucleus would support the realization of both features. To determine promoter binding as outlined in 4) above, methods for detecting protein-DNA interactions, such as Chromatin Immunoprecipitation (ChIP) assays and DNA pull-down assays could be exploited. The ChIP grade or Western blot grade antibodies derived from the C-terminus of human estrogen receptor, which was used for composing XVE, are commercially available. With an XVE antibody, the protein-DNA complex of XVE and target promoter can be selectively precipitate from the other genomic DNA fragments and protein-DNA complexes. Followed by the detection of the target DNA sequence using specific PCR primers based on the known sequence of the target promoter, we would be able to determine if XVE binds to the target DNA sequence. Given the constitutive expression of XVE in the fungal transformant of *F. verticillioides* and strict regulation of XVE by estradiol in the plant systems, we expect to see the translocation of XVE to nucleus and subsequent binding to the target promoter after the addition of β-estradiol. To deal with 5) and 6), qRT-PCR or fluorescence microscopy visualization of *GFP* can be utilized. If 1) to 4) are confirmed, the potential reason may come from the loss-of-function of the yeast-derived minimal promoter *URA3* [10] in *F. verticillioides*. If this is the case, other available minimal promoters of yeast or other fungi may be tested, for instance, the synthetic minimal yeast promoters [15, 16].

References

1. Zuo, J., Q.-W. Niu, and N.-H. Chua, *An estrogen receptor-based transactivator XVE mediates highly inducible gene expression in transgenic plants.* Plant J, 2000. **24**(2): p. 265–273.
2. Jepson, I., A. Martinez, and J.P. Sweetman, *Chemical-Inducible Gene Expression Systems for Plants—a Review.* Pestic. Sci, 1998. **54**: p. 360-367.
3. Zuo, J. and N.-H. Chua, *Chemical-inducible systems for regulated expression of plant genes.* Current Opinion in Biotechnology, 2000. **11**: p. 146–151.
4. Tang, W., X. Luo, and V. Samuels, *Regulated gene expression with promoters responding to inducers.* Plant Science, 2004. **166**(4): p. 827-834.
5. Moore, I., M. Samalova, and S. Kurup, *Transactivated and chemically inducible gene expression in plants.* Plant J, 2006. **45**(4): p. 651-83.
6. Pachlinger, R., et al., *Metabolically independent and accurately adjustable Aspergillus sp. expression system.* Appl Environ Microbiol, 2005. **71**(2): p. 672-8.
7. Shoji, J.Y., et al., *Development of Aspergillus oryzae thiA promoter as a tool for molecular biological studies.* FEMS Microbiol Lett, 2005. **244**(1): p. 41-6.
8. Ciuffetti, L.M., R.P. Tuori, and J.M. Gaventa, *A single gene encodes a selective toxin causal to the development of tan spot of wheat.* The Plant Cell, 1997. **9**(2): p. 135-144.
9. Nunberg, J.H., et al., *Molecular cloning and characterization of the glucoamylase gene of Aspergillus awamori.* Molecular and Cellular Biology, 1984. **4**(11): p. 2306-2315.
10. Roy, A., F. Exinger, and R. Losson, *cis- and trans-acting regulatory elements of the yeast URA3 promoter.* Molecular and Cellular Biology, 1990. **10**(10): p. 5257-5270.
11. Paz, Z., et al., *One Step Construction of Agrobacterium-Recombination-ready-plasmids (OSCAR), an efficient and robust tool for ATMT based gene deletion construction in fungi.* Fungal Genetics and Biology, 2011. **48**(7): p. 677-684.
12. Lorang, J.M., et al., *Green Fluorescent Protein Is Lighting Up Fungal Biology.* Applied and Environmental Microbiology, 2001. **67**(5): p. 1987-1994.
13. Andrie, R.M., J.P. Martinez, and L.M. Ciuffetti, *Development of ToxA and ToxB Promoter-Driven Fluorescent Protein Expression Vectors for Use in Filamentous Ascomycetes.* Mycologia, 2005. **97**(5): p. 1152-1161.
14. Wang, R., X. Zhou, and X. Wang, *Chemically regulated expression systems and their applications in transgenic plants.* Transgenic Research, 2004. **12**: p. 529–540.
15. Redden, H. and H.S. Alper, *The development and characterization of synthetic minimal yeast promoters.* Nature Communications, 2015. **6**: p. 7810.
16. Ajo-Franklin, C.M., et al., *Rational design of memory in eukaryotic cells.* Genes & Development, 2007. **21**(18): p. 2271-2276.

Table 4.1. Primers used in this study.

Index	Primer name	Primer sequence	Purpose
P7/37	Ceu-Hyg-For	GAGATAACTATAACGGTCCTAAGGTAGCGAAATTGAAGGAGCATTTTTTGGGCTTG	For amplification of hygR with terminal I-Ceu-I sites
P7/38	Ceu-Hyg-Rev	GAGATTCGCTACCTTAGGACCGTTATAGTTACTATTCCTTTGCCCTCGGACGAGTG	
P7/39	attB2r_SynDNA_For	GGGGACAGCTTTCTTGTACAAAGTGGAAGGATCCGATGGAATCCATGGAGGA	For amplification of the synthesized sequence (including the inserted hygR) with terminal attachment sites and confirmation of the presence of the whole insertion in fungal transformants
P7/40	attB3_SynDNA_Rev	GGGGACAACTTTGTATAATAAAGTTGTATTACCCTGTTATCCCTATAGAGT	
P7/41	Sce-GFP-For	GAGATAGGGATAACAGGGTAATTCAAAATGGTGAGCAAGGGCGAGGAGCTG	For amplification of sGFP-nos with terminal I-Sce-I sites and confirmation of the presence of sGFP-nos in fungal transformants
P7/42	Sce-GFP-Rev	GAGAATTACCCTGTTATCCCTATACATGTTTGACAGCTTATCATCG	
P1/14	HygMarker_For	TGTTTATCGGCACTTTGCATCGGC	For amplification of part of hygR
P1/15	HygMarker_Rev	AGCTGCATCATCGAAATTGCCGTC	
P7/43	qPCR_XVE_F	GCAGGGAGAGGAGTTTGTGTG	For amplification of XVE for qRT-PCR
P7/44	qPCR_XVE_R	CTTCCAGAGACTTCAGGGTGCT	
P7/45	qPCR_GFP_F	AAGCTGACCCTGAAGTTCATCTGC	For amplification of GFP for qRT-PCR
P7/46	qPCR_GFP_R	CTTGTAGTTGCCGTCGTCCTTGAA	
P1/50	TUB2-F	CAGCGTTCCTGAGTTGACCCAACAG	For amplification of β-tubulin for qRT-PCR
P1/51	TUB2-R	CTGGACGTTGCGCATCTGATCCTCG	

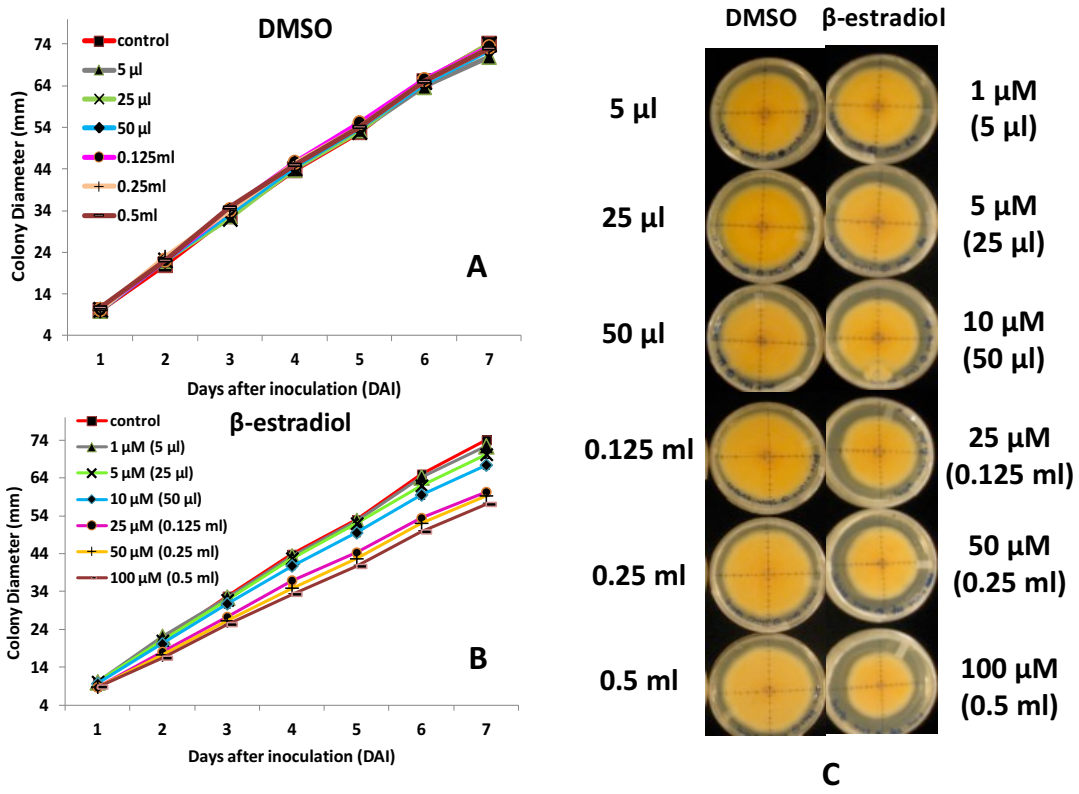

Figure 4.1: Analysis of the effect of DMSO and β-estradiol on the growth rate of *F. verticillioides*.

Four mm mycelia agar plugs of M-3125 were inverted on PDA amended with a series of concentrations of DMSO only (**A**) or β-estradiol dissolved in DMSO (**B**). Colony diameter was measured daily for seven days post inoculation (DPI). Two replicates were conducted for each treatment including a no addition PDA control. On the 7th day after inoculation, side by side comparison was made between the same amount of DMSO (**C**, left column, amount of DMSO shown on the left edge) and β-estradiol added (**C**, right column, concentration of β-estradiol shown at right edge, with DMSO volumes in parentheses). Values shown here were results generated from one experiment out two independent repeats showing the similar trend.

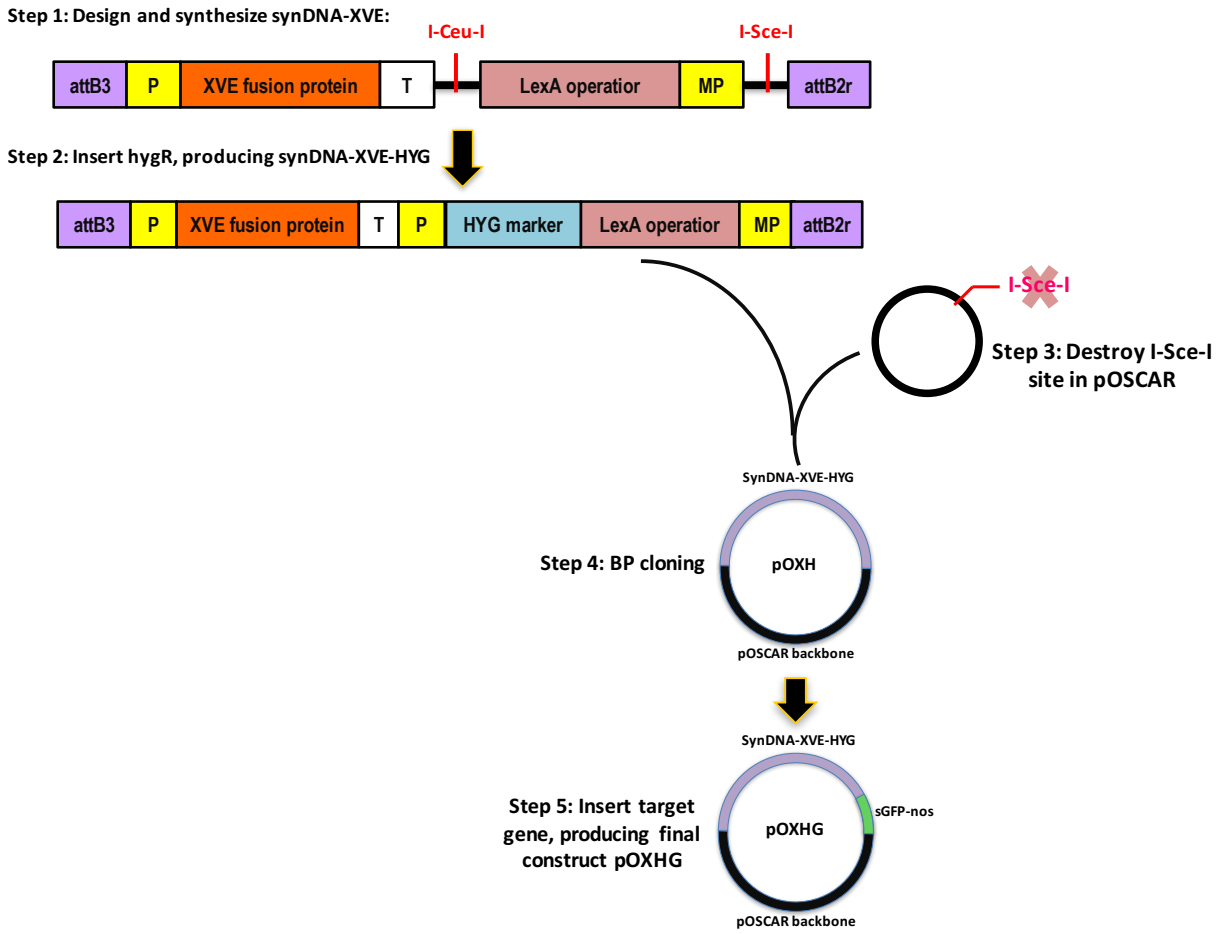

Figure 4.2: Strategy for construction of the fungal inducible vector pOXHG.
The vector construction methodology consisted of five steps. The starting fragment synDNA-XVE was designed based on the pER8 and was further modified by the insertion of the *hyg*R sequence, giving rise to synDNA-XVE-HYG. The backbone vector pOSCAR was modified to eliminate I-Sce-I site, generating pOSCAR-S$^-$. The core sequence synDNA-XVE-HYG was then inserted into the modified pOSCAR-S$^-$ via BP cloning, resulting in pOXH. The final inducible vector pOXHG was generated by the insertion of the target gene sGFP.

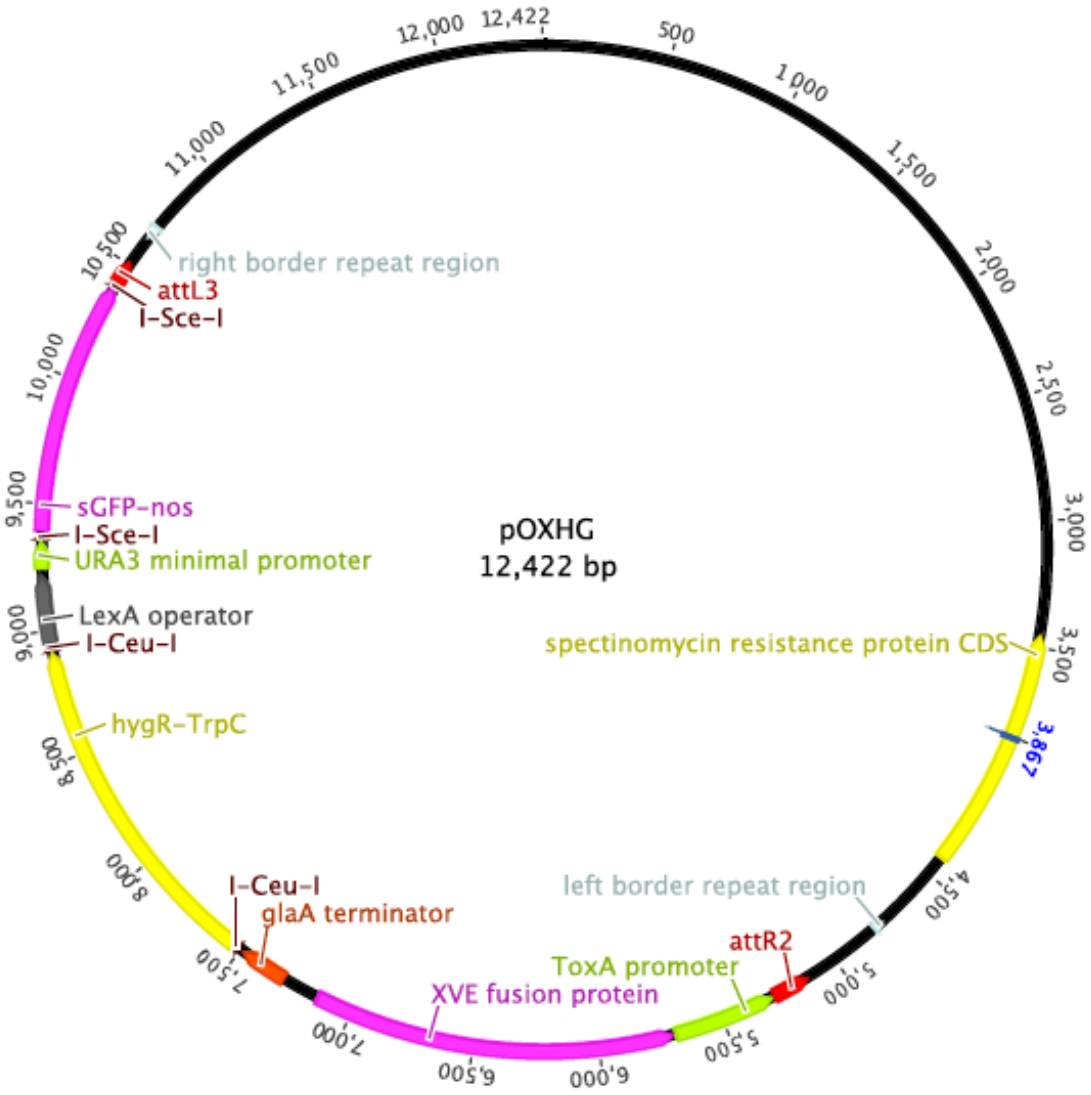

Figure 4.3: Map of the final vector pOXHG.

This map contains the core sequence, which is essential for the inducible expression system laying between the right border and left border, and the remaining sequence derived from pOSCAR. In the core sequence, there are XVE fusion protein under the regulation of *ToxA* promoter and *glaA* terminator, *hyg*R as the antibiotic resistance marker under the control of the *A. nidulans TrpC* promoter and terminator, the *LexA* operator, and the target gene sGFP under the regulation of the minimal promoter *URA3* and the *nos* terminator. The attachment sites and I-Sce-I/I-Ceu-I sites are shown. Name and total length of vector are shown in the center of the cycle map. The base numbering is labeled outside of the circular map.

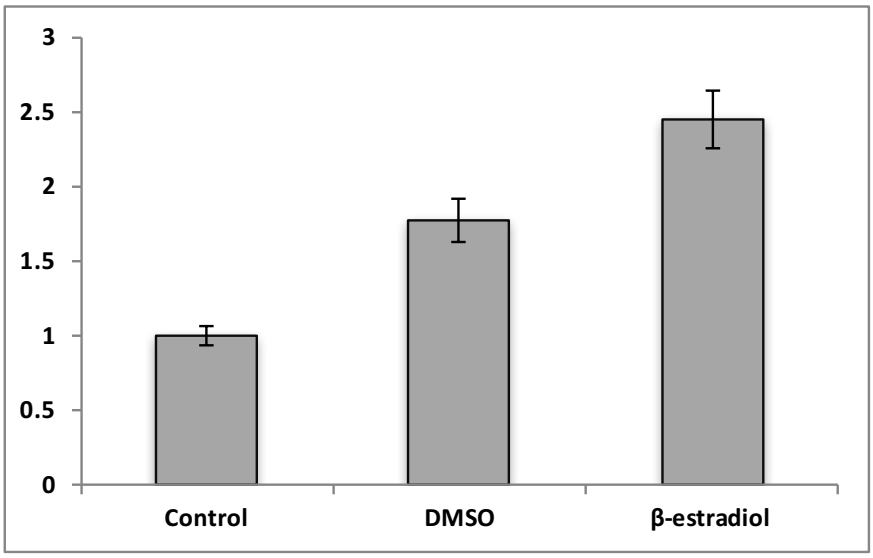

Figure 4.4. Transcriptional analysis of XVE and sGFP in fungal transformant via qRT-PCR.

Results were obtained from 50 ml PDB culture of wild-type strain M-3125 that were treated with nothing (Control), 0.25 ml DMSO (DMSO) or 50 μM β-estradiol (β-estradiol) for three days. Relative expression was calculated via the $2^{-\Delta\Delta CT}$ method by comparing the transcriptional level of "DMSO" or "β-estradiol" to those of "Control". Standard error is indicated as error bars.

CHAPTER 5

CONCLUSIONS

In this research project, the occurrence of HGT events via a semi-automatic phylogenomic pipeline and the following-up characterization of selected candidates, including FVEG_10494 and two fungal KcatG-encoding genes FVEG_10866/FVEG_12888, were pursued in *Fusarium verticillioides.* Addition efforts were made to construct a chemically-inducible and metabolism-independent expression systems for *F. verticillioides* genes *in planta*. Together, this dissertation is dedicated to evaluate the role of HGT events in the evolution and biology of *F. verticillioides* and the development of inducible expression system as a fungal tool.

Compared to the rampant cases of HGT found in prokaryotes, the rapid increase in publicly accessible eukaryotic genomic data is providing increasing evidence of laterally acquired genetic materials in eukaryotes. Efforts toward the genome-wide identification of HGT candidates in fungi and revelation of their association with core metabolisms (amino acid, carbohydrate, nucleic acid), osmotrophic capacity and pathogenesis has been accelerated dramatically with the flood of genomic data deposits [1-5]. The global analysis of a large number of strong HGT candidates obtained from the genome-wide studies will accelerate the identification of factors for answering questions like ‘which genes are transferred’ or ‘where are genes transferred to’. In fact, the biased movement of particular types of genes and ‘hot spots’ for HGT in the recipient genome have been observed. In bacterial, operational genes, which are involved in housekeeping metabolisms, are more likely to be horizontally transferred and

retained than informational genes which are involved in processes such as transcription and translation required by all organisms [6]. While in fungi, based on current case studies of HGT, genes acquired across kingdoms by fungi are largely single genes without playing direct roles in complex regulatory or biochemical pathways [7]. In contrast to preferred single genes in cross-kingdom transfer events, intra-kingdom putative HGT events of whole gene clusters have been observed in fungi [8, 9], presumably in part resulting from a friendlier genomic environment and the use of similar regulatory machinery. To address the preferred location of HGT in the genome of a recipient, locations displaying specific genomic contents described as 'regions of innovation' have been proposed as hot spots for HGT [7]. Those locations are normally gene-sparse, repeat-rich regions that may consist of genomic islands enriched in genes underlying adaptive values and displaying higher rates of evolution [10]. Potential mobile pathogenicity chromosomes in *F. oxysporum* [11] and the correlation between bacterially-derived genes in the *F. graminearum* genome with genomic regions featuring high intra-specific single nucleotide polymorphisms (SNPs) densities support the existence of hot spots for HGT in fungi.

The work described in this dissertation provides a global view of HGT candidates in *F. verticillioides*. Functional categorization of these candidates indicates several enriched biochemical activities compared to the frequency of such genes within the genome at large. It is one thing to identify high confidence HGT candidates in a large scale, but another thing to correctly interpret their functional role based on putative annotations, let alone the ultimate characterization of gene candidates using molecular techniques like mutagenesis. Except for FVEG_10494, other HGT candidates identified, especially those demonstrating interesting traits, such as genes sharing the same putative function (e.g. four putative arylsulfatases), encoding secreted proteins, induced only under specific environmental conditions (e.g. FVEG_12509),

potentially associated with secondary metabolism gene clusters, and narrowly distributed among fungal species, are also worth being functional characterized.

To promote the study of fungal gene expression inside the infected plant host, we constructed an inducible fungal gene expression system in *F. verticillioides,* but theoretically applicable to other ascomycetous fungi and easily adaptable to other fungal groups. Unfortunately, due to technical difficulties, the system is currently still under construction. Assessment of plasmid function suggests that induction failed. The most likely culprit appears to be the yeast *URA3* minimal promoter not functioning properly. In future work, we hope to exchange this sequence with a minimal promoter known to work in fungi, such as the synthetic minimal yeast promoters [12, 13]. Successful development and application of this ER-controlled system in fungi will provide a promising way to study the interaction between phytopathogenic fungi and their hosts, given the easy delivery and diffusion of β-estradiol to plant tissues. What's more, the feasibility of incorporating inducible RNAi silencing constructs into the XVE-based vector further broadens its value. Additional efforts are needed for the accomplishment of this valuable expression system.

References

1. Alexander, W.G., et al., *Horizontally acquired genes in early-diverging pathogenic fungi enable the use of host nucleosides and nucleotides.* Proceedings of the National Academy of Sciences, 2016. **113**(15): p. 4116-4121.
2. Gardiner, D.M., et al., *Comparative Pathogenomics Reveals Horizontally Acquired Novel Virulence Genes in Fungi Infecting Cereal Hosts.* PLOS Pathogens, 2012. **8**(9): p. e1002952.
3. Jaramillo, V.D.A., S.A. Sukno, and M.R. Thon, *Identification of horizontally transferred genes in the genus Colletotrichum reveals a steady tempo of bacterial to fungal gene transfer.* BMC Genomics, 2015. **16**(1): p. 2.
4. Qiu, H., et al., *Extensive horizontal gene transfers between plant pathogenic fungi.* BMC Biology, 2016. **14**(1): p. 41.
5. Richards, T.A., et al., *Gene transfer into the fungi.* Fungal Biology Reviews, 2011. **25**(2): p. 98-110.
6. Jain, R., M.C. Rivera, and J.A. Lake, *Horizontal gene transfer among genomes the complexity hypothesis.* Proc Natl Acad Sci U S A, 1999. **96**: p. 3801-3806.
7. Gardiner, D.M., K. Kazan, and J.M. Manners, *Cross-kingdom gene transfer facilitates the evolution of virulence in fungal pathogens.* Plant Sci, 2013. **210**: p. 151-8.
8. Slot, J.C. and A. Rokas, *Horizontal transfer of a large and highly toxic secondary metabolic gene cluster between fungi.* Curr Biol, 2011. **21**(2): p. 134-9.
9. Proctor, R.H., et al., *Birth, death and horizontal transfer of the fumonisin biosynthetic gene cluster during the evolutionary diversification of Fusarium.* Mol Microbiol, 2013. **90**(2): p. 290-306.
10. Gladieux, P., et al., *Fungal evolutionary genomics provides insight into the mechanisms of adaptive divergence in eukaryotes.* Mol Ecol, 2014. **23**(4): p. 753-73.
11. Ma, L.J., et al., *Comparative genomics reveals mobile pathogenicity chromosomes in Fusarium.* Nature, 2010. **464**(7287): p. 367-73.
12. Redden, H. and H.S. Alper, *The development and characterization of synthetic minimal yeast promoters.* Nature Communications, 2015. **6**: p. 7810.
13. Ajo-Franklin, C.M., et al., *Rational design of memory in eukaryotic cells.* Genes & Development, 2007. **21**(18): p. 2271-2276.

APPENDIX A

SEQUENCE OF SYNTHESIZED STARTING FRAGMENT synDNA-XVE

ACAACTTTATTATACAAAGTTGTCCCCGGATCCGATGGAATCCATGGAGGAGTTCTGTACGC

GCAATTCCGCTCTCCGTAAGGATGCTTCGGAGGTGCACATGGTCTCATACATGTAGGCCCGA

CGAGGATCGAGTCGGTTCCGAAGTAGGATCGTCTCGATTGTTGGGCATCATTGCATGGACAT

TCAGAGGGCCTACTGATACCTGGAATCCGCACCGTCCGGCTACCTAGCAATAAGATTCTGTG

TATATAAAGGGCTAAGGTGTCCGTCCTTGATAAAACCACCACCCTCAACAACTTACCTCGAC

TATCAGCATCCCGTCCTATCTAACAATCGTCCATCGGTATCCAACTCCAACTCTATTCGCAGG

GTCCTAGAATCGTAAGTACACGCTTATATCTTGTTGCCAGCGATAGCTGACAATGAATGAAT

ATAGGTCATGAAAGCGTTAACGGCCAGGCAACAAGAGGTGTTTGATCTCATCCGTGATCACA

TCAGCCAGACAGGTATGCCGCCGACGCGTGCGGAAATCGCGCAGCGTTTGGGGTTCCGTTCC

CCAAACGCGGCTGAAGAACATCTGAAGGCGCTGGCACGCAAAGGCGTTATTGAAATTGTTT

CCGGCGCATCACGCGGGATTCGTCTGTTGCAGGAAGAGGAAGAAGGGTTGCCGCTGGTAGG

TCGTGTGGCTGCCGGTGAACCGTCGAGCGCCCCCCCGACCGATGTCAGCCTGGGGGGACGAG

CTCCACTTAGACGGCGAGGACGTGGCGATGGCGCATGCCGACGCGCTAGACGATTTCGATCT

GGACATGTTGGGGGGACGGGGATTCCCCGGGTCCGGGATTTACCCCCCACGACTCCGCCCCCT

ACGGCGCTCTGGATATGGCCGACTTCGAGTTTGAGCAGATGTTTACCGATGCCCTTGGAATT

GACGAGTACGGTGGGGATCCGTCTGCTGGAGACATGAGAGCTGCCAACCTTTGGCCAAGCC

CGCTCATGATCAAACGCTCTAAGAAGAACAGCCTGGCCTTGTCCCTGACGGCCGACCAGATG

GTCAGTGCCTTGTTGGATGCTGAGCCCCCCATACTCTATTCCGAGTATGATCCTACCAGACCC

TTCAGTGAAGCTTCGATGATGGGCTTACTGACCAACCTGGCAGACAGGGAGCTGGTTCACAT

GATCAACTGGGCGAAGAGGGTGCCAGGCTTTGTGGATTTGACCCTCCATGATCAGGTCCACC

TTCTAGAATGTGCCTGGCTAGAGATCCTGATGATTGGTCTCGTCTGGCGCTCCATGGAGCAC

CCAGTGAAGCTACTGTTTGCTCCTAACTTGCTCTTGGACAGGAACCAGGGAAAATGTGTAGA

GGGCATGGTGGAGATCTTCGACATGCTGCTGGCTACATCATCTCGGTTCCGCATGATGAATC

TGCAGGGAGAGGAGTTTGTGTGCCTCAAATCTATTATTTTGCTTAATTCTGGAGTGTACACAT

TTCTGTCCAGCACCCTGAAGTCTCTGGAAGAGAAGGACCATATCCACCGAGTCCTGGACAAG

ATCACAGACACTTTGATCCACCTGATGGCCAAGGCAGGCCTGACCCTGCAGCAGCAGCACC

AGCGGCTGGCCCAGCTCCTCCTCATCCTCTCCCACATCAGGCACATGAGTAACAAAGGCATG

GAGCATCTGTACAGCATGAAGTGCAAGAACGTGGTGCCCCTCTATGACCTGCTGCTGGAGAT

GCTGGACGCCCACCGCCTACATGCGCCCACTAGCCGTGGAGGGGCATCCGTGGAGGAGACG

GACCAAAGCCACTTGGCCACTGCGGGCTCTACTTCATCGCATTCCTTGCAAAAGTATTACAT

CACGGGGGAGGCAGAGGGTTTCCCTGCCACAGTCTGAGAGCTCCCTGGCGAATTCCCAGAG

ATGTTAGCTGAAATCATCACTAATCAGATACCAAAATATTCAAATGGAAATATCAAAAAGCT

TCTGTTTCATCAAAAATGACTCGACCTAACTGAGTAAGCTAGCTTGTTCGAGTACAATCAAT

CCATTTCGCTATAGTTAAAGGATGGGGATGAGGGCAATTGGTTATATGATCATGTATGTAGT

GGGTGTGCATAATAGTAGTGAAATGGAAGCCAAGTCATGTGATTGTAATCGACCGACGGAA

TTGAGGATATCCGGAAATACAGACACCGTGAAAGCCATGGTCTTTCCTTCGTGTAGAAGACC

AGACAGAAGCTTGGAAACTGATAACTATAACGGTCCTAAGGTAGCGAACTTGCATGCCAGC

TTGGGCTGCAGGTCGAGGCTAAAAAACTAATCGCATTATCATCCCCTCGACGTACTGTACAT

ATAACCACTGGTTTTATATACAGCAGTACTGTACATATAACCACTGGTTTTATATACAGCAGT

CGACGTACTGTACATATAACCACTGGTTTTATATACAGCAGTACTGTACATATAACCACTGG

TTTTATATACAGCAGTCGAGGTAAGATTAGATATGGATATGTATATGGATATGTATATGGTG

GTAATGCCATGTAATATGCTCGACTCTAGGATCTTCGCAACAGAAGGAAGAACGAAGGAAG

GAGCACAGACTTAGATTGGTATATATACGCATATGTAGTGTTGAAGAAACATGAAATTGCCC

AGTATTCTTAACCCAACTGCACAGAACAAAAACCGACTCTATAGGGATAACAGGGTAATGG

GGACAGCTTTCTTGTACAAAGTGGAA

APPENDIX B

SEQUENCE OF THE FINAL VECTOR pOXHG

ACGGCGGTGAGGTTGCCGAGGCGCTGGCCGGGTACGAGCTGCCCATTCTTGAGTCCCGTATC

ACGCAGCGCGTGAGCTACCCAGGCACTGCCGCCGCCGGCACAACCGTTCTTGAATCAGAAC

CCGAGGGCGACGCTGCCCGCGAGGTCCAGGCGCTGGCCGCTGAAATTAAATCAAAACTCAT

TTGAGTTAATGAGGTAAAGAGAAAATGAGCAAAAGCACAAACACGCTAAGTGCCGGCCGTC

CGAGCGCACGCAGCAGCAAGGCTGCAACGTTGGCCAGCCTGGCAGACACGCCAGCCATGAA

GCGGGTCAACTTTCAGTTGCCGGCGGAGGATCACACCAAGCTGAAGATGTACGCGGTACGC

CAAGGCAAGACCATTACCGAGCTGCTATCTGAATACATCGCGCAGCTACCAGAGTAAATGA

GCAAATGAATAAATGAGTAGATGAATTTTAGCGGCTAAAGGAGGCGGCATGGAAAATCAAG

AACAACCAGGCACCGACGCCGTGGAATGCCCCATGTGTGGAGGAACGGGCGGTTGGCCAGG

CGTAAGCGGCTGGGTTGTCTGCCGGCCCTGCAATGGCACTGGAACCCCCAAGCCCGAGGAA

TCGGCGTGACGGTCGCAAACCATCCGGCCCGGTACAAATCGGCGCGGCGCTGGGTGATGAC

CTGGTGGAGAAGTTGAAGGCCGCGCAGGCCGCCCAGCGGCAACGCATCGAGGCAGAAGCAC

GCCCCGGTGAATCGTGGCAAGCGGCCGCTGATCGAATCCGCAAAGAATCCCGGCAACCGCC

GGCAGCCGGTGCGCCGTCGATTAGGAAGCCGCCCAAGGGCGACGAGCAACCAGATTTTTTC

GTTCCGATGCTCTATGACGTGGGCACCCGCGATAGTCGCAGCATCATGGACGTGGCCGTTTT

CCGTCTGTCGAAGCGTGACCGACGAGCTGGCGAGGTGATCCGCTACGAGCTTCCAGACGGG

CACGTAGAGGTTTCCGCAGGGCCGGCCGGCATGGCCAGTGTGTGGGATTACGACCTGGTACT

GATGGCGGTTTCCCATCTAACCGAATCCATGAACCGATACCGGGAAGGGAAGGGAGACAAG

CCCGGCCGCGTGTTCCGTCCACACGTTGCGGACGTACTCAAGTTCTGCCGGCGAGCCGATGG

CGGAAAGCAGAAAGACGACCTGGTAGAAACCTGCATTCGGTTAAACACCACGCACGTTGCC

ATGCAGCGTACGAAGAAGGCCAAGAACGGCCGCCTGGTGACGGTATCCGAGGGTGAAGCCT

TGATTAGCCGCTACAAGATCGTAAAGAGCGAAACCGGGCGGCCGGAGTACATCGAGATCGA

GCTAGCTGATTGGATGTACCGCGAGATCACAGAAGGCAAGAACCCGGACGTGCTGACGGTT

CACCCCGATTACTTTTTGATCGATCCCGGCATCGGCCGTTTTCTCTACCGCCTGGCACGCCGC

GCCGCAGGCAAGGCAGAAGCCAGATGGTTGTTCAAGACGATCTACGAACGCAGTGGCAGCG

CCGGAGAGTTCAAGAAGTTCTGTTTCACCGTGCGCAAGCTGATCGGGTCAAATGACCTGCCG

GAGTACGATTTGAAGGAGGAGGCGGGGCAGGCTGGCCCGATCCTAGTCATGCGCTACCGCA

ACCTGATCGAGGGCGAAGCATCCGCCGGTTCCTAATGTACGGAGCAGATGCTAGGGCAAAT

TGCCCTAGCAGGGGAAAAAGGTCGAAAAGGTCTCTTTCCTGTGGATAGCACGTACATTGGG

AACCCAAAGCCGTACATTGGGAACCGGAACCCGTACATTGGGAACCCAAAGCCGTACATTG

GGAACCGGTCACACATGTAAGTGACTGATATAAAAGAGAAAAAAGGCGATTTTTCCGCCTA

AAACTCTTTAAAACTTATTAAAACTCTTAAAACCCGCCTGGCCTGTGCATAACTGTCTGGCC

AGCGCACAGCCGAAGAGCTGCAAAAAGCGCCTACCCTTCGGTCGCTGCGCTCCCTACGCCCC

GCCGCTTCGCGTCGGCCTATCGCGGCCGCTGGCCGCTCAAAAATGGCTGGCCTACGGCCAGG

CAATCTACCAGGGCGCGGACAAGCCGCGCCGTCGCCACTCGACCGCCGGCGCCCACATCAA

GGCACCCTGCCTCGCGCGTTTCGGTGATGACGGTGAAAACCTCTGACACATGCAGCTCCCGG

AGACGGTCACAGCTTGTCTGTAAGCGGATGCCGGGAGCAGACAAGCCCGTCAGGGCGCGTC

AGCGGGTGTTGGCGGGTGTCGGGGCGCAGCCATGACCCAGTCACGTAGCGATAGCGGAGTG

TATACTGGCTTAACTATGCGGCATCAGAGCAGATTGTACTGAGAGTGCACCATATGCGGTGT

GAAATACCGCACAGATGCGTAAGGAGAAAATACCGCATCAGGCGCTCTTCCGCTTCCTCGCT

CACTGACTCGCTGCGCTCGGTCGTTCGGCTGCGGCGAGCGGTATCAGCTCACTCAAAGGCGG

TAATACGGTTATCCACAGAATCAGGGGATAACGCAGGAAAGAACATGTGAGCAAAAGGCCA

GCAAAAGGCCAGGAACCGTAAAAAGGCCGCGTTGCTGGCGTTTTTCCATAGGCTCCGCCCCC

CTGACGAGCATCACAAAAATCGACGCTCAAGTCAGAGGTGGCGAAACCCGACAGGACTATA

AAGATACCAGGCGTTTCCCCCTGGAAGCTCCCTCGTGCGCTCTCCTGTTCCGACCCTGCCGCT

TACCGGATACCTGTCCGCCTTTCTCCCTTCGGGAAGCGTGGCGCTTTCTCATAGCTCACGCTG

TAGGTATCTCAGTTCGGTGTAGGTCGTTCGCTCCAAGCTGGGCTGTGTGCACGAACCCCCCG

TTCAGCCCGACCGCTGCGCCTTATCCGGTAACTATCGTCTTGAGTCCAACCCGGTAAGACAC

GACTTATCGCCACTGGCAGCAGCCACTGGTAACAGGATTAGCAGAGCGAGGTATGTAGGCG

GTGCTACAGAGTTCTTGAAGTGGTGGCCTAACTACGGCTACACTAGAAGGACAGTATTTGGT

ATCTGCGCTCTGCTGAAGCCAGTTACCTTCGGAAAAAGAGTTGGTAGCTCTTGATCCGGCAA

ACAAACCACCGCTGGTAGCGGTGGTTTTTTTGTTTGCAAGCAGCAGATTACGCGCAGAAAAA

AAGGATCTCAAGAAGATCCTTTGATCTTTTCTACGGGGTCTGACGCTCAGTGGAACGAAAAC

TCACGTTAAGGGATTTTGGTCATGCATGATATATCTCCCAATTTGTGTAGGGCTTATTATGCA

CGCTTAAAAATAATAAAAGCAGACTTGACCTGATAGTTTGGCTGTGAGCAATTATGTGCTTA

GTGCATCTAATCGCTTGAGTTAACGCCGGCGAAGCGGCGTCGGCTTGAACGAATTTCTAGCT

AGACATTATTTGCCGACTACCTTGGTGATCTCGCCTTTCACGTAGTGGACAAATTCTTCCAAC

TGATCTGCGCGCGAGGCCAAGCGATCTTCTTCTTGTCCAAGATAAGCCTGTCTAGCTTCAAG

TATGACGGGCTGATACTGGGCCGGCAGGCGCTCCATTGCCCAGTCGGCAGCGACATCCTTCG

GCGCGATTTTGCCGGTTACTGCGCTGTACCAAATGCGGGACAACGTAAGCACTACATTTCGC

TCATCGCCAGCCCAGTCGGGCGGCGAGTTCCATAGCGTTAAGGTTTCATTTAGCGCCTCAAA

TAGATCCTGTTCAGGAACCGGATCAAAGAGTTCCTCCGCCGCTGGACCTACCAAGGCAACGC

TATGTTCTCTTGCTTTTGTCAGCAAGATAGCCAGATCAATGTCGATCGTGGCTGGCTCGAAG

ATACCTGCAAGAATGTCATTGCGCTGCCATTCTCCAAATTGCAGTTCGCGCTTAGCTGGATA

ACGCCACGGAATGATGTCGTCGTGCACAACAATGGTGACTTCTACAGCGCGGAGAATCTCGC

TCTCTCCAGGGGAAGCCGAAGTTTCCAAAAGGTCGTTGATCAAAGCTCGCCGCGTTGTTTCA

TCAAGCCTTACGGTCACCGTAACCAGCAAATCAATATCACTGTGTGGCTTCAGGCCGCCATC

CACTGCGGAGCCGTACAAATGTACGGCCAGCAACGTCGGTTCGAGATGGCGCTCGATGACG

CCAACTACCTCTGATAGTTGAGTCGATACTTCGGCGATCACCGCTTCCCCCATGATGTTTAAC

TTTGTTTTAGGGCGACTGCCCTGCTGCGTAACATCGTTGCTGCTCCATAACATCAAACATCGA

CCCACGGCGTAACGCGCTTGCTGCTTGGATGCCCGAGGCATAGACTGTACCCCAAAAAAAC

ATGTCATAACAAGAAGCCATGAAAACCGCCACTGCGCCGTTACCACCGCTGCGTTCGGTCAA

GGTTCTGGACCAGTTGCGTGACGGCAGTTACGCTACTTGCATTACAGCTTACGAACCGAACG

AGGCTTATGTCCACTGGGTTCGTGCCCGAATTGATCACAGGCAGCAACGCTCTGTCATCGTT

ACAATCAACATGCTACCCTCCGCGAGATCATCCGTGTTTCAAACCCGGCAGCTTAGTTGCCG

TTCTTCCGAATAGCATCGGTAACATGAGCAAAGTCTGCCGCCTTACAACGGCTCTCCCGCTG

ACGCCGTCCCGGACTGATGGGCTGCCTGTATCGAGTGGTGATTTTGTGCCGAGCTGCCGGTC

GGGGAGCTGTTGGCTGGCTGGTGGCAGGATATATTGTGGTGTAAACAAATTGACGCTTAGAC

AACTTAATAACACATTGCGGACGTTTTTAATGTACTGAATTAACGCCGAATTGAATTCCTCG

AGTACGTAGGATCCATTTAAATTCTAGAGGCGCGCCGATATCCTCTCTTAAGGTAGCGAGCT

CTTAATTAATAGGGCAGGGTAATTAACTATAACGGTCCTAAGGTAGCGATGGCAAACAGCT

ATTATGGGTATTATGGGTGGTTCTTTATGCGGACACTGACGGCTTTATGCCTGCAGGTCGCG

AGCGATCGCGGTACCGTAAAACGACGGCCAGTCTTAAGCTCGGGCCCTGCAGCTCTAGAGCT

CGAATTCTACAGGTCACTAATACCATCTAAGTAGTTGGTTCATAGTGACTGCATATGTTGTGT

TTTACAGTATTATGTAGTCTGTTTTTTATGCAAAATCTAATTTAATATATTGATATTTATATCA

TTTTACGTTTCTCGTTCAACTTTCTTGTACAAAGTGGGGATCCGATGGAATCCATGGAGGAGT

TCTGTACGCGCAATTCCGCTCTCCGTAAGGATGCTTCGGAGGTGCACATGGTCTCATACATG

TAGGCCCGACGAGGATCGAGTCGGTTCCGAAGTAGGATCGTCTCGATTGTTGGGCATCATTG

CATGGACATTCAGAGGGCCTACTGATACCTGGAATCCGCACCGTCCGGCTACCTAGCAATAA

GATTCTGTGTATATAAAGGGCTAAGGTGTCCGTCCTTGATAAAACCACCACCCTCAACAACT

TACCTCGACTATCAGCATCCCGTCCTATCTAACAATCGTCCATCGGTATCCAACTCCAACTCT

ATTCGCAGGGTCCTAGAATCGTAAGTACACGCTTATATCTTGTTGCCAGCGATAGCTGACAA

TGAATGAATATAGGTCATGAAAGCGTTAACGGCCAGGCAACAAGAGGTGTTTGATCTCATCC

GTGATCACATCAGCCAGACAGGTATGCCGCCGACGCGTGCGGAAATCGCGCAGCGTTTGGG

GTTCCGTTCCCCAAACGCGGCTGAAGAACATCTGAAGGCGCTGGCACGCAAAGGCGTTATTG

AAATTGTTTCCGGCGCATCACGCGGGATTCGTCTGTTGCAGGAAGAGGAAGAAGGGTTGCC

GCTGGTAGGTCGTGTGGCTGCCGGTGAACCGTCGAGCGCCCCCCCGACCGATGTCAGCCTGG

GGGACGAGCTCCACTTAGACGGCGAGGACGTGGCGATGGCGCATGCCGACGCGCTAGACGA

TTTCGATCTGGACATGTTGGGGGACGGGGATTCCCCGGGTCCGGGATTTACCCCCCACGACT

CCGCCCCCTACGGCGCTCTGGATATGGCCGACTTCGAGTTTGAGCAGATGTTTACCGATGCC

CTTGGAATTGACGAGTACGGTGGGGATCCGTCTGCTGGAGACATGAGAGCTGCCAACCTTTG

GCCAAGCCCGCTCATGATCAAACGCTCTAAGAAGAACAGCCTGGCCTTGTCCCTGACGGCCG

ACCAGATGGTCAGTGCCTTGTTGGATGCTGAGCCCCCCATACTCTATTCCGAGTATGATCCTA

CCAGACCCTTCAGTGAAGCTTCGATGATGGGCTTACTGACCAACCTGGCAGACAGGGAGCTG

GTTCACATGATCAACTGGGCGAAGAGGGTGCCAGGCTTTGTGGATTTGACCCTCCATGATCA

GGTCCACCTTCTAGAATGTGCCTGGCTAGAGATCCTGATGATTGGTCTCGTCTGGCGCTCCAT

GGAGCACCCAGTGAAGCTACTGTTTGCTCCTAACTTGCTCTTGGACAGGAACCAGGGAAAAT

GTGTAGAGGGCATGGTGGAGATCTTCGACATGCTGCTGGCTACATCATCTCGGTTCCGCATG

ATGAATCTGCAGGGAGAGGAGTTTGTGTGCCTCAAATCTATTATTTTGCTTAATTCTGGAGTG

TACACATTTCTGTCCAGCACCCTGAAGTCTCTGGAAGAGAAGGACCATATCCACCGAGTCCT

GGACAAGATCACAGACACTTTGATCCACCTGATGGCCAAGGCAGGCCTGACCCTGCAGCAG

CAGCACCAGCGGCTGGCCCAGCTCCTCCTCATCCTCTCCCACATCAGGCACATGAGTAACAA

AGGCATGGAGCATCTGTACAGCATGAAGTGCAAGAACGTGGTGCCCCTCTATGACCTGCTGC

TGGAGATGCTGGACGCCCACCGCCTACATGCGCCCACTAGCCGTGGAGGGGCATCCGTGGA

GGAGACGGACCAAAGCCACTTGGCCACTGCGGGCTCTACTTCATCGCATTCCTTGCAAAAGT

ATTACATCACGGGGGAGGCAGAGGGTTTCCCTGCCACAGTCTGAGAGCTCCCTGGCGAATTC

CCAGAGATGTTAGCTGAAATCATCACTAATCAGATACCAAAATATTCAAATGGAAATATCAA

AAAGCTTCTGTTTCATCAAAAATGACTCGACCTAACTGAGTAAGCTAGCTTGTTCGAGTACA

ATCAATCCATTTCGCTATAGTTAAAGGATGGGGATGAGGGCAATTGGTTATATGATCATGTA

TGTAGTGGGTGTGCATAATAGTAGTGAAATGGAAGCCAAGTCATGTGATTGTAATCGACCGA

CGGAATTGAGGATATCCGGAAATACAGACACCGTGAAAGCCATGGTCTTTCCTTCGTGTAGA

AGACCAGACAGAAGCTTGGAAACTGATAACTATAACGGTCCTAAGGTAGCGAAATTGAAGG

AGCATTTTTTGGGCTTGGCTGGAGCTAGTGGAGGTCAACAATGAATGCCTATTTTGGTTTAGT

CGTCCAGGCGGTGAGCACAAAATTTGTGTCGTTTGACAAGATGGTTCATTTAGGCAACTGGT

CAGATCAGCCCCACTTGTAGCAGTAGCGGCGGCGCTCGAAGTGTGACTCTTATTAGCAGACA

GGAACGAGGACATTATTATCATCTGCTGCTTGGTGCACGATAACTTGGTGCGTTTGTCAAGC

AAGGTAAGTGGACGACCCGGTCATACCTTCTTAAGTTCGCCCTTCCTCCCTTTATTTCAGATT

CAATCTGACTTACCTATTCTACCCAAGCATCCAAATGAAAAAGCCTGAACTCACCGCGACGT

CTGTCGAGAAGTTTCTGATCGAAAAGTTCGACAGCGTCTCCGACCTGATGCAGCTCTCGGAG

GGCGAAGAATCTCGTGCTTTCAGCTTCGATGTAGGAGGGCGTGGATATGTCCTGCGGGTAAA

TAGCTGCGCCGATGGTTTCTACAAAGATCGTTATGTTTATCGGCACTTTGCATCGGCCGCGCT

CCCGATTCCGGAAGTGCTTGACATTGGGGAGTTCAGCGAGAGCCTGACCTATTGCATCTCCC

GCCGTGCACAGGGTGTCACGTTGCAAGACCTGCCTGAAACCGAACTGCCCGCTGTTCTCCAG

CCGGTCGCGGAGGCCATGGATGCGATCGCTGCGGCCGATCTTAGCCAGACGAGCGGGTTCG

GCCCATTCGGACCGCAAGGAATCGGTCAATACACTACATGGCGTGATTTCATATGCGCGATT

GCTGATCCCCATGTGTATCACTGGCAAACTGTGATGGACGACACCGTCAGTGCGTCCGTCGC

GCAGGCTCTCGATGAGCTGATGCTTTGGGCCGAGGACTGCCCCGAAGTCCGGCACCTCGTGC

ATGCGGATTTCGGCTCCAACAATGTCCTGACGGACAATGGCCGCATAACAGCGGTCATTGAC

TGGAGCGAGGCGATGTTCGGGGATTCCCAATACGAGGTCGCCAACATCCTCTTCTGGAGGCC

GTGGTTGGCTTGTATGGAGCAGCAGACGCGCTACTTCGAGCGGAGGCATCCGGAGCTTGCA

GGATCGCCGCGCCTCCGGGCGTATATGCTCCGCATTGGTCTTGACCAACTCTATCAGAGCTT

GGTTGACGGCAATTTCGATGATGCAGCTTGGGCGCAGGGTCGATGCGACGCAATCGTCCGAT

CCGGAGCCGGGACTGTCGGGCGTACACAAATCGCCCGCAGAAGCGCGGCCGTCTGGACCGA

TGGCTGTGTAGAAGTACTCGCCGATAGTGGAAACCGACGCCCCAGCACTCGTCCGAGGGCA

AAGGAATAGTAACTATAACGGTCCTAAGGTAGCGAACTTGCATGCCAGCTTGGGCTGCAGG

TCGAGGCTAAAAAACTAATCGCATTATCATCCCCTCGACGTACTGTACATATAACCACTGGT

TTTATATACAGCAGTACTGTACATATAACCACTGGTTTTATATACAGCAGTCGACGTACTGTA

CATATAACCACTGGTTTTATATACAGCAGTACTGTACATATAACCACTGGTTTTATATACAGC

AGTCGAGGTAAGATTAGATATGGATATGTATATGGATATGTATATGGTGGTAATGCCATGTA

ATATGCTCGACTCTAGGATCTTCGCAACAGAAGGAAGAACGAAGGAAGGAGCACAGACTTA

GATTGGTATATATACGCATATGTAGTGTTGAAGAAACATGAAATTGCCCAGTATTCTTAACC

CAACTGCACAGAACAAAAACCGACTCTATAGGGATAACAGGGTAATTCAAAATGGTGAGCA

AGGGCGAGGAGCTGTTCACCGGGGTGGTGCCCATCCTGGTCGAGCTGGACGGCGACGTGAA

CGGCCACAAGTTCAGCGTGTCCGGCGAGGGCGAGGGCGATGCCACCTACGGCAAGCTGACC

CTGAAGTTCATCTGCACCACCGGCAAGCTGCCCGTGCCCTGGCCCACCCTCGTGACCACCTT

CACCTACGGCGTGCAGTGCTTCAGCCGCTACCCCGACCACATGAAGCAGCACGACTTCTTCA

AGTCCGCCATGCCCGAAGGCTACGTCCAGGAGCGCACCATCTTCTTCAAGGACGACGGCAA

CTACAAGACCCGCGCCGAGGTGAAGTTCGAGGGCGACACCCTGGTGAACCGCATCGAGCTG

AAGGGCATCGACTTCAAGGAGGACGGCAACATCCTGGGGCACAAGCTGGAGTACAACTACA

ACAGCCACAACGTCTATATCATGGCCGACAAGCAGAAGAACGGCATCAAGGTGAACTTCAA

GATCCGCCACAACATCGAGGACGGCAGCGTGCAGCTCGCCGACCACTACCAGCAGAACACC

CCCATCGGCGACGGCCCCGTGCTGCTGCCCGACAACCACTACCTGAGCACCCAGTCCGCCCT

GAGCAAAGACCCCAACGAGAAGCGCGATCACATGGTCCTGCTGGAGTTCGTGACCGCCGCC

GGGATCACTCACGGCATGGACGAGCTGTACAAGTAAAGCGGCCGCCCGGCTGCAGATCGTT

CAAACATTTGGCAATAAAGTTTCTTAAGATTGAATCCTGTTGCCGGTCTTGCGATGATTATCA

TATAATTTCTGTTGAATTACGTTAAGCATGTAATAATTAACATGTAATGCATGACGTTATTTA

TGAGATGGGTTTTTATGATTAGAGTCCCGCAATTATACATTTAATACGCGATAGAAAACAAA

ATATAGCGCGCAAACTAGGATAAATTATCGCGCGCGGTGTCATCTATGTTACTAGATCCGAT

GATAAGCTGTCAAACATGTATAGGGATAACAGGGTAATACAACTTTATTATACAAAGTTGGC

ATTATAAAAAAGCATTGCTTATCAATTTGTTGCAACGAACAGGTCACTATCAGTCAAAATAA

AATCATTATTTGGAGCTCCATGGTAGCGTTAACGCGGCCGCGATATCCCCTATAGTGAGTCG

TATTACATGGTCATAGCTGTTTCCTGAAGCTTAGCTTGAGCTTGGATCAGATTGTCGTTTCCC

GCCTTCAGTTTAAACTATCAGTGTTTGACAGGATATATTGGCGGGTAAACCTAAGAGAAAAG

AGCGTTTATTAGAATAACGGATATTTAAAAGGGCGTGAAAAGGTTTATCCGTTCGTCCATTT

GTATGTGCATGCCAACCACAGGGTTCCCCTCGGGATCAAAGTACTTTGATCCAACCCCTCCG

CTGCTATAGTGCAGTCGGCTTCTGACGTTCAGTGCAGCCGTCTTCTGAAAACGACATGTCGC

ACAAGTCCTAAGTTACGCGACAGGCTGCCGCCCTGCCCTTTTCCTGGCGTTTTCTTGTCGCGT

GTTTTAGTCGCATAAAGTAGAATACTTGCGACTAGAACCGGAGACATTACGCCATGAACAA

GAGCGCCGCCGCTGGCCTGCTGGGCTATGCCCGCGTCAGCACCGACGACCAGGACTTGACC

AACCAACGGGCCGAACTGCACGCGGCCGGCTGCACCAAGCTGTTTTCCGAGAAGATCACCG

GCACCAGGCGCGACCGCCCGGAGCTGGCCAGGATGCTTGACCACCTACGCCCTGGCGACGT

TGTGACAGTGACCAGGCTAGACCGCCTGGCCCGCAGCACCCGCGACCTACTGGACATTGCCG

AGCGCATCCAGGAGGCCGGCGCGGGCCTGCGTAGCCTGGCAGAGCCGTGGGCCGACACCAC

CACGCCGGCCGGCCGCATGGTGTTGACCGTGTTCGCCGGCATTGCCGAGTTCGAGCGTTCCC

TAATCATCGACCGCACCCGGAGCGGGCGCGAGGCCGCCAAGGCCCGAGGCGTGAAGTTTGG

CCCCCGCCCTACCCTCACCCCGGCACAGATCGCGCACGCCCGCGAGCTGATCGACCAGGAA

GGCCGCACCGTGAAAGAGGCGGCTGCACTGCTTGGCGTGCATCGCTCGACCCTGTACCGCGC

ACTTGAGCGCAGCGAGGAAGTGACGCCCACCGAGGCCAGGCGGCGCGGTGCCTTCCGTGAG

GACGCATTGACCGAGGCCGACGCCCTGGCGGCCGCCGAGAATGAACGCCAAGAGGAACAA

GCATGAAACCGCACCAGGACGGCCAGGACGAACCGTTTTTCATTACCGAAGAGATCGAGGC

GGAGATGATCGCGGCCGGGTACGTGTTCGAGCCGCCCGCGCACGTCTCAACCGTGCGGCTGC

ATGAAATCCTGGCCGGTTTGTCTGATGCCAAGCTGGCGGCCTGGCCGGCCAGCTTGGCCGCT

GAAGAAACCGAGCGCCGCCGTCTAAAAAGGTGATGTGTATTTGAGTAAAACAGCTTGCGTC

ATGCGGTCGCTGCGTATATGATGCGATGAGTAAATAAACAAATACGCAAGGGGAACGCATG

AAGGTTATCGCTGTACTTAACCAGAAAGGCGGGTCAGGCAAGACGACCATCGCAACCCATC

TAGCCCGCGCCCTGCAACTCGCCGGGGCCGATGTTCTGTTAGTCGATTCCGATCCCCAGGGC

AGTGCCCGCGATTGGGCGGCCGTGCGGGAAGATCAACCGCTAACCGTTGTCGGCATCGACC

GCCCGACGATTGACCGCGACGTGAAGGCCATCGGCCGGCGCGACTTCGTAGTGATCGACGG

AGCGCCCCAGGCGGCGGACTTGGCTGTGTCCGCGATCAAGGCAGCCGACTTCGTGCTGATTC

CGGTGCAGCCAAGCCCTTACGACATATGGGCCACCGCCGACCTGGTGGAGCTGGTTAAGCA

GCGCATTGAGGTCACGGATGGAAGGCTACAAGCGGCCTTTGTCGTGTCGCGGGCGATCAAA

GGCACGCGCA